DESIGN AND CONSTRUCTION OF

A NEW PSYCHROMETRIC CHAMBER

By

SPENCER OWEN LIFFERTH

Bachelor of Science in Mechanical Engineering

Brigham Young University

Provo, Utah

2007

Submitted to the Faculty of the
Graduate College of the
Oklahoma State University
in partial fulfillment of
the requirements for
the Degree of
MASTER OF SCIENCE
May, 2009

DESIGN AND CONSTRUCTION OF

A NEW PSYCHROMETRIC CHAMBER

Thesis Approved:

Dr. Lorenzo Cremaschi

Thesis Adviser

Dr. Daniel Fisher

Dr. Dana Hobson

Dr. A. Gordon Emslie

Dean of the Graduate College

ACKNOWLEDGMENTS

I would to thank that many people that made this project possible. I could not have done this with out the assistance and support from so many people.

First and foremost, I'd like to thank my wonderful wife, Whitney. She has allowed me to work long days and many nights on this project, and has whole-heartedly supported me through it all. I will be forever indebted to my parents, who have shown me what a full day of work means. I especially give thanks to my dad who, with patience, showed me how to create items using all kinds of tools and methods.

I thank the mechanical and aerospace engineering department at OSU for allowing me to take on such an interesting project. I also thank them for providing excellent faculty and staff to enhance my education.

I am grateful to Dr. Lorenzo Cremaschi, who got the ball rolling for the psychrometric chamber. I appreciate the invitation to work on this project. I'm thankful for the amazing trust that he has had in my abilities, and for the guidance he has shown to me.

Also, thanks to Dr. Jeffery Spitler and Dr. Daniel Fisher for their guidance over the Building System and Thermal Research group at OSU, and for their instruction on these topics.

A huge thank you goes to AAON for their generous contribution in materials and expertise. Specific thanks to Stephen Wakefield and Patrick Chapman for guidance in the structural design of the chamber. Enormous thanks to Richard Davis, for answers to hundreds of questions and close guidance through out the project. Thanks also to Tyson Hinther, Mark Fly, Kevin Teakell, and Brent Stockton.

Concerning the mezzanine, I thank Dr. Dana Hobson for his help and guidance in design. My gratitude to Justin Combs and Joe Donarumo, of Double J Welding, for their work constructing the mezzanine and welding various other parts of the chamber.

I appreciate the other graduate students that have contributed to the success of the chamber; namely, Sam Hobson, Edwin Lee, and Ozgur Aslan.

I could not have gotten far without the excellent help of the many students who have worked on the chamber over the past year; their willingness to work hard has made the chamber construction a success: Forrest Austin, Wendell Cook, Chris Carroll, Seth Hayes, Adam Parker and Johnathan Peterson.

Also, I appreciate the Oklahoma State University Physical Plant for supplying us with power and water. Specific thanks to Gary Thacker for his work on the electrical systems. Thanks to the university truck services for their help in lowering the chamber pieces into the basement and allowing us to borrow their scaffolding for the duration of the chamber construction.

I'd like to thank Jerry Dale for being an invaluable source of information and help. Also, I express gratitude to him for his patience in putting up with our messes in the basement of the ATRC. My appreciation goes to John Gage, for allowing us to

borrow tools from the DML, and to Ron Markham for his generosity in allowing us to use much of his equipment.

Finally, I'd like to express my gratefulness to Kyong Edwards for her excellent help in handling the finances of the psychrometric chamber. Her service has been invaluable in ensuring that we have had the tools and supplies necessary to move the chamber forward.

Thanks again to everybody who made this project a success.

TABLE OF CONTENTS

Chapter Page

LIST OF TABLES

LIST OF FIGURES

Figure Page

Figure Page

Figure Page

NOMENCLATURE

A_n	exit area of nozzle (ft^2)
A_i	area of surface i
C	coefficient of discharge for the nozzle (dimensionless)
COP	coefficient of performance
C_p	specific heat capacity of the wall A is the heat transfer area
$c_{p,air}$	specific heat capacity of air
D	diameter (in)
E	modulus of elasticity (psi)
f	f factor – as seen in ASHRAE 37-1988
F	force exerted on beam under load
F_m	flux history coefficients
g_{ij}	radiation heat transfer factor between interior surface i and j
$\bar{h}$	average convection coefficient
h_{ci}	convective heat transfer coefficient at interior surface i and j
h_{in}	enthalpy of inlet stream
h_{out}	enthalpy of outlet stream
i_{fg}	enthalpy of vaporization of water
I	moment of inertia (in^4)

k	coefficient of conduction
k_{fluid}	conduction coefficient of connecting fluid
l	length between supports of beam under stress
m	number of surfaces in the room
$\dot{m}_{air}$	mass flow rate of air
M_{end}	bending moment at the ends of a beam
M_{center}	bending moment at center of beam
M_{max}	maximum bending moment (psi)
N_{Re}	Reynolds Number
$\overline{Nu}_L$	average Nusselt number
p_n	pressure at the nozzle throat (in Hg)
p_v	pressure difference across the nozzle (in H_2O)
Pr	Prandtl number
$q_{i,\theta}$	rate of heat conducted into surface *i* at inside surface at time θ
$\dot{Q}_{Low}$	total heat removed from a system
$\dot{Q}_{Low,latent}$	latent portion of heat removed from a system
$\dot{Q}_{Low,sensible}$	sensible portion of heat removed from a system
Ra_L	Rayleigh number
$RE_{i,\theta}$	rate of heat radiated form the equipment and occupants and absorbed by surface *i* at time θ
$RS_{i,\theta}$	rate of solar energy coming through windows and absorbed by surface *i* at time θ

$RL_{i,\theta}$	rate of heat radiated from lights and absorbed by the surface i at time θ
$t_{a,\theta}$	inside air temperature at time θ
$t_{o,\theta}$	outdoor air temperature at time θ
$t_{i,\theta}$	average temperature of interior surface i at time θ
$t_{v,\theta}$	ventilation air temperature at time θ
$t_{e,\theta-n\delta}$	sol-air temperature at time θ-$n\delta$, (°F)
T_{in}	temperature of inlet stream
T_{out}	temperature of outlet stream
$T_{surface}^{p}$	temperature of the surface at the current time step
$T_{surface}^{p+1}$	temperature of the surface at the future time step
T_{mid}^{p}	current temperature of the inner wall node
T_{m}^{p}	current temperature of a specified node, m
T_{m}^{p+1}	future temperature of a specified node, m
$\dot{V}$	volumetric flow rate of air through a single nozzle (cfm)
V_a	air velocity
$V_{i,\theta}$	volume flow rate of outdoor air infiltrating into room at time θ
$V_{v,\theta}$	volume rate of flow of ventilation air at time θ
v_n	specific volume of the air as measured from wet and dry bulb temperatures
v_n'	adjusted specific volume of the air at the nozzle (ft^3/lb)
$\dot{W}_{in}$	electrical power consumed by the test unit
X	exterior CTF values
Y	cross CTF values

y_{max}	maximum deflection of beam under load
Z	interior CTF values
α	thermal diffusivity of the wall
δ	time interval
Δx	distance between nodes
ρ	density
σ	air density
$\sigma_{c,max}$	maximum compressive forces (psi)
$\sigma_{t,max}$	maximum tensile forces (psi)
ω_{in}	absolute humidity of inlet stream
ω_n	absolute humidity at the nozzle (lbs moisture/lbs dry air)
ω_{out}	absolute humidity of exiting stream

CHAPTER I

INTRODUCTION

Most of us sleep, eat, and work in the conditioned space provided by heating and air-conditioning systems; we live in an air-conditioned world – that is – the buildings that surround us are conditioned for our comfort. However, the reality is that the world beyond our walls is anything but conditioned: Temperatures ranging from -129 °F (-89°C) to 136 °F (58°C) have been recorded on the earth's surface (NCDC and Commerce 2009). Air conditioning and heating systems that provide us with comfortable living spaces endure temperatures imposed by the climate in which they operate. A psychrometric chamber is a laboratory simulator that is used to study the operation of these systems in various climate conditions.

Psychrometrics is the study of water, or humidity, in the air, which is largely dependent on temperature. A psychrometric chamber then, is a set of rooms in which the temperature and humidity can be precisely controlled. The chamber is controlled to simulate actual field operating conditions that an air conditioner or heat pump would typically be exposed to during its service.

The performance characteristic data of these systems are measured for design and off-design conditions. A system may be an air conditioner, heat pump, roof top unit, or refrigerator. These data sets can be used to determine energy consumption, reliability, and maintenance schedules. It is also possible to research design modifications and develop optimization features for system improvement using the data retrieved from tests in a psychrometric chamber.

The thermal systems research group at Oklahoma State University (OSU) actively performs research on heating and air-conditioning systems. Funds have been allocated to design and build a psychrometric chamber on the Stillwater campus. This thesis summarizes the design, construction, and start up of the new psychrometric chamber at OSU.

The Need for HVAC&R Research

Among the several fields of engineering exists the field of heating, ventilation, air-conditioning, and refrigeration; or HVAC&R as it commonly called. Although most don't think about it, people throughout the world enjoy the benefits of HVAC&R equipment on a daily basis. This equipment cools our homes and offices in the summer and heats them in the winter, it provides adequate ventilation for where we work and play and it enable us to keep medicine and food from spoiling. Indeed, the world would be a much different place if it weren't for the technology of the HVAC&R industry.

It is easy to see how the industry has helped to make the world a healthier place to live: safer food, readily available medicine, temperate living spaces, etc. However, the benefits go beyond health: studies have shown that a properly air-conditioned workplace has strong connections to productivity – a connection that is worth millions to businesses each year (Tom 2008). Of course, the increased productivity comes at a cost: cooling and heating buildings is expensive; the equipment that makes up the air conditioning system is often the most expensive portion of the utility bill.

Because of relatively high operating costs, there is a great need for research to be done in the field of HVAC&R. As the world becomes more energy dependant, it is increasingly more important for society to more efficiently make use of the energy that is consumed. One aspect of increasing our energy efficiency must be through the improvement of HVAC&R equipment. As is the case with any technology, improvement will come as research is done, and design modifications are implemented to existing systems and components. The overall benefit comes as new ideas are tried and tested.

Test Chambers

Innovations are first created on paper before they can be implemented in real life. Unfortunately, engineers have neither the time nor ability to create something perfect the first time – therefore an intermediate step is required.

Many equipment operations are largely dependent on surrounding conditions. This fact gives way to the need for test chambers. Test chambers allow scientists and engineers to test new and existing technology under real life conditions. A new type of

wing would not be put on a plane without first testing the thrust in a wind tunnel; similarly, a new heat pump technology should not be put on your home until it has been tested in a psychrometric chamber.

Numerous environmental test chambers have been developed for testing various systems and components. Test chambers can be purchased in all sizes, and differ in their control variables. These variables include temperature, humidity, air pressure, altitude, solar exposure, and precipitation. Chambers can be designed to maintain a constant condition; they can also be transient, or even cyclic. One chamber on the market even simulates the change in air pressure of a free-falling object. Most of these condition variations are beyond the scope of necessary controls in a performance characterization of HVAC equipment. For testing of HVAC equipment, the temperature, humidity, and airflow rate are the usual controlled variables.

A psychrometric chamber allows the operation of a unit under controlled conditions. One unique aspect of a psychrometric chamber that differentiates it from a typical environmental test chamber is that it is able to maintain conditions with the addition of a live thermal load. The psychrometric chamber must respond to the rejection or absorption of heat by the test unit in order to maintain the desired conditions. In other words, the psychrometric chamber simulates the environment by acting as an infinite heat source or sink.

A Brief Timeline of the Project

In 2006 Dr. Lorenzo Cremaschi began work as an assistant professor at Oklahoma State University. As part of his start up fund he ventured to create a psychrometric chamber on campus at OSU. The Building and Environmental Thermal Systems Research Group (BETSRG) previously had other laboratories. Prominent laboratories include an airflow and contaminants laboratory, and several setups for testing ground source heat pumps. The psychrometric chamber adds the ability to test air source heat pumps, air-conditioning equipment, refrigerators and other thermal systems in a controlled environment.

Later that year the faculty members of the BETSRG group and Dr. Cremaschi approached AAON, a Tulsa based HVAC company, and proposed the idea of building a chamber with them. A deal was struck that AAON would meet OSU half way for the funding of a half million dollar facility that would be located on OSU campus. AAON would provide the construction materials and OSU would provide the location, man power and many of the materials related to the chamber.

As part of the deal with OSU, a site in the lower basement of the Advanced Technical Research Center (ATRC) was dedicated to the project. With the site selected and AAON on board for the project, the general specifications of the chamber were laid out, including the temperature ranges, overall capacity, and basic floor plan of the chamber area.

By May 2007 the final design work began. Two graduate students from OSU were hired as interns at AAON to design the chamber structure, seen in Figure 1.1. Each

piece of the chamber was designed to be manufacture by AAON. Concurrently at AAON, three undergraduate students from Montana State University were hired as interns to develop some of the preliminary design of the conditioning system and code tester.

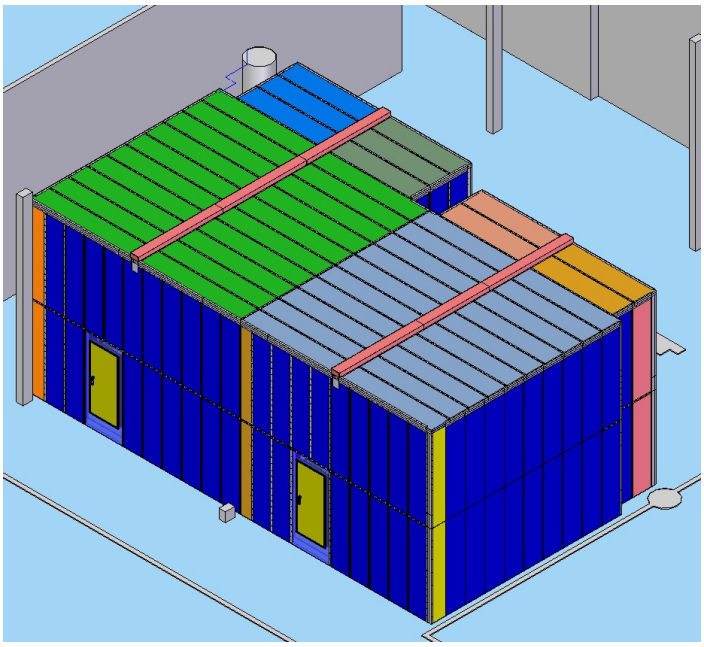

Figure 1.1: Electronic rendering of chamber design in setting of the ATRC basement

All interns completed their stay at AAON by mid August. At this time the complete structural enclosure of the chamber had been designed. The equipment mounting pieces in the chamber had had the preliminary work done on them, but the final drafts of those would not be completed until November. The code tester design had been completed and conditioning system had several viable parts identified; however the actual system would be re-designed in the fall of 2008.

From September to November 2007 the design on the mezzanine was accomplished. Also during this time, and stretching into early March, the site in the

ATRC was prepared for the chamber construction. Preparation included the design and construction of a foundation for the chamber to rest on, seen in Figure 1.2.

Figure 1.2: Photo showing a portion of the steel floor support for chamber

Engineers and drafters at AAON converted all the part designs into files for their automated machinery during the late fall and early winter. AAON utilized the annual winter slowdown to manufacture the parts for the chamber. Manufacturing was completed by the end of January 2008. The first shipment of parts, seen in Figure 1.3, came on four semi trailers and arrived at OSU on January 31, 2008. Other shipments came much later and included purchased parts: such as motors, door handles, dampers, piping, etc.

Figure 1.3: Top: lowering the crates into the ATRC basement via the wind tunnel shaft. Bottom: Unopened crates at chamber construction site.

The unpacking and arranging of the shipment from AAON took several weeks; during which time the mezzanine was constructed. There was little room for movement anywhere in the basement and progress was slow; much of the effort at the time was directed to organization in order to keep construction moving once it was started. The first panels of the chamber were screwed together near the end of March. The lower half

of the first (south) wall was erected during the beginning of April. As seen in Figure 1.4, the upper half of the wall was added before the end of the month.

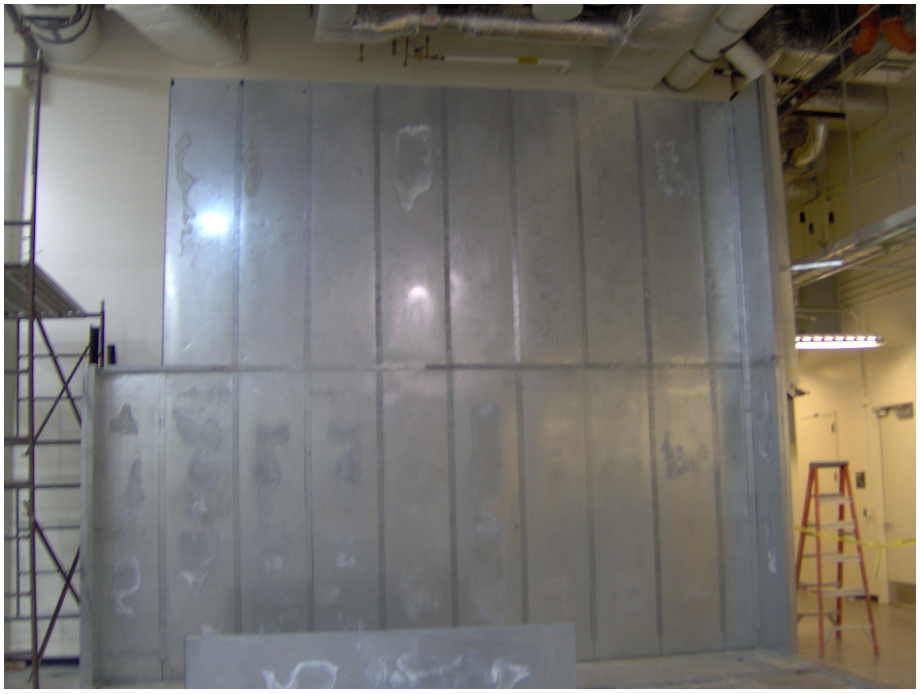

Figure 1.4: Chamber construction begins, erected south wall of chamber

By the beginning of May the construction of the chamber sped up considerably; this was in conjunction with the end of the semester and a substantial increase in man power and time.

Figure 1.5: Chamber construction. Left: Indoor chamber walls Right: outdoor conditioning loop

The construction, seen in Figure 1.5, of the chamber continued throughout the summer. By the end of July 2008 the last of the panels that comprise the chamber envelope, seen in Figure 1.6, had been secured in place. By the middle of August a shift in emphasis and man power moved construction to a slower pace. From August to December and beyond, the hanging of doors, mounting of equipment, and finishing touches on chamber construction were being accomplished. Also during this time, a major revamp of the conditioning system design was accomplished. The redesign eliminated some uncertainties in the system and served to balance cost and functionality of the chamber. By late November parts began arriving for the conditioning system; parts continued to trickle in throughout February 2009.

Figure 1.6: Photographs of completed chamber envelope – Clockwise from top: North wall and main access for units, East wall, West wall containing personnel access doors, and roof

In conjunction with the conditioning system revamp was a design of the electrical requirements for the chamber. The basic requirements had been laid out previously; during this time actual components were selected. The piping system installation began in December 2008 and continued into May 2009. The cooling coils, pumps, and other cooling system components were also installed during this time. Parts for the electrical system were ordered at the end of December. Electrical work commenced early February, and continued through May.

Objectives of this Thesis

The overall scope of this thesis was to design and build a new psychrometric chamber at OSU. The specific objectives of my thesis are to (1) design the structure of the chamber, mezzanine, and trolley crane. (2) Build the chamber structure. (3) Install the mechanical equipment used such as coils, heaters, and steam lines. (4) Determine the soaking time of the chamber.

I began working on the chamber in May 2007. I was one of two graduate students at AAON in charge of designing the chamber structure. At this stage, the basic plan and specifications had already been decided. Later on, I designed the mezzanine and crane lift that are used for equipment staging. I supervised the construction of the chamber. I have done very little work in the electrical planning but have, with the help of others, designed the conditioning system; that is the cooling coils, heater, and steam system for temperature and humidity control in the chamber. I have contributed to the many aspects

of the chamber, and have had great assistance. I have spent my time at OSU keeping the work going; that is what I have tried to do.

CHAPTER II

PSYCHROMETRIC CHAMBER: REVIEW AND SPECIFICATION

Psychrometric chambers are a sub-market of environmental test chambers, which can be purchased in a variety of sizes and temperature ranges. Sizes can be as small as a micro-wave oven or large enough to drive a semi truck into. Table 2.1 shows what is available on the market; it may not be possible to get all the options in a single chamber. Regardless, the options available are certainly amazing.

	SCSI	CSZ	Cambridge	Tescor	ESPEC	Thermotron	Envirotronics	Temptronics	Design Environmetnal	TestEquity
Temp Min °F (°C)	-65 (-54)	-100 (-73)	-13 (-25)	-15 (-26)	-85 (-65)	-99 (-73)	-99 (-73)	-76 (-60)	-94 (-70)	-99 (-73)
Temp Max °F (°C)	212 (100)	375 (190)	131 (55)	266 (130)	302 (150)	350 (177)	350 (177)	347 (175)	356 (180)	347 (175)
Humidity min	<1%	10%	50%	NA	10%	20%	20%	NA	10%	10%
Humidity max	99%	95%	100%	NA	95%	95%	95%	NA	98%	95%
Change Rate °F/min (°C/ min)	9 (5)	NA	NA	NA	1.8 - 27 (1-15)	7.2 - 9 (4-5)	NA	NA	1.5 - 5 (0.8 - 2.7)	NA
Area (ft^2)	50 to 25,000	Any	576	NA	174	161	NA	Bench Top	1.6	27 cu ft

Table 2.1: Features available in commercial environmental test chambers. Note that all features may not be available in a single unit – company web advertisements

With so many options available in commercial environmental chambers, determining the need for OSU psychrometric chamber was not very straightforward. There are a lot of

aspects that could be taken on this topic, but the idea was to make the chamber as versatile as possible within the cost constraints.

Room Size

The first decision, and possibly easiest to make, was the size of the chamber. As part of the agreement with OSU, the maximum floor space for the project was predetermined. The area allotted in the basement was approximately 53' long, 25' wide and 20' high. As seen in Figure 2.1, the space was mostly open except for a few columns near the edges on the east and west sides.

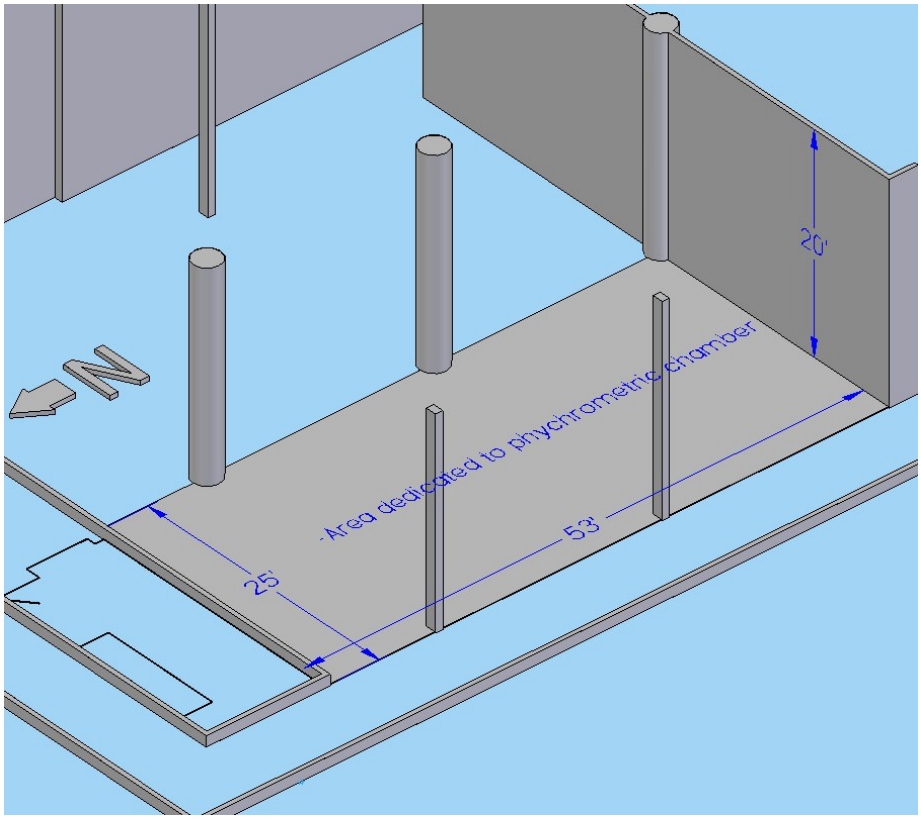

Figure 2.1: Rendering of area dedicated to the psychrometric chamber in the ATRC basement

All equipment necessary to the chamber was to be contained within the allotted space. Additional parameters imposed by OSU required that another test facility could be set up in the space east of the chamber location, and a pathway should remain on the north end of the chamber. These parameters limit the access doors of the chamber to be on the North and West faces. The floor plan developed allows access through the North wall. A mezzanine houses the chamber conditioning equipment. An integrated trolley crane will assist in lifting and moving the testing equipment into the chamber, as shown in Figure 2.2.

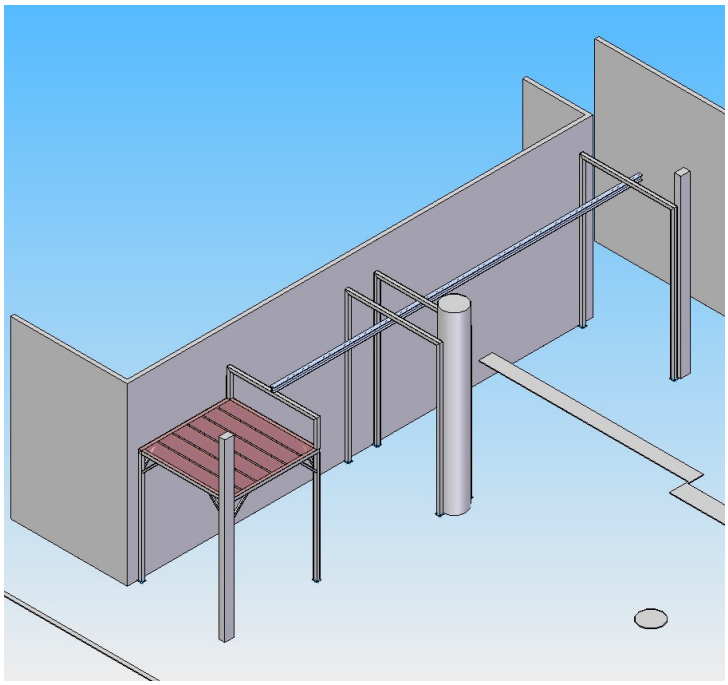

Figure 2.2: 3-D rendering of mezzanine in basement of ATRC

Because of the nature of research work; and for limiting the cost of construction, it was desirable to have a space available that could house two separate research projects. This would allow each researcher to keep their experimental setup without hindering the

progress of the other. Some collaboration would be needed in scheduling tests, but the setup would remain untouched while a testing unit is on standby.

A review of the standards set forth by American Society of Heating, Refrigerating, and Air-condition Engineers, ASHRAE, concerning the testing of air-conditioning units reveals that there must be at least three feet between any unit and the wall of the chamber. Additionally, there must be at least six feet from any wall to any discharging surface of the test unit.

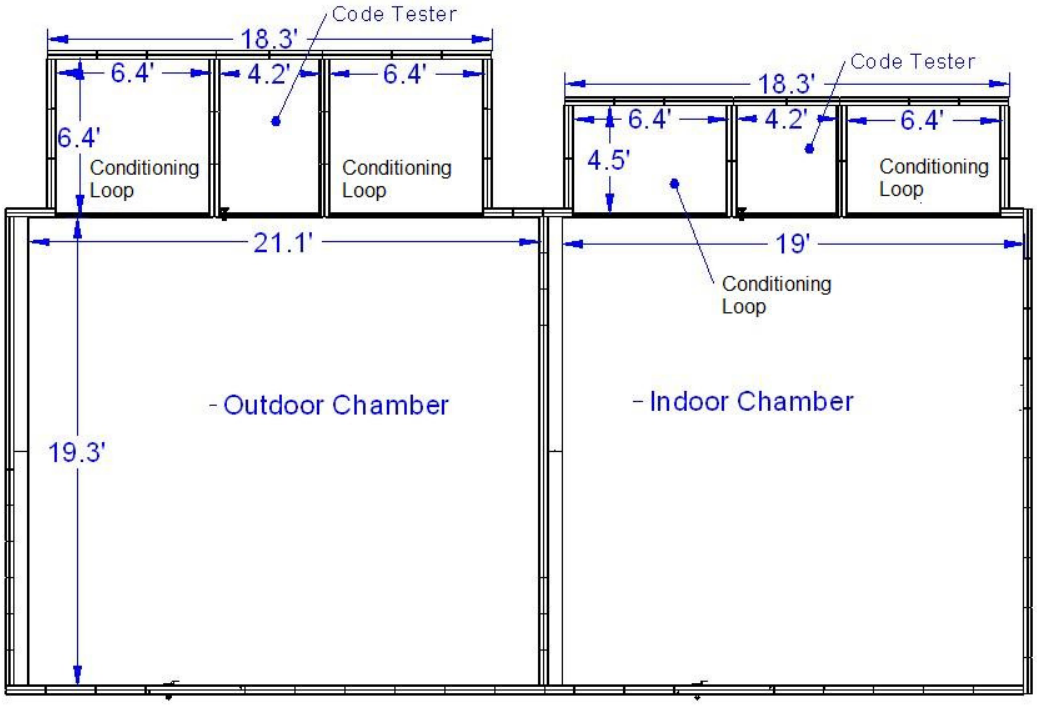

Figure 2.3: Floor plan of psychrometric chamber, note that internal height is 16'.

While packaged air-conditioning units come in many shapes and sizes, AAON products were used as a reference. AAON houses several different capacities of air-conditioners in the same packaging. For example, one of the RM rooftop models houses options of 8, 10, 13, and 15 ton capacity. The packaging for these options has a footprint

of 87" x 78" and height of 45". Using the longest dimension, 87", or 7.25', the maximum required space would be 7.25' for the unit, 6' for the discharging surface, and 3' spacing from the opposite wall; the total space needed is 17.25', Figure 2.3 shows that there is plenty of room for a unit. If two units are to sit side by side, assuming that the do not discharge toward each other, they would require 23.5' of space. Unfortunately, the space is sufficiently limited that if two of the largest test units were used, some shifting would be necessary to shift from one test to the other. A unit that discharges from top and bottom, as can be the case with rooftop units, requires a total of 15.75'. The total inside chamber space is 16'; revealing some of the difficulty in building a psychrometric chamber in the limited space of a basement. .

Chamber Access

Three different access routes are available to the get units into the basement and chamber. Depending on the unit size, different routes will need to be used. For small units, maximum dimensions not exceeding about 48" wide and 100" long, the nearest elevator can be used. Larger units will require the use of the larger freight elevator or the wind tunnel shaft. The freight elevator access path allows nothing wider than 76"; however, one must also ensure that the unit will be able to navigate the turns. Table 2.1 lists the clearances of each of the access routes. These dimensions present general guidelines; however, when the maximum limits are approached, specific cases should be considered.

Regardless of route, the chamber entrance door is limited to 103” x 100”. All large equipment to be located in the indoor chamber will be positioned via the outdoor chamber. Two personnel access doors; each measuring 34” by 77”, will allow people ad smaller items into the chamber.

1	**Wind Shaft Limitations**	
	Door Opening:	144" W x 120" T
	*Shaft opening:	79" x 231"
2	**Large Elevator Route**	
	Opening:	72" W x 82" T
	Interior:	89" W x 108" T x 135" D
	*Diagonal:	194"
	Minimum hallway clearance:	76"
3	**Small Elevator Route**	
A	Opening:	48" W x 102" T
B	Interior:	64" W x 108" T x 101" D
	**Diagonal:	169"

*Shaft opening can be expanded to 155" x 231" if center beam is removed
**Diagonals demonstrate max length of thin rod that could fit in elevator

Table 2.2: Access route limitations

The wind tunnel air shaft (1) provides the most direct route to the chamber, allowing the largest possible items into the chamber; however using this route is time consuming and requires the collaboration of several people – including university truck services. Figure 2.4 demonstrates the possible routes to transport equipment to the chamber.

The shaft is accessed on the East side of the ATRC. A crane, and operator, can be rented from the university to lower equipment from the outside to the basement floor roughly 26’ below. The initial shaft opening is 79” x 231”; however, a little tilting and twisting has allowed access of several narrow items exceeding this length. If needed, the

center supporting beam could be removed enlarging the opening to 155” x 231” (12 x 19 ft).

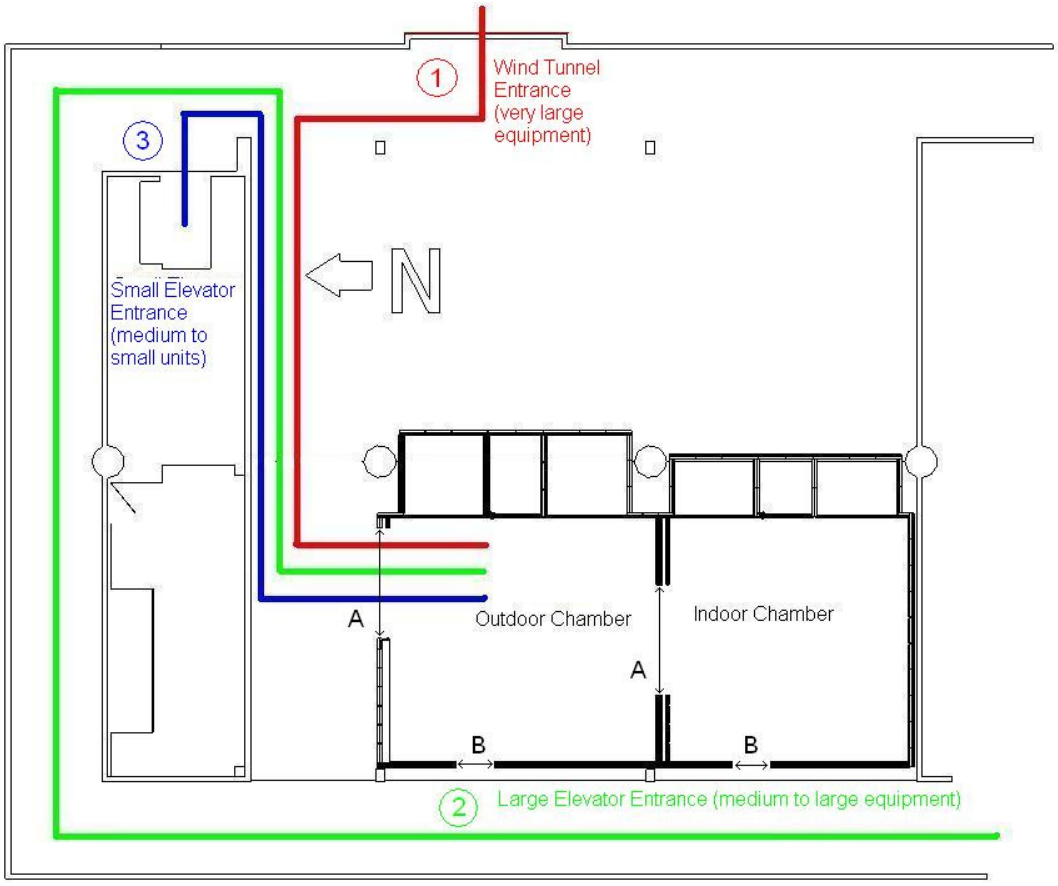

Figure 2.4: Equipment access routes to chamber see Table 2.1 for information on dimensional limitations

Temperature and Humidity Limits

Reference to testing standards for heat pumps and air conditioning systems reveals the starting point for temperature range specification. Heat pumps are tested as low as 17/15°F (-8/-9°C) and as high as 62/56.5°F (8/6°C). Air conditioners are tested between 67/53.5°F (19.4/11.9°C) and 95/75°F (35/23.9°C). So at a minimum, if all that will ever be tested is heat pumps and air conditioners, it is necessary to have a chamber

that has a dry bulb/wet bulb temperature range from 17/15°F (-8/-9°C) to 95/75°F (5/6°C) (AHRI 2008).

It is conceivable, especially because this will be primarily a research facility, that temperature beyond this minimum range would be beneficial. A comparison of commercial chambers reveals that a very common minimum temperature as -40°F; maximum temperatures vary widely. Furthermore, control of humidity between 10 and 95% seems to be common in industry; the only manufacturer advertising ranges significantly outside these parameters is SCSI, a developer of clean rooms. This range certainly falls within the range dictated by the testing standards.

Chamber Capacity

The overall capacity of the chamber was decided to be 15 tons of refrigeration (52.7 kW). This decision reflects a balance between testing area, access route and mechanical systems. As previously discussed, a 15 ton unitary air conditioning unit from AAON has the dimensions of 87" x 78" x 45"; the predetermined chamber size will house this unit reasonably well; however, in order to get a larger unit into the chamber, the access route would need to be wider, which would in turn reduce the room size. A 15 ton capacity room balances the space needed for testing, conditioning equipment, and room access the best.

Floor load capacity was also determined using an AAON unit as a reference. A 15 ton unit weighs about 3,000 pounds. When testing a unit, it will likely be on castors, creating four point loads. Even in the poorest distributions of weight, no more than 80%

of the total load would be expected to fall on one wheel, therefore 2400 lbs as a point load was determined to be number used for maximum floor load capacity.

Air Supply

One element of the chamber design makes it stand out from the typical commercial chamber; this is the air supply path. Most of the chambers available on the market have one or more registers that supply the room with conditioned air. In an attempt to obtain more uniform air distribution, the OSU psychrometric chamber was specified to have air delivered through a perforated floor plenum system. The conditioned air will come through the floor and exit through the ceiling in the same manner. With this method the distribution of the air should be more uniform, hopefully eliminating stagnation points and severely turbulent points which can commonly be found near the supply registers of a typical room. Uniform air distribution increases the repeatability of experiments, thus enhancing the accuracy of test results.

Preliminary Heat Transfer Analysis

Some work was done by Cremaschi and Lee concerning heat transfer and the thickness of the panels (Cremaschi and Lee 2008). Using finite element analysis software, they modeled the heat transfer through insulated panels. The modeled panels are used on many of the units produced by AAON. The thickness of the panels was varied to test for heat transfer through the panels. Thicker panels will provide better

insulation to the chamber. The decided benchmark in the paper was whether or not there would be condensate on the outside of the chamber.

Fundamental heat transfer equations for conduction and both free and forced convection were used in the calculations. The conclusion, seen in Figure 2.5, was that 5" panels would ensure that the outside surface temperature of the chamber would not drop below the dew point even when the inside of the chamber was as low as -40°F.

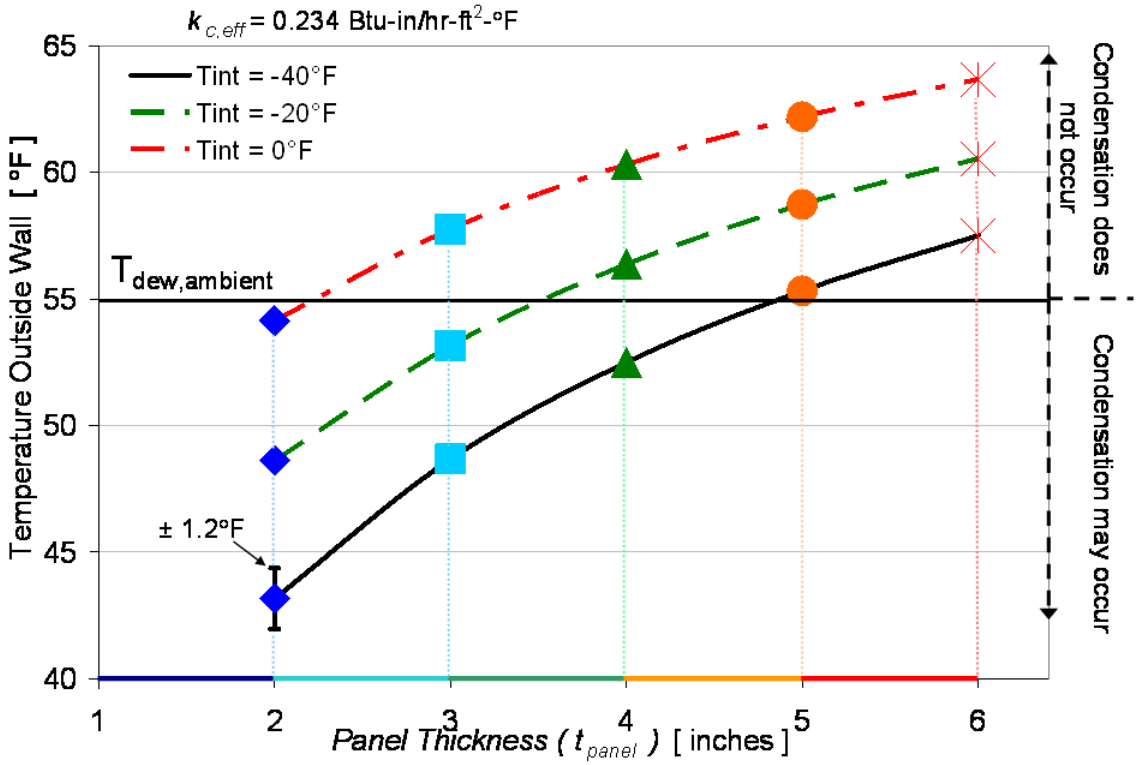

Figure 2.5: Dependence of condensate formation on the outer wall of the chamber based on panel thickness (Cremaschi and Lee 2008)

Previously AAON made panels up to 3" thick; manufacturing panels thicker than 4" would require AAON to purchase new machinery. Even the manufacturing of a 4" panel required modification to existing machinery. According to the results, for a 4" panel,

condensate is likely to collect on the outer walls of the chamber temperature approaches approximately -25°F (-32°C).

CHAPTER III

INDUSTRY TESTING STANDARDS

Two major organizations in the United States publish standards that apply to heating and air conditioning equipment. These organizations are the Air-Conditioning, Heating and Refrigeration Institute, AHRI, and the American Society of Heating, Refrigerating, and Air-Conditioning Engineers, or ASHRAE. Both organizations provide standards for guidance in testing and rating equipment.

Methods for Testing

According to ARI standard 210, four methods exist to conduct performance rating test evaluation on unitary equipment and split unit systems. These methods are included in the following list (AHRI 2008):

a) Indoor air enthalpy method

b) Outdoor air enthalpy method

c) Compressor calibration method

d) Refrigerant enthalpy method

Standard 116 from ASHRAE lists the same methods. Both standards define the indoor air enthalpy method as the primary method for testing. The other methods are for verification of the indoor side air enthalpy method (ASHRAE 1995). The four main methods for testing equipment are explained below.

The psychrometric chamber is set up to easily incorporate both the indoor and outdoor enthalpy methods without modifying the test equipment. Implementing these methods will be the primary way of testing units inside the psychrometric chamber. The compressor calibration method and refrigerant enthalpy method could also be used as a testing tool, but both methods require modifications to the typical commercial unit and will be used less extensively. Because the air enthalpy methods are so useful and straightforward to implement, details of how the measured variables from these methods are used to determine equipment performance are explained in the next section.

Indoor Air enthalpy Method

As previously stated, the primary method for testing air-conditioners and heat pumps is the indoor air enthalpy method. As implied by the name of the method, the idea behind the method is to measure the change of enthalpy of the indoor air. This is done by monitoring the wet and dry bulb temperatures of the inlet and outlet sides of the conditioning coils. The mass flow of the air is monitored as well as the power consumption of the test unit.

Outdoor Air Enthalpy Method

Similar to the indoor air enthalpy method, this test relies on measurements of the air flow and the wet and dry bulb temperatures of the air stream to determine the change in enthalpy that occurs across the outdoor coil. Power consumption measurements allow one to determine the performance using equations.

Compressor Calibration Method

In the compressor calibration method the refrigerant temperature and pressures are measured. The evaporator superheat is determined as well as the refrigerant enthalpies for the inlet and outlet of the indoor coils, these variable are used to determine the capacity of the test unit.

Refrigerant Enthalpy Method

In this method, instruments are placed to measure the temperature, pressure and flow of the refrigerant. The enthalpy of the refrigerant is determined on either side of the indoor coils. Total capacity of the system can be calculated from these measured variables.

Performing Tests

During testing, it is crucial to maintain the specified conditions inside the test chamber. Because heat transfer is driven by temperature gradients, variations in chamber conditions result in variations of performance. Standard 210/240, issued by AHRI, specifies chamber conditions for various unit categories. A sample of the conditions appear in Table 3.1 (AHRI 2008).

Table 3. Cooling Mode Test Conditions for Units Having a Single-Speed Compressor and a Fixed-Speed Indoor Fan, a Constant Air Volume Rate Indoor Fan, or No Indoor Fan

Test Description	Air Entering Indoor Unit Temperature				Air Entering Outdoor Unit Temperature				Cooling Air Volume Rate
	Dry-Bulb		Wet-Bulb		Dry-Bulb		Wet-Bulb		
	°F	°C	°F	°C	°F	°C	°F	°C	
A Test - required (steady, wet coil)	80.0	26.7	67.0	19.4	95.0	35.0	75.0[1]	23.9[1]	Cooling Full-load [2]
B Test - required (steady, wet coil)	80.0	26.7	67.0	19.4	82.0	27.8	65.0[1]	18.3[1]	Cooling Full-load [2]
C Test - optional (steady, dry coil)	80.0	26.7	[3]		82.0	27.8	–		Cooling Full-load [2]
D Test - optional (cyclic, dry coil)	80.0	26.7	[3]		82.0	27.8	–		[4]

Notes:

[1] The specified test condition only applies if the unit rejects condensate to the outdoor coil.
[2] Defined in section 6.1.3.3.1.
[3] The entering air must have a low enough moisture content so no condensate forms on the indoor coil. (It is recommended that an indoor wet-bulb temperature of 57.0 °F [13.9 °C] or less be used.)
[4] Maintain the airflow nozzles static pressure difference or velocity pressure during the ON period at the same pressure difference or velocity pressure as measured during the C Test.

Table 3.1: Sample testing conditions as specifies by ARI standard 210 (AHRI 2008)

As seen from the title of the table pulled from the standard, specific classifications exist for each type of unit. The psychrometric chamber plays a key role by ensuring that the air properties entering the coils in each chamber meet the specifications dictated by the standards.

Calculations

The goal behind testing is to determine the performance of the test units. This is done by measuring several variables and using the results to calculate the performance. In an air conditioning unit, the cooling capacity can be estimated by measuring the inlet and outlet temperature of the air passing through the indoor cooling coils, this can be done by utilizing equation 3.1 in conjunction with the airflow.

$$\dot{Q}_{Low} \cong \dot{m}_{air} c_{p,air} (T_{in} - T_{out}) \qquad 3.1$$

where

$\dot{Q}_{Low}$ is the total cooling capacity of the air conditioner

$\dot{m}_{air}$ is the mass flow rate of the air passing through the cooling coils

$c_{p,air}$ is the average heat capacity air

T_{in} and T_{out} are the entering and exiting air temperature passing through the indoor coils

Equation 3.1 gives a good estimate; however, a more accurate approach is to measure the wet and dry bulb temperature of the air flow. The result allows one to break the total capacity into dry and wet cooling, or more properly, sensible and latent cooling. This approach requires the use of a psychrometric chart or other means to obtain the absolute humidity, ω, from the wet and dry bulb temperatures at each location. One could also use enthalpy, h, at each condition to calculate the total capacity. The enthalpy can be estimated from the psychrometric chart using the wet and dry bulb temperatures, or calculated using other means Equations 3.2 through 3.5 show the relation between these capacities.

$$\dot{Q}_{Low} = \dot{m}_{air}\left(h_{in} - h_{out}\right) \quad 3.2$$

$$\dot{Q}_{low,sensible} = \dot{m}_{air} c_{p,air}\left(T_{in} - T_{out}\right) \quad 3.3$$

$$\dot{Q}_{Low,latent} = \dot{m}_{air} i_{fg}\left(\omega_{in} - \omega_{out}\right) \quad 3.4$$

$$\dot{Q}_{Low} = \dot{Q}_{Low,latent} + \dot{Q}_{Low,sensible} \quad 3.5$$

where

h_{in} and h_{out} are the entering and exiting enthalpies of air passing through the indoor coils

i_{fg} is the enthalpy of vaporization of water

ω_{in} and ω_{out} are the entering and exiting humidity ratio of the air passing through the indoor coils

The dimensionless coefficient of performance, or COP, can be determined using Equation 3.6.

$$COP = \frac{\dot{Q}_{Low}}{\dot{W}_{in}} \quad 3.6$$

where $\dot{W}_{in}$ is the electrical power consumed by the test unit

The above equations pertain to the indoor air enthalpy method. As a secondary measurement, or check on the system, the temperatures and air flow of the outdoor stream can be measured. The amount of heat rejected, $\dot{Q}_{High}$, is determined using expressions analogous to Equations 3.1 through 3.5. The relation between the electrical work in, and the heat rejected and absorbed should be as seen in Equation 3.7.

$$\dot{Q}_{High} = \dot{Q}_{Low} + \dot{W}_{in} \quad 3.7$$

For a test to be valid, correlation 3.7 must hold to within 6%(AHRI 2008).

Measuring the wet and dry bulb temperatures is straightforward and calculating the capacity and COP is trivial. The only part of the process described above that may be a little unclear is the measurement of the air flow. This is done using the air flow measuring apparatus, also known as code tester, seen in Figure 3.1.

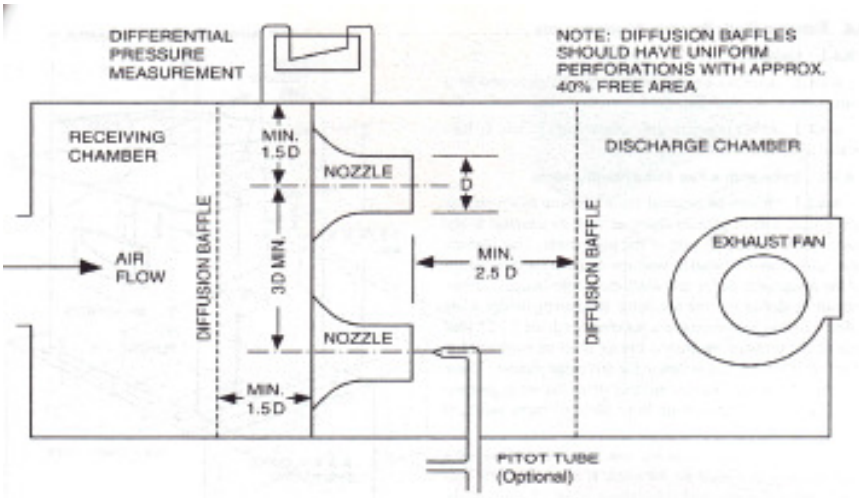

Figure 3.1: Schematic of code tester (ASHRAE 2005)

A code tester operates on the fundamentals of fluid flow. In the psychrometric chamber it consists of a vertical column. Air flow from the unit is ducted to the base of the column using large diameter flexible tubing. A diffusion baffle on either side helps to settle the airflow as passes through a bank of elliptical air flow nozzles. The nozzles are precision manufactured; therefore the differential pressure drop between the inlet and outlet of the nozzles can be used to determine the volumetric flow rate using Equations 3.8 and 3.9 (ASHRAE 1995).

$$\dot{V} = 1096 C A_n \left(p_v v_n'\right)^{0.5} \tag{3.8}$$

$$v_n' = \frac{29.92 v_n}{p_n \left(1 + \omega_n\right)} \tag{3.9}$$

where

$\dot{V}$ is the volumetric flow rate of air through a single nozzle (cfm)

C is the coefficient of discharge for the nozzle (dimensionless)

A_n is the exit area of the nozzle (ft^2)

p_v is the pressure difference across the nozzle (in H_2O)

v_n' is the adjusted specific volume of the air at the nozzle (ft^3/lb)

v_n is the specific volume of the air as measured from wet and dry bulb temperatures assuming standard atmospheric conditions

p_n is the pressure at the nozzle throat (in Hg)

ω_n is the absolute humidity at the nozzle (lbs moisture/lbs dry air)

In order to ensure that the effect of the measurement device on the flow is minimal, a variable speed blower is placed at the exit of the code tester. The blower is adjusted to neutralize the pressure losses through testing apparatus; this is done by equalizing the static pressures at the unit and code tester outlets

Efficiency Measurements

Several methods exist for measuring the efficiency of an air conditioner. Commonly in engineering classes the coefficient of performance is used, or COP, seen in Expression 3.6. As with most measures of efficiency, the basic equation is the desired output over the required input. However, unlike typical efficiencies, the COP can be greater than unity.

COP ratings have no units, so it is typical to do the measurements in kilojoules, kJ, or British thermal units, Btu. These units work well for engineers, but to appeal to the consumer other rating systems have been developed. Some widely used efficiency ratings are the seasonal energy efficiency ratio, SEER and the energy efficiency ratio, EER. The EER is basically the COP multiplied by 3.413; the new units become Btu/(Watt-hour). This rating system utilizes the fact that electrical power is purchased by the kilowatt-hour (kW*hr). The slight adjustment to Watt-hour makes gives the EER a magnitude to the left of the decimal, typical values of 13 rather than 0.013, which is much more palatable to the consumer. The EER is based on specific test points set forth by AHRI, and represent the full load capacity of a unit. The SEER, or seasonal energy efficiency ratio, is based on a range of settings to better gauge the efficiency throughout the usage season because units are not running at full capacity all the time.

The goal in testing units is to give a reliable EER or SEER rating; these are all the consumer sees when selecting a piece of equipment. Having a specific standard for testing ensures the consumer is comparing apples to apples when using the EER as a guide for selecting new air-conditioning equipment. The EER is also used by government to guide the industry to better overall efficiency. Currently, any air conditioner sold in the United States must have a SEER of at least 13; in this way, the industry is being pushed to higher standards, this gives researchers the incentive for innovation. Regardless of the efficiency measurement, the goal is to get more for less; and that is what drives the industry.

CHAPTER IV

STRUCTURAL DESIGN

Because of AAON's pledge, it was essential to design the chamber in such a way that the majority of parts could be manufactured in-house. Thus the structural design of the chamber commenced in May 2007 by two OSU graduate students: Sam Hobson and Spencer Lifferth. Stephen Wakefield, of AAON, managed the design; Patrick Chapman contributed greatly to helping turn ideas into valid designs.

Structural Design Specifications

As mentioned in chapter two, several parameters pre-determined the design of the chamber. The overall dimension of the chamber was to be "as big as possible" with all necessary equipment enclosed in the portion of the ATRC Basement that was allotted. The envelope is approximately 53' long, 25' wide, and 20' tall, as seen in Figure 2.1. The walls, floor, and ceiling were to be made of foam panels similar to the ones used on AAON's air conditioning units. The chamber is to contain two separate rooms, one to simulate indoor conditions, the other to produce outdoor conditions. The chamber should be self standing. Conditioned air is to be delivered via an underfoot air supply plenum with return air extracted in an overhead ceiling plenum. Means for moving units of up

to 15 ton capacity into and out of the chamber should be provided. Entry to the chamber is limited to the North and West walls; the east side of the chamber should not require any access; the south side is bordered by a wall.

Chamber Walls

The majority of the chamber is made up of foam panels. Similar panels have been used at AAON to build some of their units. Previously, AAON worked with 1, 2, and 3" thick panels; however, the chamber panels are 4" thick. The rigid, foam filled panels provide structural support and insulation to the chamber. Rectangular panels of varying sizes make up the walls, floor, doors, and roof to completely surround the chamber test area in a rigid, insulated enclosure.

The panels are made up of a sheet metal shell filled with polyurethane foam. The shell is made out of two pieces of galvanized sheet metal; depending on the panel, the sheet metal thickness of a side may range from 24 to 14 gauges (0.0276 to 0.071 inches). The thicknesses of either side of a panel are not necessarily equal. The edges of each of the sheet metal sides are bent into a "C" shape, and the sides are secured together with a piece of double sided neoprene tape. The Tape serves the purpose of temporarily aligning the side as well as providing a thermal break across the panel for insulation purposes. After securing the sides together, the panel is filled with foam. The foam expands to fill the panel (density of 2 lbs/ft^3) and adheres to the sheet metal. The resulting panel, even with very light gauge sheet metal, is surprisingly rigid and durable. Figure 4.1 demonstrates construction process of each of the foam panels.

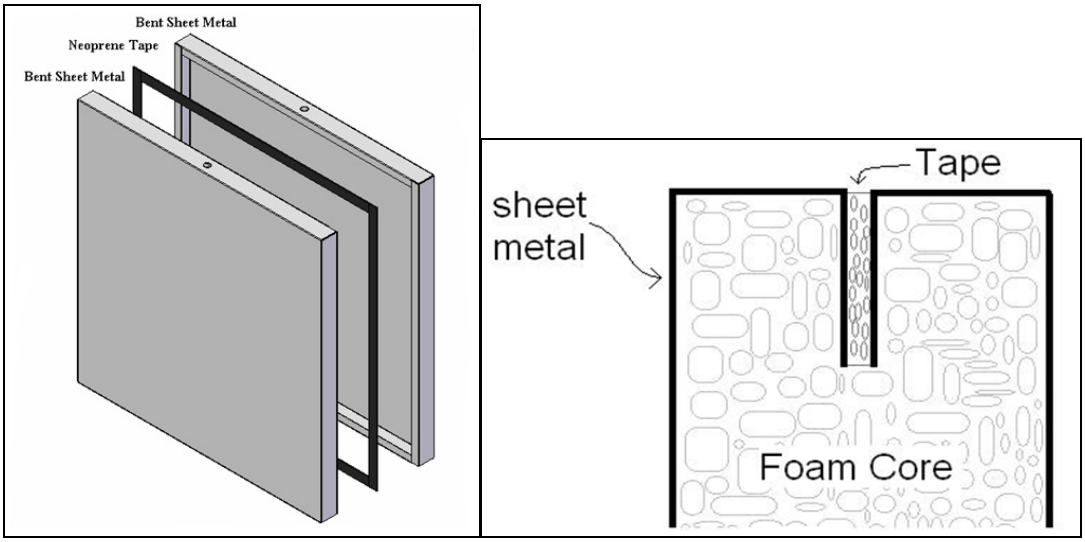

Figure 4.1: Construction of foam panels

The chamber structure is made of several panels joined together. Panels are joined together using splices and neoprene. The edges of the panel are lined with neoprene, and joining panels are pressed together to compact the neoprene. Panels are fastened together using splices which are also lined with neoprene. The neoprene serves to create an air tight seal and a thermal break. Splices consist of 12 gage sheet metal with holes punched about every six inches. The neoprene between panels is ¼" thick before compression and approximately 1/8" thick after compression. Neoprene used to line the splices is 1/8" thick before compression and 1/16" thick after compression. Figure 4.2 demonstrates the assembly of two panels.

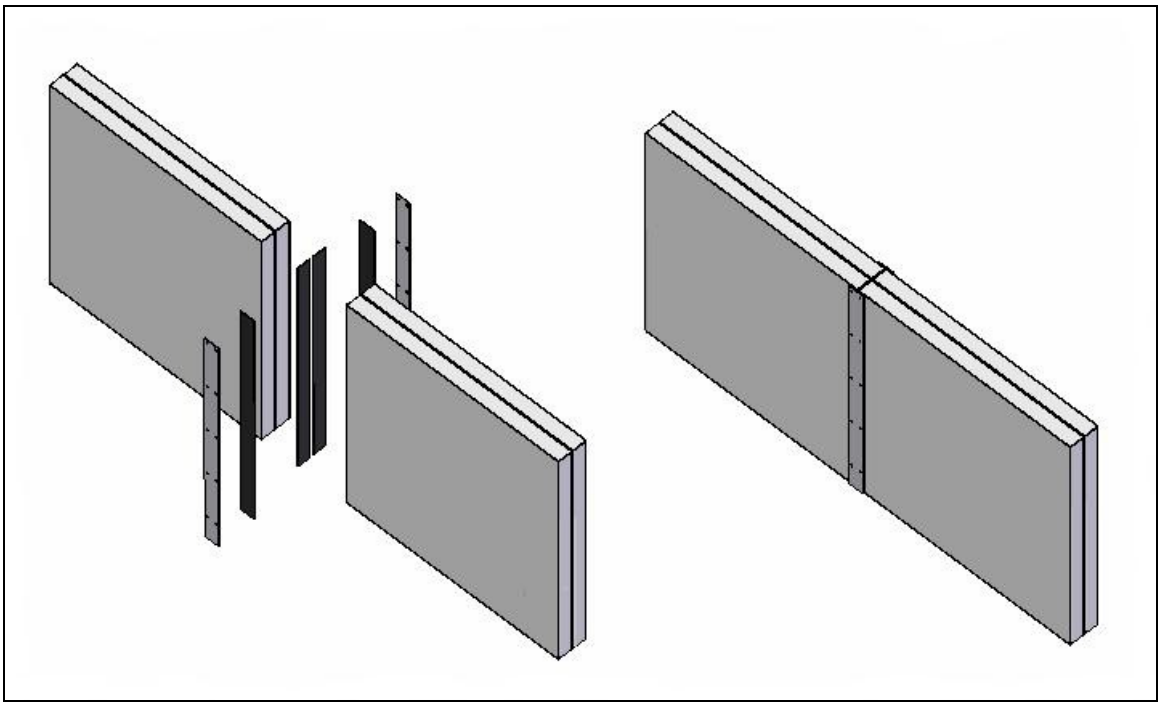

Figure 4.2: Process of joining two panels

The entire chamber enclosure is assembled in this manner. Appendix A contains some drawing of individual chamber parts; Figure 4.4 shows an electronic rendering of the complete chamber design. The chamber consists of two levels of panels. With the exceptions of the doors, the upper row of panels is the same as the lower row of panels. Each of the wall panels stands 9 feet high. A splice connects the upper and lower rows of panels in the same manner that it connects panels side by side. The corners of the chamber are assembled in much the same way as the straight runs of panels, the only difference is that the splices for the corners are bent to wrap around the outside of the panel ad meet on the inside as seen in Figure 4.3.

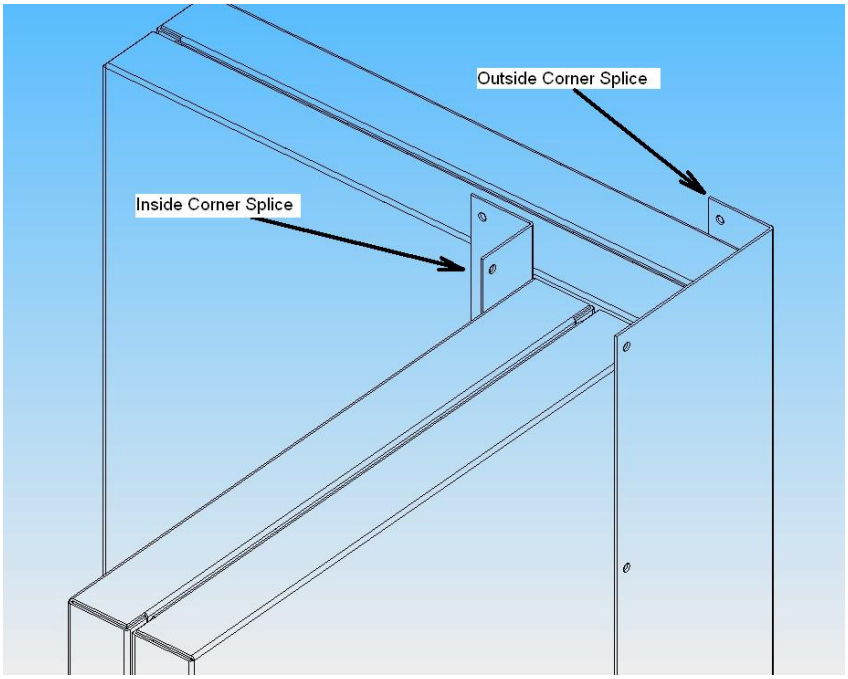

Figure 4.3: Inside and outside corner splices

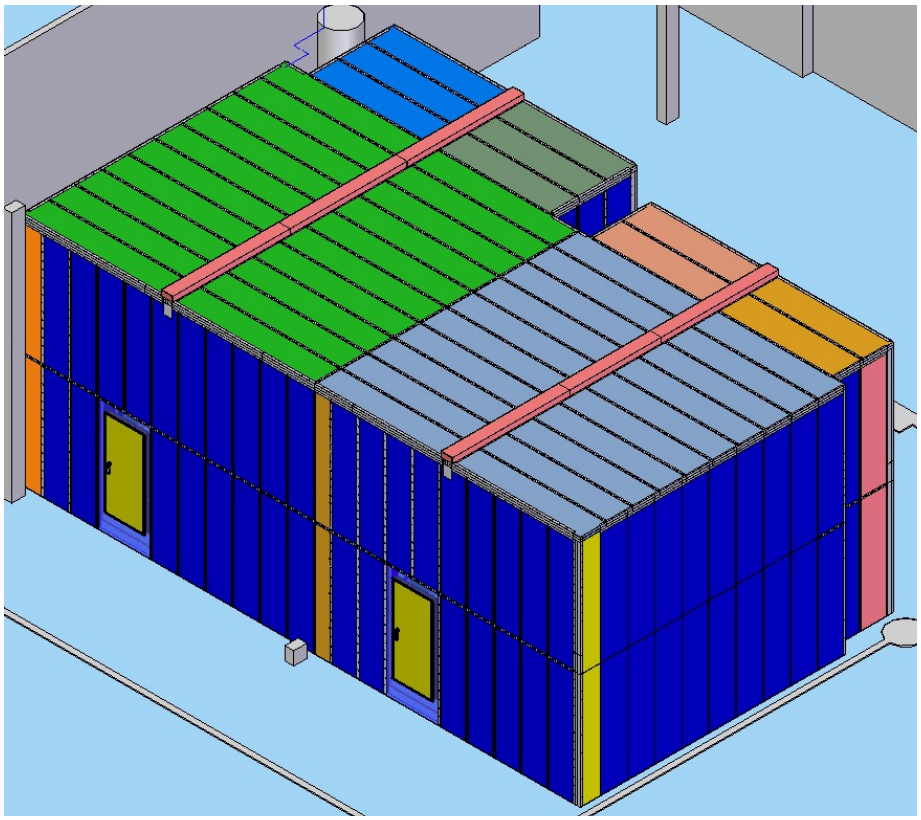

Figure 4.4: Rendering of chamber as it sits inside the ATRC basement

The panels are certainly a very important part of the chamber; however much of the design effort went into other parts of the chamber. The parts include the doors, plenums, and the cooling and testing equipment mounting pieces.

Doors

There are four doors in the chamber. Each of the two rooms has a personnel entry door that is 34" x 77". Additionally, the North wall of the chamber houses the primary door for moving in equipment. Its dimension is 104" x 100". An identically sized door separates the two rooms; this door is the means of getting equipment into the indoor chamber.

It is essential for the conditioning of the chamber to have doors that seal well. The doors should seal tightly to prevent air infiltration into the chamber. They also should not compromise thermal conductivity with respect to the rest of the chamber. The final door designs have fulfilled both of these requirements.

Personnel access doors are a modified version of a panel door that AAON uses on some of their product lines. Dimensions of the door were changed – not only the opening size, but the thickness of the door was increased to 4", thus matching the thickness of the rest of the panel walls. Construction of the door panel is similar to other panels; however it consists of many more pieces.

The door panel consists of two assembled panels. The first panel provides a door opening; this panel is relatively large – twice as wide as a typical wall panel – and has a cut out in it. A jamb is riveted inside the cutout. After assembling the panel pieces, the

panel cavity is injected with foam. The door is made of two pieces. It is designed in order to mate smoothly with the jamb, the whole mating section is made of piece of metal, and this forces the thermal break to the panel edge instead of center. The door, seen in Figure 4.5, is connected to the doorway using a piano hinge. A purchased latch system provides compression on bulb seals that line the door jamb.

Figure 4.5: Personnel access doors on the west wall

The equipment doors operate on a much different concept than the personnel doors. They are custom designed for the psychrometric chamber. The main entrance door is situated in the north wall on the west side of the wall. The door consists of two main panels that stack on top of each other. The upper door panel mates with the lower panel using a tongue and groove interface, seen in Figure 4.6. The interface was glued together. To increase rigidity to the door, each end of the door has a splice attached. In addition to providing rigidity, it also protects the thin metal of the door and ensures the tongue and groove interface remains tight.

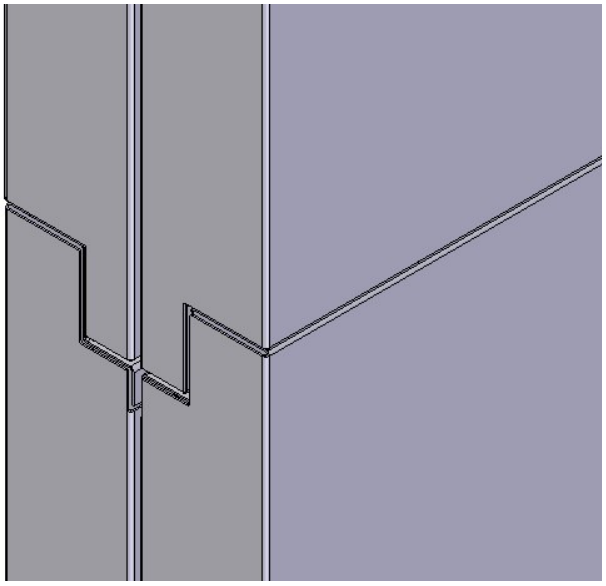

Figure 4.6: Tongue and groove of sliding door assembly

The bottom of the door is fastened with wheels, seen in Figure 4.7. The wheel track was integrated into the assembly before the foaming process. Recessing the wheels into the panel provides a very low profile door, minimizing the area necessary to seal. A recessed handle is also integrated into the door side to allow easy opening; it also allows the door to open further than it otherwise would be able. Because the recessed handles will not be accessible when the door is completely ajar, an additional handle is located on the end of the door to allow for easy closing. Bent pieces of metal secured to the top of the door keep the door from tipping side to side

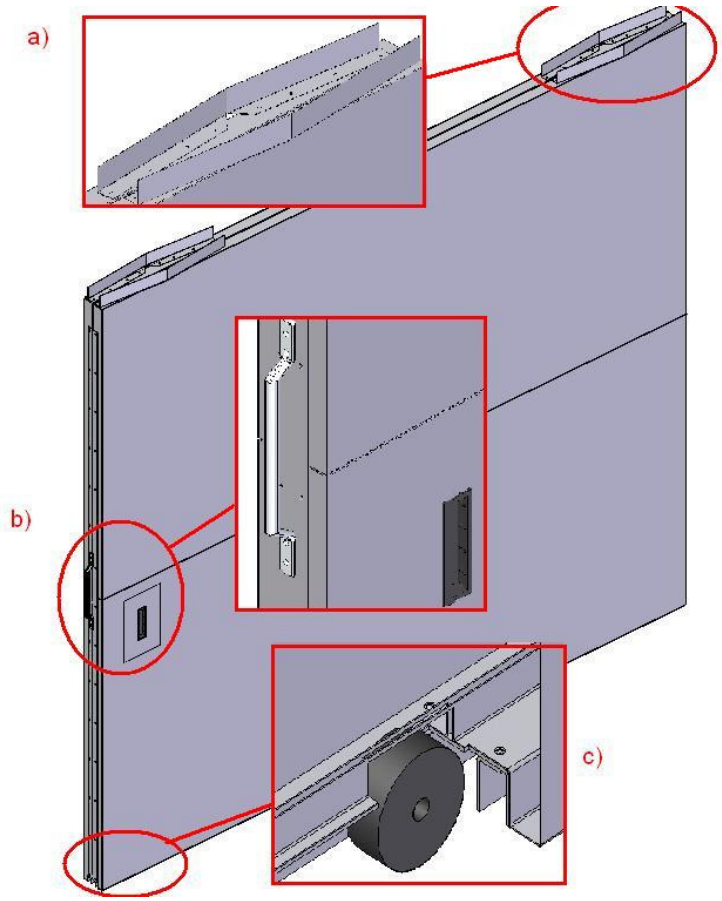

Figure 4.7: Main door detail. a) balancing pieces b) handles c) cut-away showing wheels

The door opening complements the door design. The North wall is built with 4" thick panels. Unlike the rest of the chamber, however, the lower panels surrounding the door do not mirror the upper panels. The top of the door opening is higher than the other panels and therefore is not able to be symmetrical. Additional differences can be seen with the lintel, seen in Figure 4.8, which holds up several panels above the doorway entrance.

Figure 4.8: Main equipment entrance door – lintel seen at top of the doorway (north wall)

A pocket is built around the doorway into which the door rolls, see Figure 4.9. The base of the doorway is constructed from heavy gage steel panels that are also foam filled. The wheels of the door roll on one of these panels. The track panel is 1" wide and is recessed slightly with respect to the rest of the door's threshold to guide the wheels. The pocket of the door is constructed of 2" thick panels. The cavity that is created by the pocket is 5" wide. The door rests in the middle and is balanced by the guides previously mentioned. Also built into the cavity are rubber door stops to dampen the door as it opens and closes.

Figure 4.9: Door pocket – without door and with door inside

The door separating the two chambers is built similarly to the main entry door; however, a few differences exist. The door between the rooms is centered between the east and west walls, as seen in Figure 4.10, rather than being located on one side, which is the case of the main access door. This allows for the door to consist of two doors that roll to meet each other in the middle. This will allow for ducting between the two rooms if needed. Using two separate doors allowed the use of a single panel per door. Except for the positioning of the handles, which are not recessed, these doors are of the same design as the main entry doors. They roll on low profile wheels into a pocket created by 2" panels spaced from the regular wall panels.

Figure 4.10: Center door – looking from the indoor chamber through the intermediate wall into the outdoor chamber

The personnel doors are sealed using a bulb seal which compresses when the door is closed. The equipment access door utilizes wiper seals to prevent air from flowing around the pocket into the chamber; both types of seals can be seen in Figure 4.11.

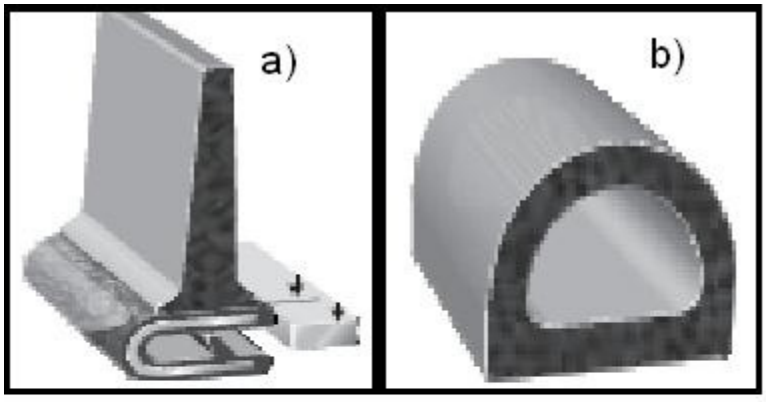

Figure 4.11: neoprene seals a) flexible wiper type seal: used for rolling personnel doors b) bulb type seal: used on all hinged doors

Floor

A main distinction of the Oklahoma State University psychrometric chamber is the underfoot air supply plenum. The plenum structure presented a challenging task. It was previously determined that the plenum, and supporting floor, should be able to support a 2400 lb point load. This was to be done using no larger than 14 gage sheet metal – the heaviest sheet metal that AAON can manufacture using their automated machinery. The floor structure consists of several parts; the final design is outlined below.

Foundation

The basement floor of the Advanced Technology Research Center is bare concrete. Several drains and other abnormalities are located throughout the space where the chamber rests. Because of the many drains, the floor beneath the chamber is far from level. Random measurements of the area revealed a difference of 2 ½" between the highest and lowest points in the concrete. The panels and the chamber would inevitably show instability if the bare floor was used as a foundation; therefore a better foundation was developed.

The solution to the varying floor height was to create a steel grid strategically placed under the seams of the chamber walls and floor panels. Flat steel stock of 3/8" thick was used as a base. As seen in Figure 4.12, holes, drilled and tapped, were placed not less than 36" apart from each other. Through each hole was threaded a bolt which

pivoted on the floor and elevated the height of the base plate to the desired level. Nearly 200 screws were adjusted to set the height of the base plate. A laser level was used to check the height; the resulting plane is within 1/8" of level.

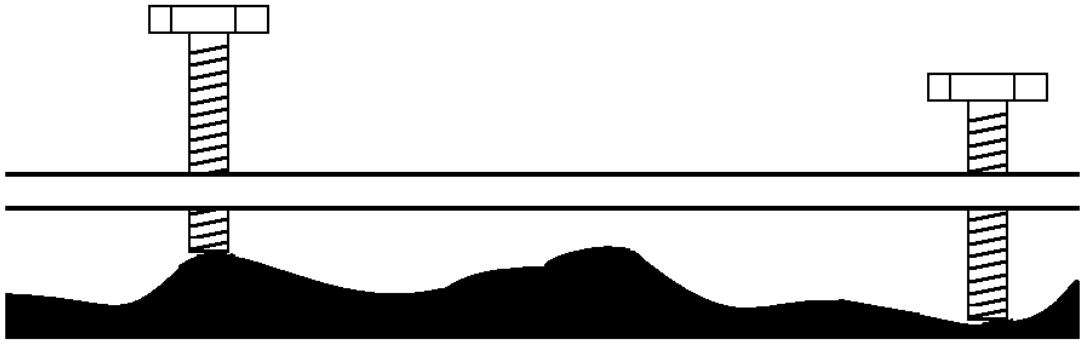

Figure 4.12: Method of leveling base plates over uneven concrete surface using bolts

After being leveled, grout was packed under the base plates to strengthen them and reduce sagging. The heads of the bolts were cut off and the plate surface ground smooth in preparation for building, see Figure 4.13.

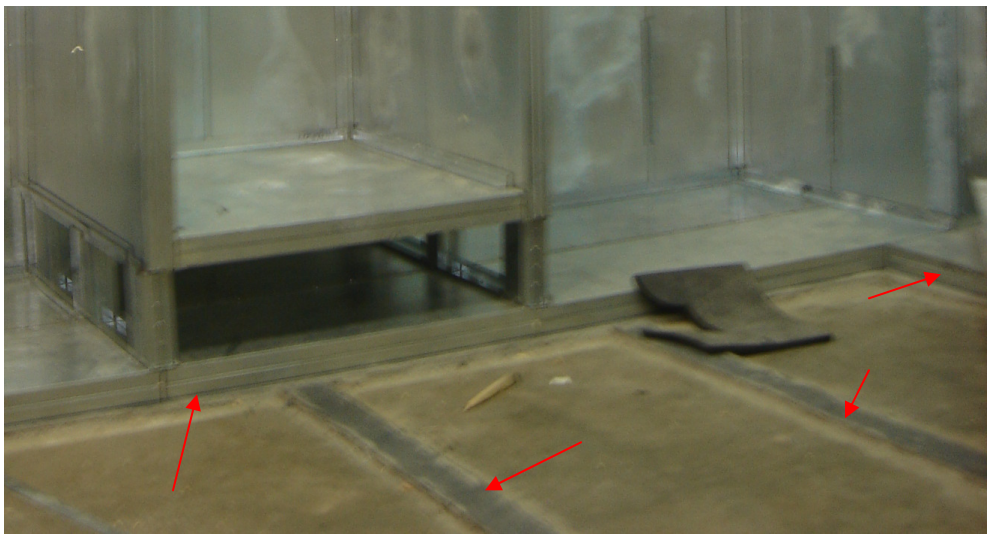

Figure 4.13: Chamber construction on top of base plates; base plates provided level surface for chamber construction

Insulation

Like the rest of the structure, the floor is designed with 4" thick insulation panels. The seams of the panels rest on centers of the base plate foundation. Campus physical plant requested that the four sanitary cleanout access points located under the chamber be readily accessible. After compromising from both sides, the decision was made to create a few panels that would have pre-punched, or perforated access points. The panels will only need to be penetrated if the cleanout point is ever used; however, the panel would have no difference in performance until that point in time.

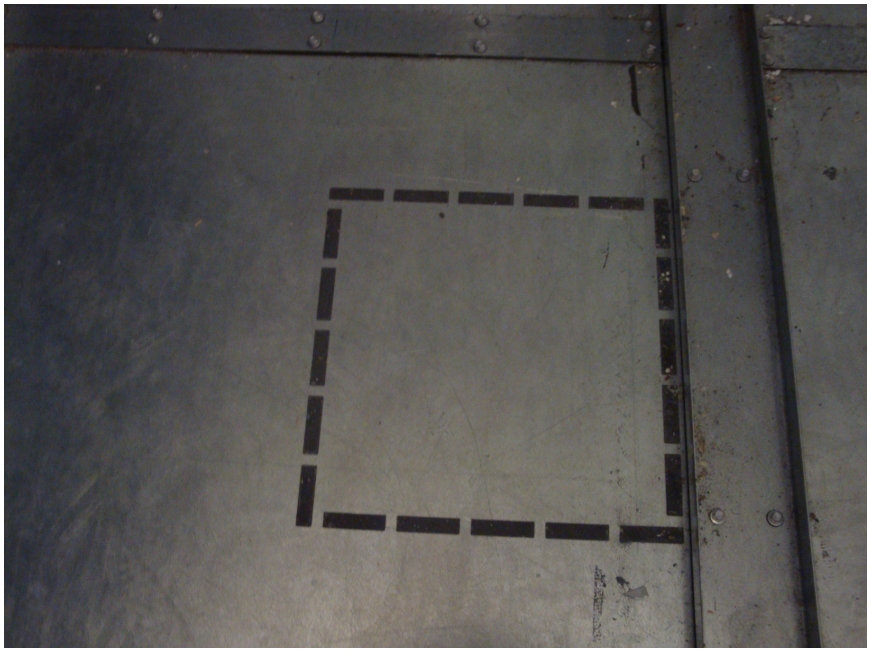

Figure 4.14: Picture of floor panel with precut access to sanitary cleanout

The perforated panels, seen in Figure 4.14, allow plumbers the access they need with minimal work required to get to the cleanouts. The panels also mark the location of the cleanout, thus ensuring that little additional disruption of tests need be done to fix a

potential problem. All of the cleanouts are located in the indoor room. Cutout points were not made for drains and other items in the floor.

Plenum Structure

The plenum structure consists of two main parts; the floor grating and the supporting structure. The supporting structure is secured at the base with a "U" channel that is fastened over the seams of the floor paneling; thus securing the paneling together and transferring the weight through the most rigid part of the floor panels down to the base plate. Sheet metal posts are secured inside the "U" channel. On top of the posts rests a saddle structure on which the floor grating rests; the plenum structure can be seen in Figure 4.15.

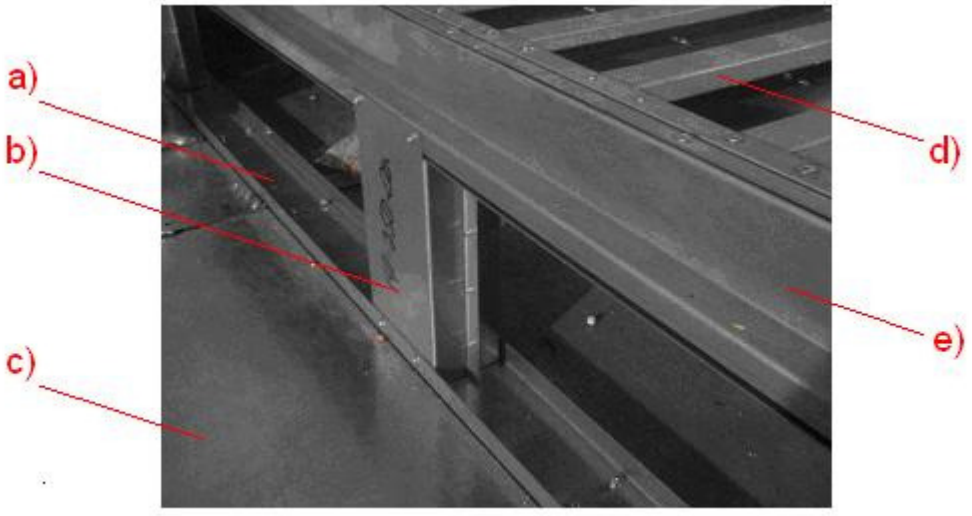

Figure 4.15: Floor plenum assembly: a) u-channel b) plenum post c) floor insulation d) grating e) saddle rail

An important consideration in the design of the saddle rail was to ensure that the automated bending machines at AAON could manufacture it. While these machines are

versatile in their overall ability to manufacture complex parts, they also subject to some very specific constraints concerning the length, height, depth, and number of bends that can be performed on a single piece of steel. These limitations have to do with the tooling on the machines. These constraints led to the two-piece saddle rail design seen in Figure 4.16.

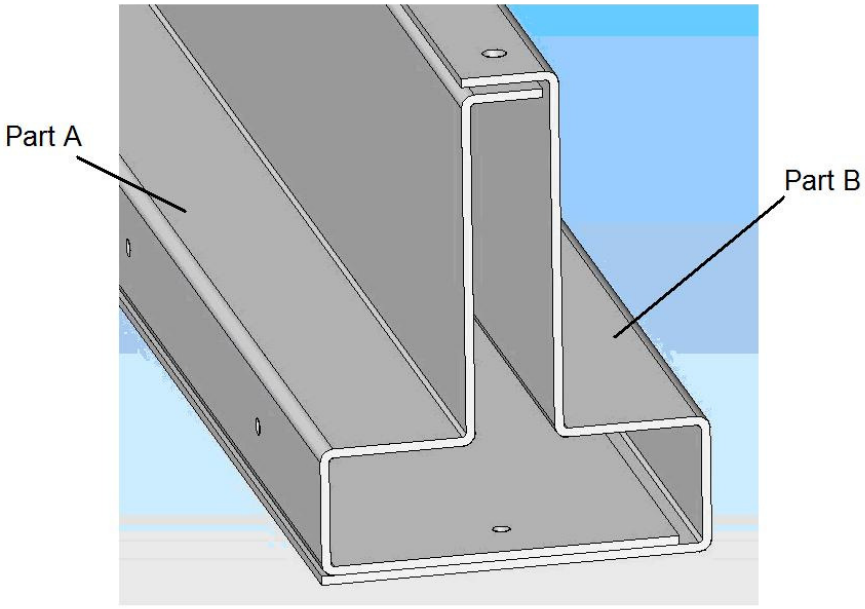

Figure 4.16: Cross section of saddle rail, the supporting component of floor grating sections showing parts A and B of the saddle rail assembly

Equations 4.1 and 4.2 (Shigley and Mischke 2002) were used to determine the validity of the structural design. The former equation demonstrates the deflection of a beam that is simply supported, while the latter demonstrates the deflection of a beam that is cantilevered on each end. The sections of beams between each post are a mixture between these two scenarios. Table 4.1 demonstrates the effect that the post spacing has on the beam deflection.

$$y_{\max} = \frac{Fl^3}{48EI} \qquad 4.1$$

$$y_{\max} = \frac{Fl^3}{192EI} \qquad 4.2$$

where

F is Force (lbs)

l is length (in)

E is the modulus of Elasticity, a material property; 28,000 psi was used for the galvanized sheet metal that comprises the chamber

I is the bending moment of inertia, a geometric property that is computed using the cross-sectional area of the member (in^4)

	y_{max} (in) Cantelivered			y_{max} (in) Simply Supported			y_{max} (in) Average		
L (in)	Part A	Part B	Combined	Part A	Part B	Combined	Part A	Part B	Combined
20	0.004	0.003	0.002	0.016	0.013	0.007	0.010	0.008	0.005
35	**0.022**	**0.017**	**0.010**	**0.086**	**0.070**	**0.039**	**0.054**	**0.044**	**0.024**
40	0.032	0.026	0.014	0.129	0.104	0.058	0.081	0.065	0.036
60	0.109	0.088	0.049	0.435	0.352	0.195	0.272	0.220	0.122
80	0.258	0.209	0.115	1.031	0.835	0.461	0.644	0.522	0.288

Table 4.1: Deflection of part A and part B of the saddle rail acting separately and combined as one. The bending moment of inertia, I, is 0.887, 1.095, and 1.982 in^4 for part A, part B, and their combined total respectively; the demonstrated load is 2400 lbs.

The table demonstrates what we intuitively know; larger spacing of posts results in the greater deflection of the beam. Spacing of 35" is selected. This allows 7 posts to be roughly evenly spaced across the East-West axis of the room. In the worst of case, if part B acts alone as a simply supported beam, assuming no twisting, the deflection is only 0.070", which would be undetectable when rolling equipment around inside the chamber.

Intuitively, we would assume that a beam subject to such little deflection would have no danger of failure; a quick check confirms this assumption. Equations 4.3 and 4.4

are used to demonstrate this. Again, the first demonstrates the stresses in a simply supported beam and the latter in a cantilevered beam.

$$M_{\max} = \frac{Fl}{4} \tag{4.3}$$

$$M_{\max} = \frac{Fl}{8} \tag{4.4}$$

Where F and l are force (lbs) and length (in) respectively and M_{max} is the maximum bending moment (lb-in) in the beam

The neutral axis runs through the centroid of the cross section of the beam, the maximum stress is determined using Equations 4.5 and 4.6. Table 4.2 demonstrates the maximum compression and tension stress that act on the saddle rail components.

$$\sigma_{c,\max} = -\frac{M_{\max} c_1}{I} \tag{4.5}$$

$$\sigma_{t,\max} = \frac{M_{\max} c_2}{I} \tag{4.6}$$

Where

$\sigma_{c,max}$ and $\sigma_{t,max}$ are the maximum compressive and tensile forces (psi) in the beam

M_{max} is the maximum bending moment (psi)

c_1 and c_2 are the distances (in) from the neutral axis to the top and bottom of the beam respectively

I is the bending moment of inertia (in^4)

	Cantelivered			Simply Supported			Average		
	Part A	Part B	Combine	Part A	Part B	Combine	Part A	Part B	Combined
Mmax (lb-in)	10500	10500	10500	21000	21000	21000	15750	15750	15750
σ_t (psi)	14773	12773	7057	29547	25545	14113	22160	19159	10585
σ_c (psi)	-29085	-24673	-13631	-58170	-49345	-27262	-43628	-37009	-20446

Table 4.2: Maximum stresses in saddle rail parts. Note that failure occurs at about 30,000 psi in steel, when combined, the rails are not in danger of failure

The grating rests on top of the saddle rails. Again, the design, seen in Figure 4.17, was constrained to the manufacturing capabilities at AAON. The grating is made of three parts, all of which are replicated at least once in the assembly. The assembly consists of two end caps, which rest on the saddle rails; between the end caps span the main support rails, each section of grating has 10 support rails that are spaced roughly 5" apart on center. Stabilizers run across the bottom of the grates to tie the main load bearing members together. The design results in 885.9 in^2 open area for every 2286 in^2 of grate, or 38.7% open area.

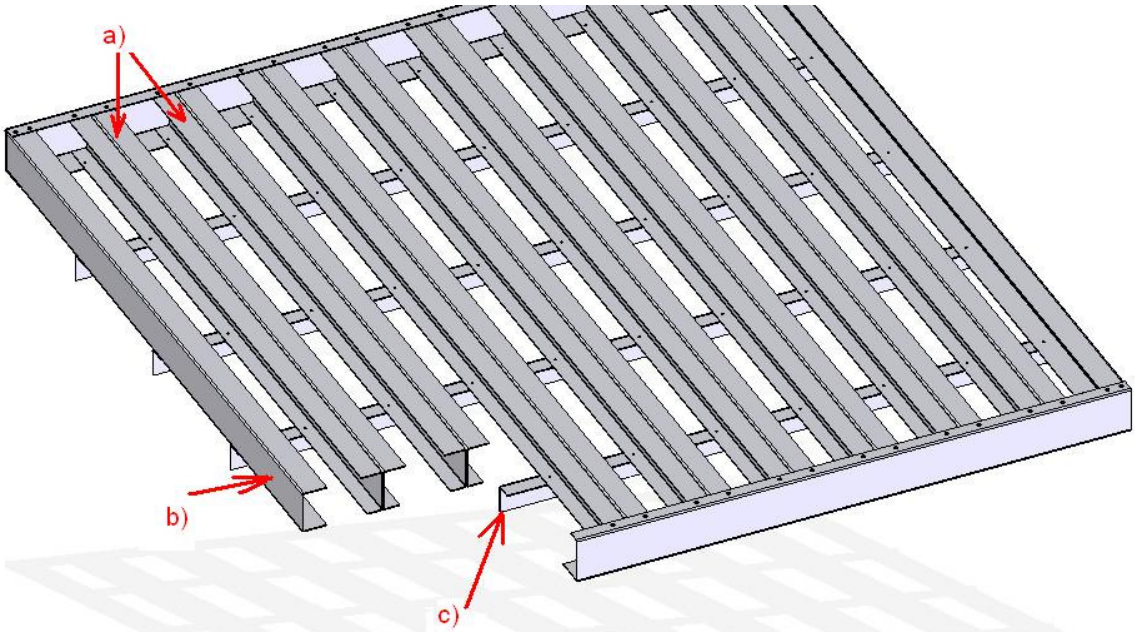

Figure 4.17: Grating with cutout view; a) main supporting rails b) side support rail c) stabilizer

A two dimensional finite analysis would have to be used in order to get the full picture of the deflection and maximum stresses of the grate system, however, each component is analyzed separately using Equations 4.1 and 4.2; results appear in Table 4.3. It can be seen that under the maximum expected load, even when the pieces are functioning alone, the deflection is still within an acceptable value.

		Cantelivered				Simply Supported				Average			
Object	I (in^4)	y_{max} (in)	M_{max} (lb-in)	σ_t (ksi)	σ_c (ksi)	y_{max} (in)	M_{max} (lb-in)	σ_t (ksi)	σ_c (ksi)	y_{max} (in)	M_{max} (lb-in)	σ_t (ksi)	σ_c (ksi)
Side support rail	0.426	0.127	14871	45.82	-45.82	0.511	29742	91.63	-91.63	0.319	22306.5	68.73	-68.73
main supporting rail (one section)	0.351	0.154	14871	59.82	-51.39	0.620	29742	119.65	-102.78	0.387	22306.5	89.73	-77.09
main supporting rail (combined)	0.702	0.077	14871	29.91	-25.70	0.310	29742	59.82	-51.39	0.193	22306.5	44.87	-38.54
grate stabilizer	0.061	0.718	13837.5	263.37	-133.61	2.873	27675	526.73	-267.22	1.795	20756.25	395.05	-200.42

Table 4.3: Deflections and stresses in each of the rail members acting independently from one another under a centrally located 2400 lb point load

Floor Surface

Solid sheet metal is used around the perimeter of each room to cover the gaps between the grating rails. The center portion of the room will use a perforated sheet metal, which will serve as a diffuser for the conditioning air. As seen in Figure 4.18, fine perforated steel is used near the conditioning loop where the pressure of the airflow is high. Courser perforated steel is used farther back in the chamber. The difference in open area should allow the airflow to be more evenly distributed across the entire chamber. Currently, the chamber is broken into three distinct sections: 23%, 40% and 58% open area for the perforated steel. After the grating is taken into account, the open area of the floor translates to 8.9%, 15.5%, and 22.4%.

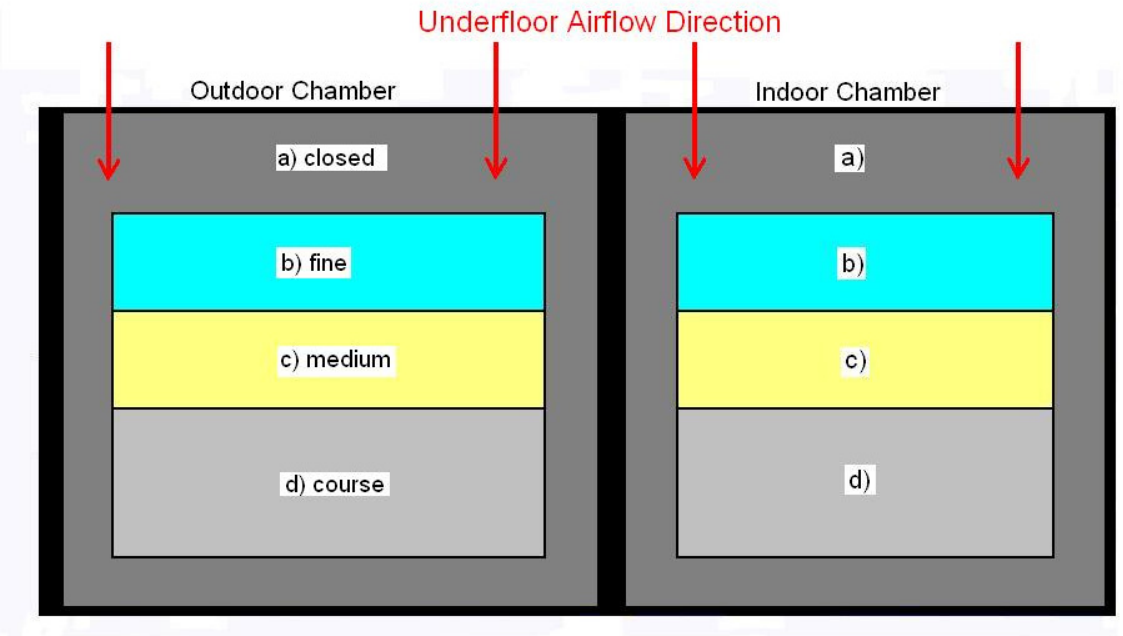

Figure 4.18: Distribution of perforated flooring. a) closed sheet metal; remaining flooring is perforated sheet metal with the open area of b) 23% c) 40% d) 58%

Plenum Ceiling

As is the case with the floor, the plenum ceiling, consists of several parts. Consistent with the rest of the chamber, 4" thick insulated panels comprise the roof. Similar to the wall panels, the ceiling panels are secured together using splices. A center beam supports the panels, and a plenum hangs from the roof panels. Each part will be described below.

Ceiling Beams

The ceiling beams are made of ten gauge sheet metal, and are the only parts of the chamber made using the manual, rather than automatic, press brake at AAON. Each chamber has a beam extending between the East and West walls. The indoor and outdoor

ceiling beams are 295” and 318” respectively; due to the length limit on the press brake, the beams were made in sections, and welded together on-site. Two identical sections of beam are welded back-to-back for the complete beam design, shown in Figure 4.19. The tops and bottoms of the beams are capped and insulted to reduce thermal conductivity between the plenum space and the ambient air.

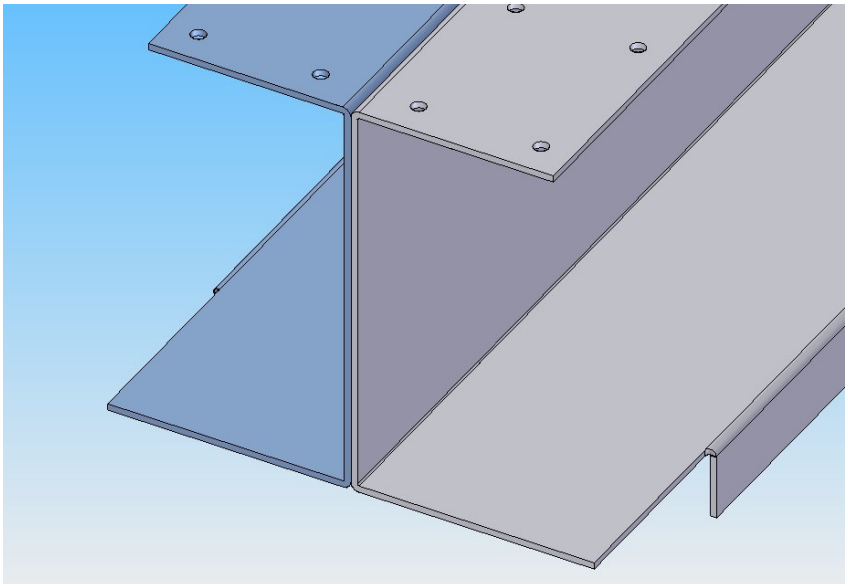

Figure 4.19: Ceiling beam cross section

The primary stresses on the beams are due to the roof panels; the deflection of a cantilevered beam with uniform load is determined using Equation 4.7, and the maximum bending moment is represented as Equation 4.8 for the ends of the beam, and Equation 4.9 for maximum in the middle of the beam. The ceiling beam is modeled as a cantilevered beam because of the supporting posts used to secure the ends of the beam. Because interstitial space between the roof of the chamber and the ceiling of the ATRC exists, it is likely that the ceiling beam will experience more loading than just the roof panels. To account for addition loading in the center of the beam, Equations 4.7 and 4.8

can be combined with previously mentioned cantilevered expressions to get a total resulting deflection and bending moment. As before, Equation 4.5 and 4.6 will show the resulting stresses in the beam. Table 4.4 shows the total deflection of the beam and the resulting stresses occurring. The total roof weighs about 7,000 lbs, distributed evenly between the two rooms. The maximum load that the outdoor ceiling beam should endure in addition to the panels is 3,300 lbs; this corresponds to a maximum stress in the beam of about 15 ksi; the indoor can theoretically handle more because it is shorter. The very simple analysis of a single ceiling panel indicates that, acting alone, it can support approximately 100 lbs before it is subject to the same stress.

$$y_{\max} = \frac{wl^4}{384EI} \tag{4.7}$$

$$M_{end} = \frac{wl^2}{12} \tag{4.8}$$

$$M_{center} = \frac{wl^2}{24} \tag{4.9}$$

		Design Conditions				σ_{max} = (15 ksi)	
Object	I (in^4)	y_{max} (in)	M_{max} (lb-in)	σ_t (ksi)	σ_c (ksi)	new load (lbs)	y_{max} (in)
Ceiling beam (one side)	29.69	2.154	47700	7.93	-7.55	1100	2.376
ceilig panel (one side)	0.306	0.094	2062.5	1.64	-11.42	27	0.189
Ceiling beam (combined)	59.38	1.077	47700	3.96	-3.78	3300	1.410
Ceiling panel (combined)	0.612	0.047	2062.5	6.74	-6.74	102	0.225

Table 4.4: Analysis of ceiling beam and panels

Supporting Columns

For safety and rigidity, the ceiling beams are supported by columns erected next to the structure. The supporting columns, made out of 4" square steel tube, are anchored to the floor and ceiling of the ATRC, as seen in Figure 4.20.

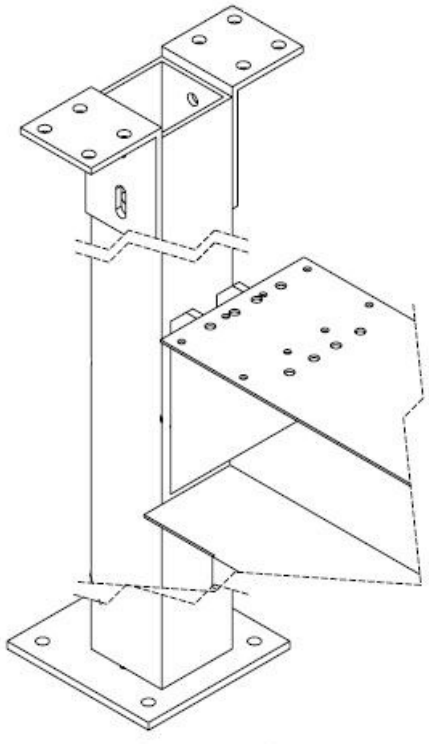

Figure 4.20: Ceiling beam – post interface

Roof Panels

The roof panels are supported by the ceiling beam and the walls. Corner splices, as described previously, are used at the junction of the roof and walls; panel to panel junctions are also done in the same manner as the walls. As previously stated, it is likely

that the roof will be subject to loads that are not part of the chamber structure. The strength and probable deflection of the ceiling panels can be determined from Equations 4.6 and 4.6; results are shown in Table 4.4. The equations assume that panels remain rigid under deflection, an assumption warranted by the stiffness of the panels after foam injection.

Plenum Structure

The ceiling plenum hangs from the roof panels, and is made out of very lightweight steel. It consists of several parts, as seen in Figure 4.21; the first being hangers which are fastened to the roof to support the plenum, or false ceiling. The hangers support a sleeve into which the plenum blanks and filters are inserted.

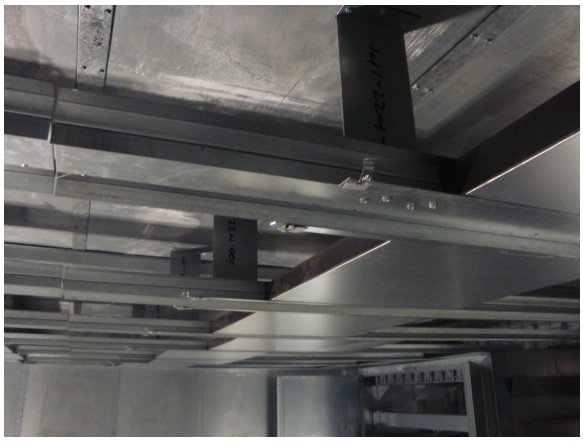

Figure 4.21: Left: Filter sleeves and ceiling plenum assembly

The bulk of the false ceiling consists of blanks and filters, these are use to create the plenum space. Fourteen filters provide means for the air to enter the plenum space. The filters act as a diffuser and pressure differential as well as to help ensure the conditioning equipment remains clean and dust free. The blanks, made out of very thin

sheet metal have the same shape as the filters and provide the plenum space for air to return to the conditioning loops. The filters and blanks can be arranged in any configuration in case the air flow inside the chamber needs to be adjusted. Both filters and blanks are inserted into the sleeve using the cutaway slot and filter clips as seen in Figure 4.22.

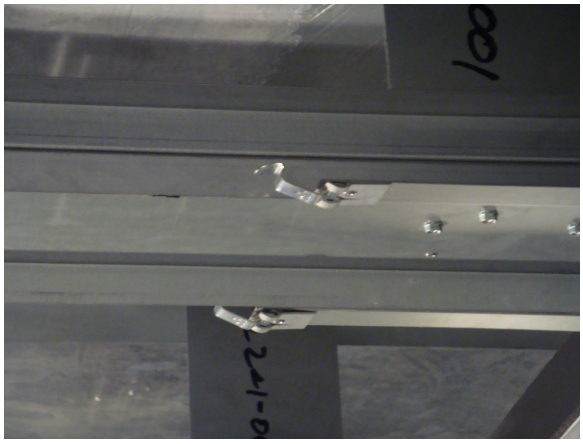

Figure 4.22: Filter sleeve entrance and retaining clips

Conditioning Loops and Code Tester

The limited space required unique planning for the conditioning and code tester loops. These loops are located on the East side of the chamber and are separated from the chamber, as seen in Figure 4.23, using a wall consisting of panels and doors 2" thick.

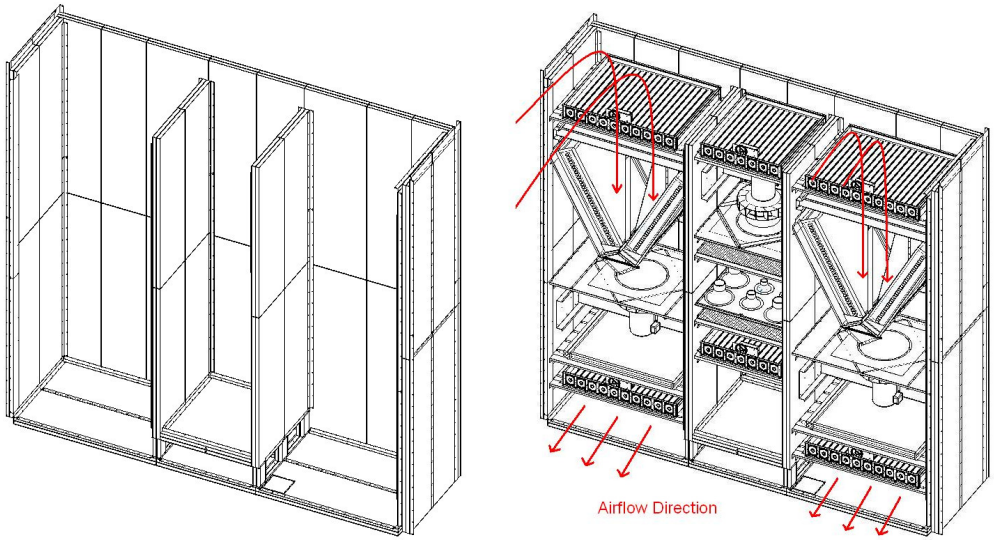

Figure 4.23: Conditioning loop and code tester. Left: without equipment. Right: with equipment. Center column is code tester, side columns are conditioning loops.

Behind the wall are three sections separated by 4" thick partitions. The partitions extend between the floor and ceiling plenums. The center section is capped at the bottom, but left open on to the ceiling plenum on top and serves as the code tester. Each side section functions as a conditioning loop.

The code tester, described in chapter three, consists of several levels of equipment necessary for testing the air flow from a unit. The majority of the code tester equipment is mounted using a triangular bracket, seen in Figure 4.24.

Figure 4.24: Triangular mounting bracket secured in code tester

The conditioning loops have equipment mounting brackets of several shapes and sizes. They support coils, dampers, blowers and electric heaters, all of which are necessary to condition the chamber. Each component is discussed more in chapter six; however, pictures of the different bracketing styles are shown in figure 4.25.

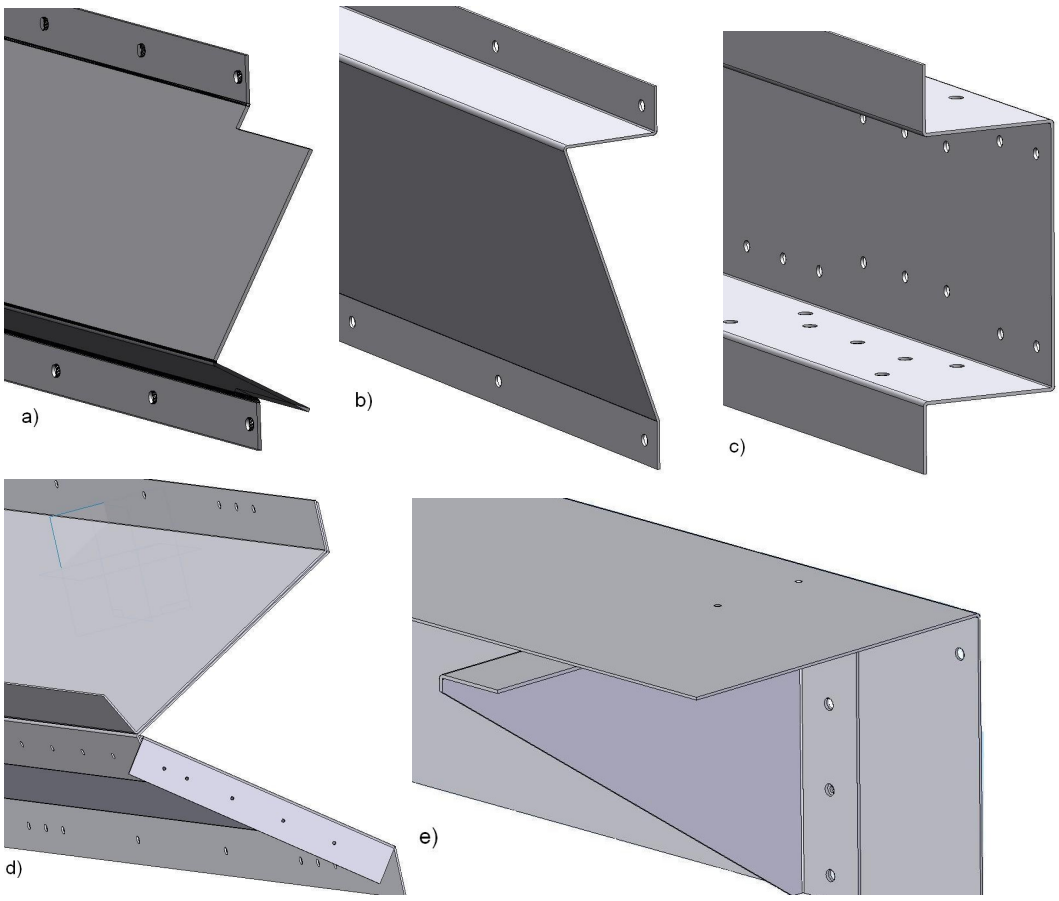

Figure 4.25: Various types of brackets used in mounting conditioning equipment: a) top coil mount b) blower nozzle plat mount c) front coil hanger mount d) bottom coil mount e) damper and heating coil mount

A 20 hp blower is located near the top of the code tester and near the bottom of the conditioning loop. As seen in Figure 4.26, the motor mount designed allows the motor to be suspended in the center of each of the loops. The motor mounts are secured to each wall and to the back of the conditioning loop.

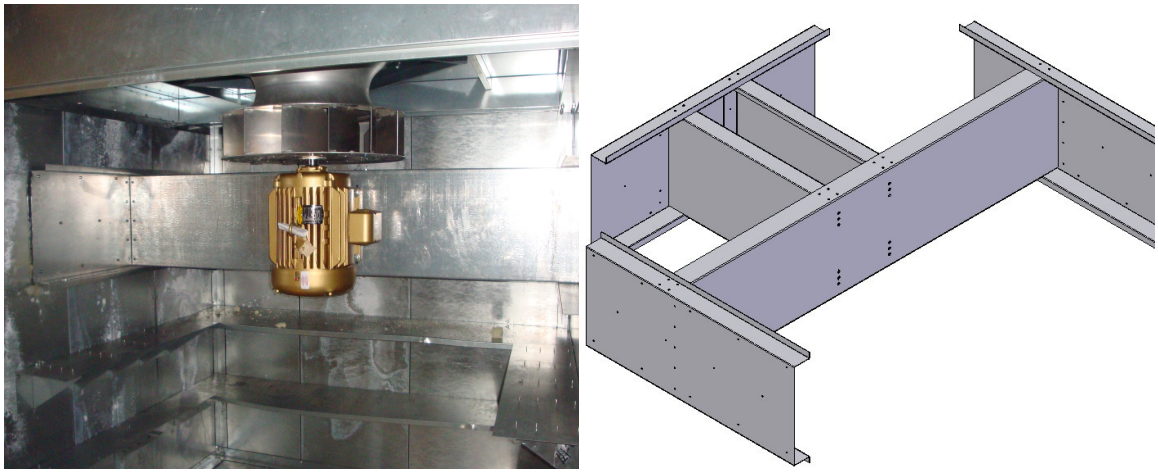

Figure 4.26: Left: Blower mounted in conditioning loop Right: rendering of motor mount

Figure 4.27 shows the partition separating the chamber and the conditioning and code testing loops. Several doors and removable panels allow access to the equipment if needed.

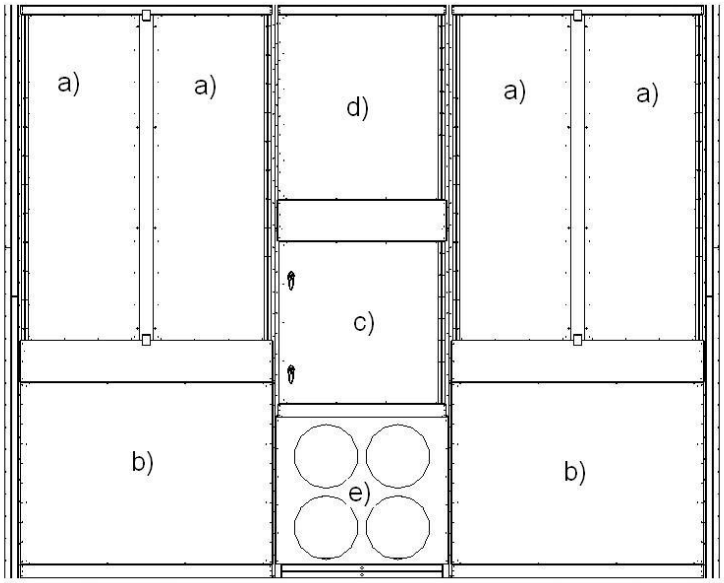

Figure 4.27: Façade for conditioning loops and code tester revealing access doors a) coils access b) conditioning blower and electric heater access c) flow nozzle access d) code tester blower access e) flex duct connection for code tester

Mezzanine and Crane Lift

One solution to getting around the limited available floor space was to build a mezzanine on which to place several of the components necessary for conditioning the chamber: Pumps, tanks, heat exchangers and other items are placed on the mezzanine to free up room for equipment entering and exiting the chamber. Integrated into the mezzanine design is a crane lift for lifting test units up to the level of the plenum floor.

The mezzanine and crane lift, designed separate from AAON, are comprised of structural steel rather than sheet metal. Dr. Dana Hobson, P.E., assisted in the selection of the beam material for the mezzanine in order to ensure that it met standards of safety. The mezzanine platform is 10' x 10'; there is a clearance under the mezzanine of roughly 12'. The beam for the crane approach is 40' long and will support well over the required weight of 3000 lbs. The mechanical lift and trolley selected will support 4000 pounds. A picture of the mezzanine and crane lift can be seen in Figure 4.28 and 4.29.

Figure 4.28: Mezzanine with accompanying trolley beam erected in basement of ATRC before construction of chamber

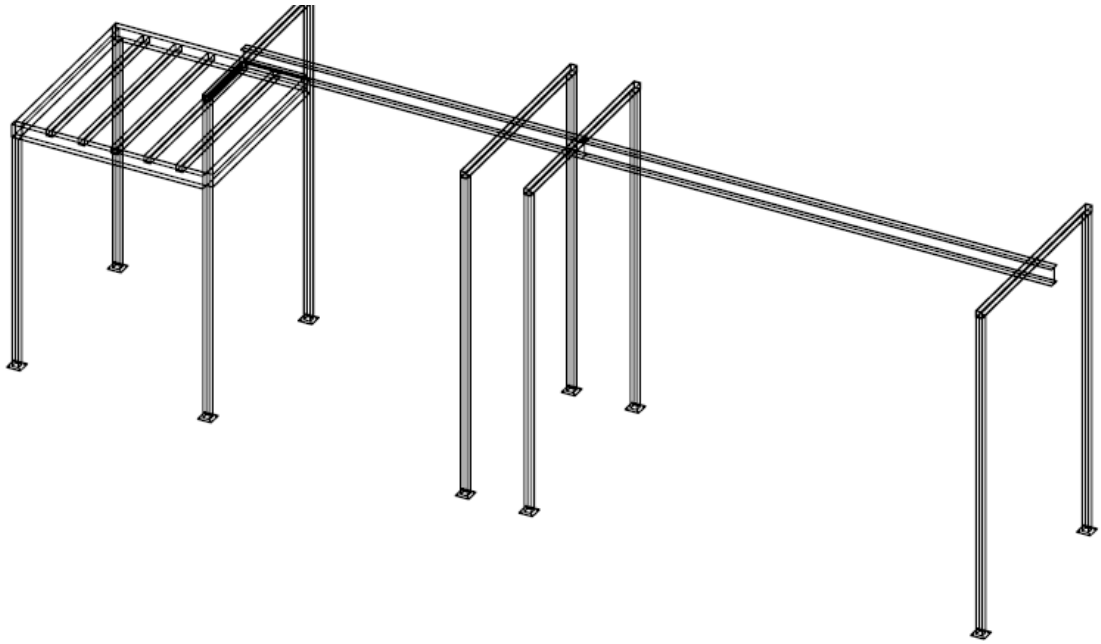

Figure 4.29: Full design sketch of mezzanine and crane lift

Staging Area

Because the floor of the chamber is nearly 20 inches higher than the ATRC basement floor, it is important to have a way of getting into the chamber. As an intermediate step between the crane and the chamber, a staging area has been designed. The staging area is similar in design to the mezzanine, as seen in Figure 4.30. The staging are will be used to position units onto a test cart. When the unit is ready for testing, the cart can be rolled from the staging area into the chamber. Detailed schematics of the staging area are contained in Appendix B.

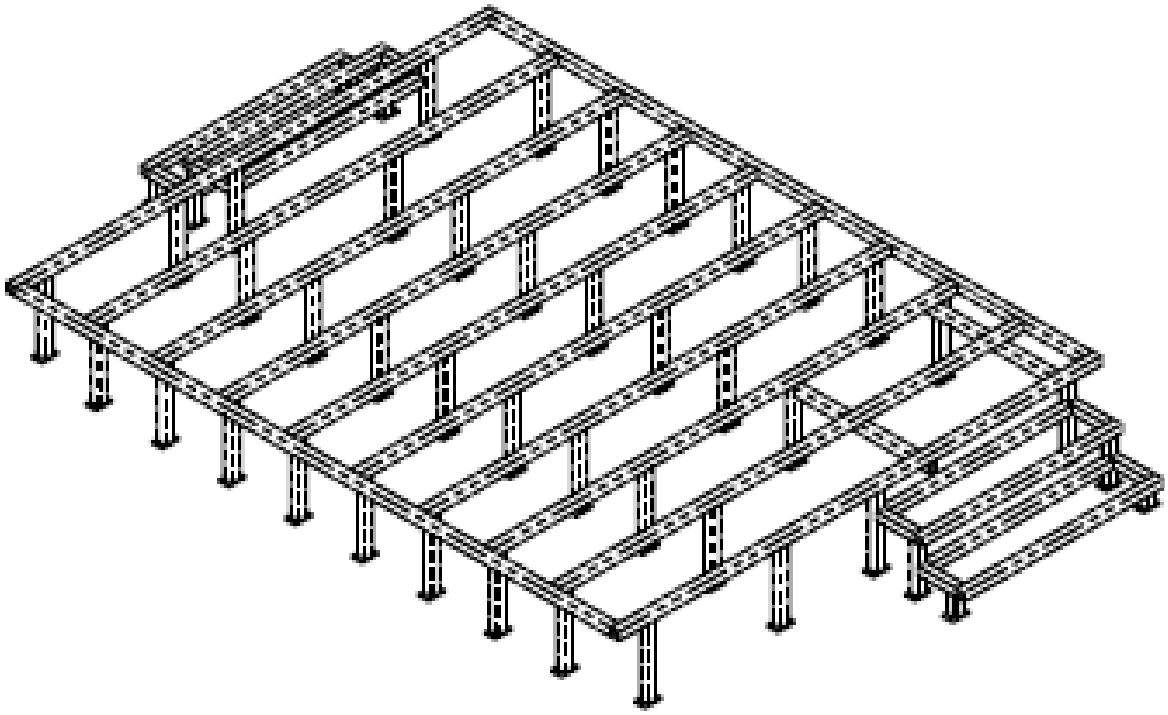

Figure 4.30: Design sketch of staging area used for accessing the chamber

CHAPTER V

METHOD OF CONDITIONING AND CONTROL

This chapter focuses on the specifics of the conditioning and how the psychrometric chamber is to be controlled. It will also touch on the unique difficulties of conditioning to temperatures as low as -40°F (-40°C).

Air Flow

As previously discussed, the OSU psychrometric chamber is unique in that it is conditioned by an underfoot air supply plenum. Conditioned air enters the underfoot plenum as it leaves the conditioning loop. The air diffuses through the perforated steel floor, as seen in Figure 5.1, to enter the conditioned space, and continues through filters in the ceiling to enter the ceiling plenum. From the ceiling plenum air is pulled back into the conditioning loops to complete the cycle.

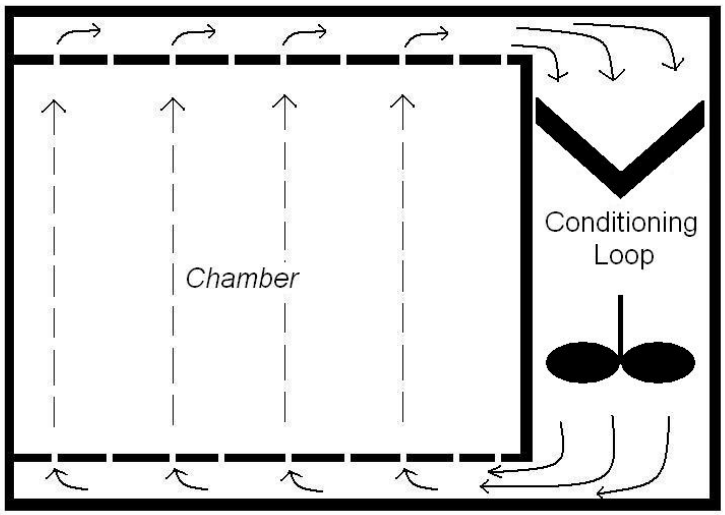

Figure 5.1: Airflow pattern inside chamber

Air enters the vertical conditioning loop through a set of control dampers located at the top. In the conditioning loop, air is first cooled by the coils. The blower, located directly below the coils, pulls the air through the coils and propels it downward past the set of electrical resistance heaters and into a control damper located at the bottom of the conditioning loop. Just before the air reenters the plenum, it is humidified by steam injection.

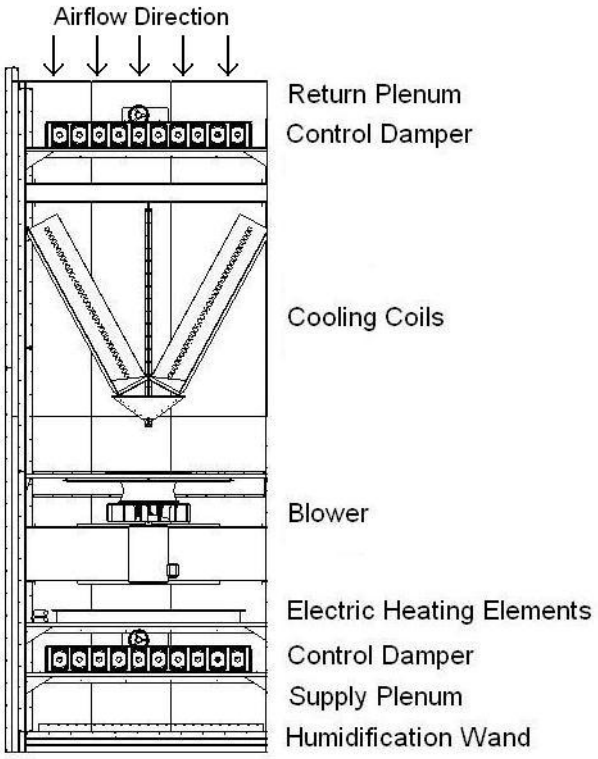

Figure 5.2: Conditioning loop components

Good system design is essential for maintaining tight control of the chamber. A brief overview of the psychrometrics involved with the conditioning of the chamber will be helpful; the process is outlined below.

Psychrometrics

Three components are used to change the properties of the air: Cooling coils, electric resistance heater, and a steam humidifier. The coils provide sensible cooling down to the saturation curve, and latent cooling beyond the saturation curve. The electric resistance heaters provide sensible heating. Any point on the psychrometric chart could

technically be reached using only the cooling coils and heater. However, condensate collected on the coils leaves the chamber system; an overall drying effect would result without the addition of humidity back into the system. The steam generator provides latent heating, or humidification to restore system water. Figure 5.3 demonstrates the processes on the psychrometric diagram.

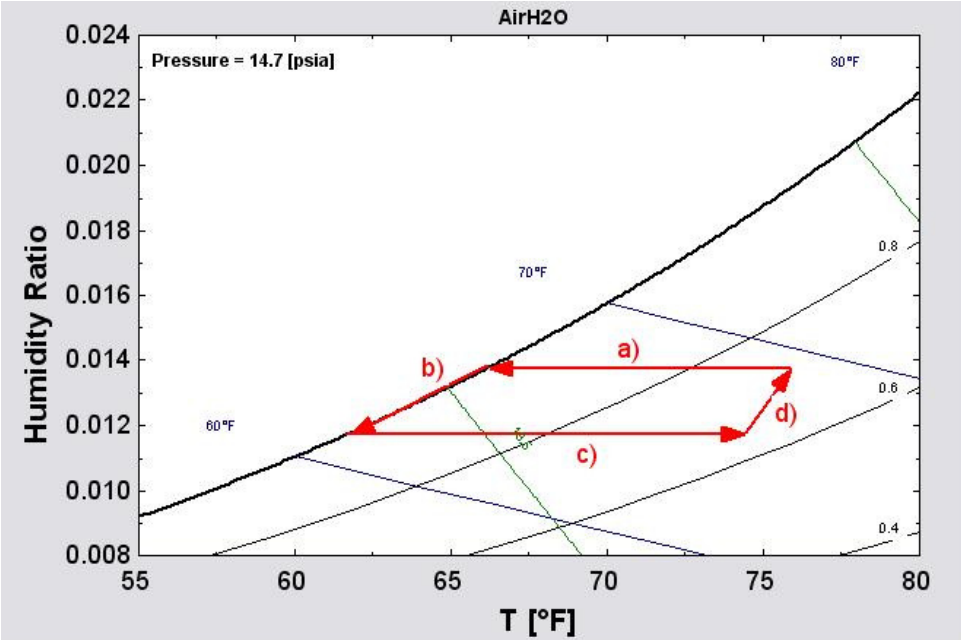

Figure 5.3: Psychrometric chart and processes. a) Sensible cooling b) latent cooling c) sensible heating d) steam humidification

The fundamental concepts of controlling and conditioning the chamber from an air side perspective are fairly straightforward. The air flow can be adjusted by varying the blower speed or adjusting the dampers located at the top and bottom of the conditioning loop. The exiting temperature and humidity of the air depends on the temperature of the cooling coils, the amperage delivered to the heating coils, and the whether or not the steam valves are open.

In the outdoor chamber only one of the conditioning loops will operate at any given time. This will allow defrosting of one set of outdoor coils while maintaining chamber conditions with the other conditioning loop. In the indoor chamber, both conditioning loops will operate simultaneously because there are no plans to operate at sub-freezing temperatures.

Of course, the actual operation of the system and the coordination of the specific pieces of equipment are a lot more complex than explained above. The details behind each of the systems and getting everything to work harmoniously will require hours of testing and operation.

Cooling Loop and Coils

The most heavily relied upon pieces of equipment to keep the chamber within conditions are the cooling coil. Each room has a set of four fin and tube coils that will be working at any given time. All coils are fin and tube type custom designed by AAON for use in the chamber. Coils are placed in the conditioning loops using a "V" configuration, as seen in Figure 5.4.

The indoor coils are two tube rows deep; each coil has a capacity of about 5.5 tons (19.28 kW). The outdoor coils are each four rows deep. The outdoor conditioning loop is two coils deep, or rather; it consists of a double "V".

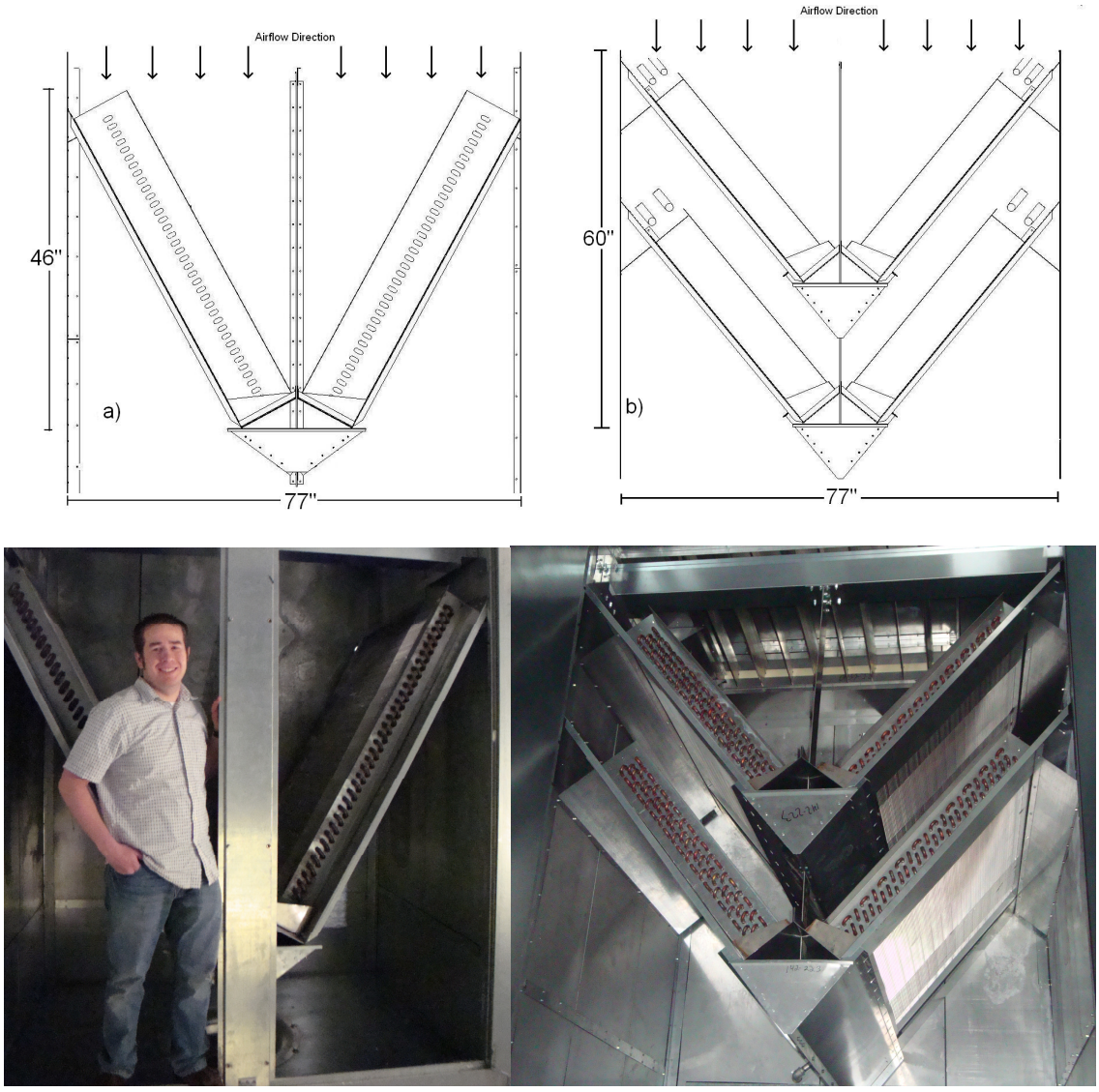

Figure 5.4: Cooling coils inside conditioning loops a) indoor coils b) outdoor coils

Indoor Cooling Loop

The indoor cooling system is a basic hydronic system; the operating fluid is water. Figure 5.5 shows a flow diagram of the indoor cooling system. Heat from the air in the chamber is removed using the coils. Heat is removed from the water using a brazed plate heat exchanger connected to the campus chilled water system. The campus system

delivers water at 44° F, with a strict need to return the water from the plate heat exchanger at 56° F. Proportional valves in each of the lines to the plate heat exchanger will be used to control the temperature of the coil.

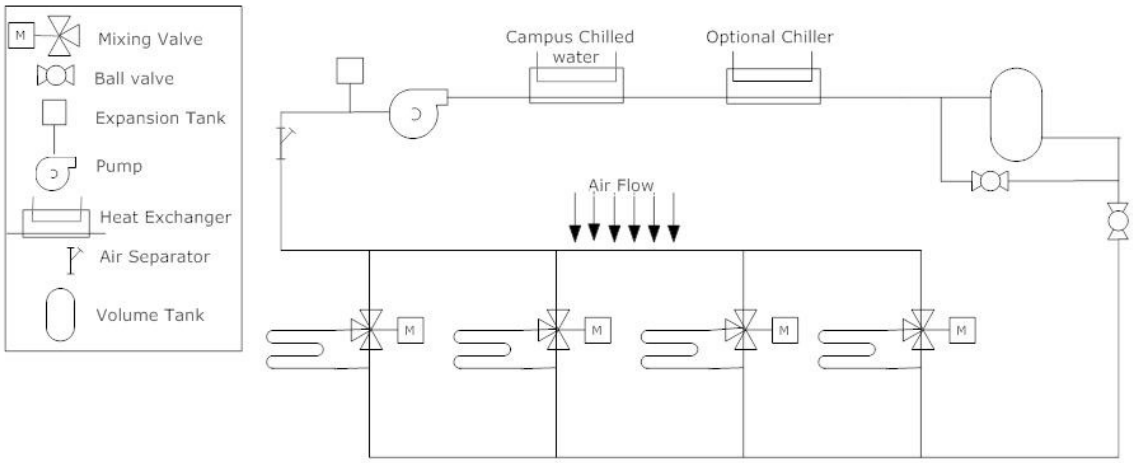

Figure 5.5: Piping Schematic for indoor cooling loop

Additional control of the coil heat transfer rate is done using proportion mixing valves at the outlet of each of the coils. These valves allow a portion of the water flow to bypass the coils. The modulation of these valves helps to control the water side, and thus the air side, heat transfer rate. Additional control may be obtained through adjustment of pump speed. A volume tank in the system acts as a flywheel to help maintain the system against small disturbances; the volume tank may be bypassed for faster system response. Other necessary components of any hydronic system include balancing valves, air separators, pumps, and an expansion tank. A detailed piping schematic is contained in Appendix C.

An additional plate heat exchanger is installed after the campus chilled water heat exchanger. The other side of this heat exchanger will be available for connection to

another device. This will give flexibility to the system. A likely possibility for connection to the "extra" heat exchanger would be a DX system or a chiller; this would allow cooling to temperatures below that of the campus chilled water. Additional humidity removal and cooler chamber temperatures could be reached using the additional heat exchanger.

Outdoor Cooling Loop

The outdoor chamber cooling loop is much more complex than the indoor. In order to meet the low temperature requirements, the outdoor system is filled with Dynalene HC-50, a glycol-type substance which freezes at -58°F. Many of the complexities inherent to the outdoor system are introduced because of the low temperature of the circulating fluid. Figure 5.6 shows the schematic of the outdoor cooling loop.

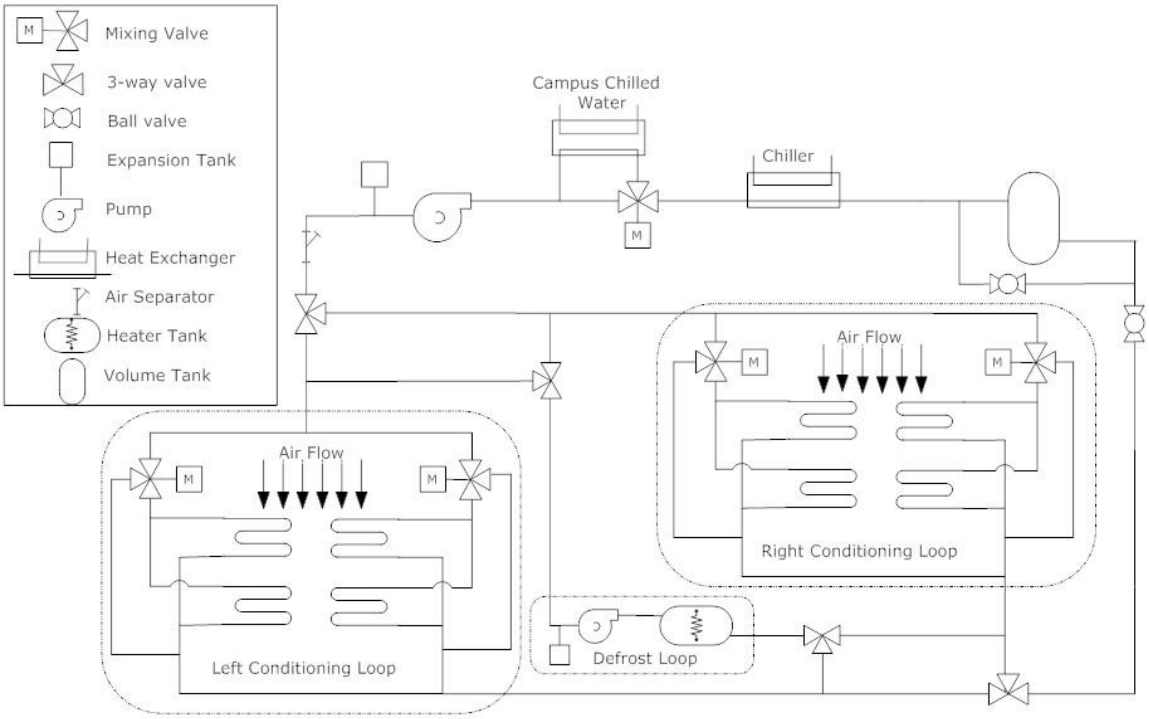

Figure 5.6: Piping Schematic of the outdoor cooling loop with defrost capabilities

Each of the stacked coil pair is connected in parallel to a proportional control valve. This gives the effect of controlling a single eight-row coil. Proportional mixing valves allow the precision control of the heat transfer rate of the coils.

Similar to the indoor cooling loop, there are two plate heat exchangers, one of which rejects heat to the campus chilled water system, the other to a chiller or DX system to get to lower temperatures. It is expected that the second heat exchanger will be used extensively. Because this is basically a hydronic system, the same components exist in the outdoor cooling loop as in the indoor cooling loop.

The main differences of the outdoor loop with respect to the indoor cooling loop are the changes made to facilitate smooth operation at low temperatures. The mixing valves used to control the coils are only rated to -20°F; therefore a manual bypass is

installed for both valves on one of the outdoor conditioning loops. When temperature of the fluid is below -20°F, the bypass should be manually opened. The coils will then run full open, with the only control of them being through the adjustment of the variable speed pump. An actuated valve allows the complete bypass of the campus chilled water plate frame heat exchanger. Bypassing the heat exchanger at low temperatures will prevent freezing of the campus chilled water, which would likely damage the system.

When the temperature of the outdoor coils approach freezing, there will be frost accumulation. As frost accumulates at low temperatures; the effectiveness of the coils will decrease. Decreased air flow and degraded heat transfer will eventually render the coils completely ineffective. In order to combat this process, a defrost system has been designed. The defrost loop incorporates four 3-way valves, a pump, and a heating tank, as seen in Figure 5.6.

In the event that the need for defrost is detected, the heater in the tank will be turned on. Circulating fluid is diverted from the coils needing defrosting to the ice free coils as the system switches to the other conditioning loop. The heated fluid will then be circulated through the frosted coils to melt the ice from them. When the frosting renders the other coils inoperable, the process will be repeated.

The electric heating elements will work on proportional control. Each room has four 20 watt heaters. Steam will be injected under the floor right after the conditioning loop. Steam is mainly controlled with signals to the steam generator. Table 5.1 shows the pieces of equipment used to control indoor chamber conditions; Table 5.2 demonstrates control items for the outdoor chamber. Notice the several possible control strategies.

Indoor Chamber				
Description	**Quantity**	**Control Type**	**Effect of Controlling**	**Location**
Damper	4	proportional	Operate between close ond open to regulate airflow	One at the top and bottom of each conditioning loop
Blower	2	proportional	Adjust to vary air volume to chamber or velocity through conditioning loop and across coils	One in each of the conditioning loops, just under eye level
Mixing Valve	4	proportional	Regulate fluid flow to each coil, changing the capacity and heat tranfer characteristics	One connected to the outlet of each cooling coil - valve located in interstitial space above the chamber
Mixing Valve	1	proportional	Regulate flow to the brazed plate heat exchanger connected to the campus chilled water - effects capacity and heat tranfer of the system	Above mezzanine, near plate heat exchanger
Proportional Valve	1	proportional	Regulates return temperature of campus chilled water to plate heat exchanger - must ensure 56 F return	Above mezzanine, near plate heat exchanger
Circulation Pump	1	proportional	Increase fluid flow in cooling system - effects capacity and water side heat transfer	On mezzanine
Electric Heating Elements	1	proportional	Heat air stream	Located below blower, but above damper in one conditioing loop.
Electric Heating Elements	3	on/off	Heat air stream	Conditioining loops near bottom. Located below blower, but above damper
Steam Generator	1 (shared)	on/off	Increase humidity in room - manual control valve to determine which room	Interstital space above chamber - over partition wall

Table 5.1: Items for control in the indoor chamber

It is not hard to imagine the possible complexities involved in controlling the chamber. Many of the same variables can be controlled using different interdependent pieces of equipment. Perhaps the simplest example is demonstrated by the control of the volume of air delivered to the chamber. In the indoor room, this aspect depends on two blowers and four dampers, all of which are independently operated. Slightly closing any one of the dampers will immediately increase the pressure differential across that

particular conditioning loop, thus reducing the airflow through the conditioning loop. The decreased air flow will created a drop in pressure in the supply plenum. The blower in the opposite conditioning loop would in turn need to do less work to push the same amount of air; however, because it operates independently, equilibrium will be reached at a slightly higher flow rate.

Adjusting a damper in one conditioning loop directly decreases the flow in that loop; however it indirectly increases flow in the opposite conditioning loop. Where, then will the new equilibrium point be? The solution is increasingly more complex because the concern will not only be with the amount of air flow, but also the temperature of said air. The changes in airflow will affect the flow characteristics, and thus the heat transfer properties at the cooling coil. Variation in heat transfer at the coils affects the return water temperature, and eventually the supply temperature. Ultimately, a change in the damper position could affect every aspect of the system! Experimental data will be invaluable in determining the set method for controlling the system.

Outdoor Chamber				
Description	**Quantity**	**Control Type**	**Effect of Controlling**	**Location**
Damper	4	proportional	Operate between close ond open to regulate airflow	One at the top and bottom of each conditioning loop
Blower	2	proportional	Adjust to vary air volume to chamber or velocity through conditioning loop and across coils	One in each of the conditioning loops, just under eye level
Mixing Valve	4	proportional	Regulate fluid flow to each coil, changing the capacity and heat tranfer characteristics	One connected to the outlet of each stacked coil set - located in interstital space above chamber
3-way Valve	4	directional: 1 or 2	Regulates coil connection to cooling system or to defrost system	Interstitail space above chamebr over the outdoor conditioning loop
Mixing Valve	1	proportional	Regualte flow to the plate heat exchanger connected to campus chilled water	On mezzanine, near plate heat exchanger
Circulation Pump	1	proportional	Regulate fluid flow in outdoor cooling loop	On mezzanine
Circulation Pump	1	on/off	Turn on to circulate water in defrost system	Interstitail space above chamebr over the outdoor conditioning loop
Tank heater	1	on/off	Heats the deforst tank - set temperature manually selected	On defrost tank in interstitial space above chamber
Electric Heating Elements	2	proportional	Heat air stream before delivery to chamber	One in each conditioining loop near bottom. Located below blower, but above damper
Electric Heating Elements	6	on/off	Heat air stream before delivery to chamber	Three in each conditioining loop near bottom. Located below blower, but above damper
Steam Generator	1 (shared)	on/off	Increase humidity in room - manual control valve to determine which room	Interstital space above chamber - over partition wall

Table 5.2: Control items for outdoor chamber

The control of the chamber will be done using a data acquisition (DAQ) system. The system will continuously gather data about temperature and air flow. It will adjust the many components according to the needs involved to reach and maintain the required conditions. The topic of actually controlling the chamber is reserved for another paper.

CHAPTER VI

AN OPERATIONAL MODEL

As part of the chamber planning and design, an operational model was developed to test the soaking time of the chamber. The soaking time is the time it takes for the chamber to transition from the start up temperature to the set point temperature. This section focuses on modeling this aspect of the chamber.

Literature on Computer Modeling

It seems that it is only when we stand on the shoulders of others that we are able to see the picture clearly enough to attempt to build a trail. The idea of modeling heat transfer in a structure is not new. Several papers have been published on this topic, far too many to review here. Research is particularly plentiful in the HVAC industry, where much of it is based on the modeling of living or working spaces in order to provide comfortable conditions for people (Clark, Hurley et al. 1985; Clark and May 1985; Sowell 1989; Brandemuehl, Lepore et al. 1990; Sowell and Hittle 1995; Kasahara, Kuzuu et al. 2000; Sowell and Haves 2001; Chatzidakis, Athienitis et al. 2002; Armstrong, Leeb et al. 2006). Other areas of research focus on animal housing, green houses, or environmental

test facilities(Chatzidakis, Athienitis et al. 2002). The general approach of most researchers seems to have been aimed at either modeling a room or a building in which several rooms are located.

As is the case with most fields that have been around for decades, an exhaustive literature review is not practical. Far too many papers have been published on the topic of building simulation to do more than touch on the available pertinent information. The main difference with mainstream building modeling and modeling the chamber is the dynamic aspect of the chamber.

In general, buildings are maintained at a set temperature. Building controls may allow small perturbations from the set point temperature; however, it is much more common for temperature of a building to remain constant. Modeling of buildings focus on the thermal loads associated with weather and occupants. The key point is to understand how much energy is required to maintain the set point temperature of the buildings. This purpose is often extended to investigate energy saving options. Regardless, building models focus on the steady state operation because the vast majority of operational time for building conditioning systems is spent maintaining the set point temperature. Even with some energy saving practices, where conditioning is minimized during nights or weekend, the overall deviation from the standard set point is relatively small.

In contrast, the psychrometric chamber will operate intermittently, dedicating a large portion of its operating time to soaking, or transitioning to the set point conditions. Additionally, the temperature changes between start up and the set point temperature can

be greater than 100°F (38°C). Therefore a new model needs to be developed in order to estimate the soaking time of the chamber.

Regardless of the differences from the typical building model, there is a lot of pertinent information to be gleaned from main stream building model literature. This section of the paper attempts to present the main ideas and methods used in building simulation. An overview of the building system modeling is provided with examples and references to work done by previous researchers in the field. Governing equations of the most popular solution methods are presented with documentation directing interested readers to their sources.

Some examples of research that have used models that are pertinent to the psychrometric room project are also presented. The literature review is concluded with a brief discussion of programs and a short explanation of some of the HVACSIM+ supporting literature.

Simulating Systems

People have long been interested in the overall energy needs associated with maintaining comfortable conditions inside a space. In the early days simple steady state models were used to determine the amount of coal delivered to a home. These models were referred to as degree-day models (Armstrong, Leeb et al. 2006). The steady state model obviously left things to be desired. Modeling approaches have evolved to become more complicated over the years. The time of the degree-day has passed. New models use computers and complicated algorithms written in lengthy programs to predict energy

consumption over several years based on past weather data. These programs can break down the data into small time steps in order to give an accurate representation of the modeled system at any given moment.

The response to an input, such as an air conditioner, is determined by much more than the indoor and outdoor temperatures. Parameters such as geometry of the building, internal partitions, and obstructions in the room all influence what actually happens inside a building. Significance is also found in the building's capacitance, or ability to store heat, as well as its thermal transmission properties (Armstrong, Leeb et al. 2006). It is not hard to imagine why the early models were insufficient.

Early models lacked not only complexity in calculation, but also lacked sufficient components and appropriate parameters. A small house with one room may have been adequately heated by a stove in the middle of the room, but a similar sized house with two rooms and an identical stove in the corner certainly could not be assumed to have the same warmth to it. A simulation must be broken into parts and sub parts. A common way of breaking down a simulation by current programs by breaking it into four main parts: Load, System, Plant, and Economics; or LSPE as Sowell has termed it (Sowell and Hittle 1995). Each of these components may be broken down even further depending on the overall goal of a simulation and the desired level of detail.

Components of the LSPE Model

Load. The first, and possibly most obvious, part of the LSPE model is that of the load. Loads are the reason behind HVAC equipment. Their sources are numerous.

Typical building loads specific to air conditioning are present in the form of lights, people, machinery, computers, conduction through walls, and radiation incident on exterior walls and through windows. Loads are dealt with using either a nodal or zonal model. Both models break a space up into manageable pieces and assign a value to each piece representative of the loads generated in the space. An example of a zonal model is presented by Kasahara in Figure 6.1 (Kasahara, Kuzuu et al. 2000).

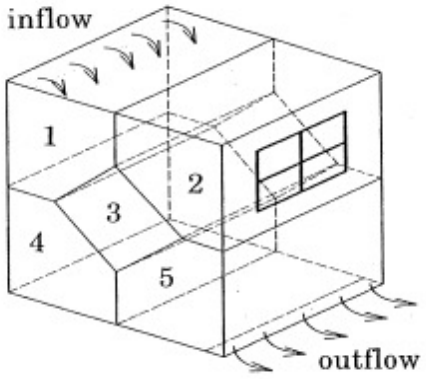

Figure 6.1: Example of a zone model (Kasahara, Kuzuu et al. 2000)

Each zone will have a load value associated with it and will interact with the zones immediately around it. For example, from Figure 6.1, zone 2 will have loads associated with the window, perhaps conductive heat loss to a lower outside temperature; it will exchange heat with zones 1, 3, and 5. Zone 4 may have electronic equipment producing heat that needs to be accounted for and will exchange heat with zones 1, 3, and 5. Adding more zones makes the model more accurate but also complicates the model. Nodal models are really an extension of zone. They allow more freedom, but can also become increasingly more complex. Complexity can improve simulation results, but always add the cost of computation time.

Sowell presented a complex nodal model, which he solved using HVACSIM+ (Sowell 1989). In Sowell's model, each surface or volume in the room is represented by a node in the network. Nodes appear inside and at the boundary of a zone and do not necessarily contain mass. Heat transfer in any form can occur between any of the nodes. This method allows one to very accurately show the interactions inside and around a building. Sowell suggests, when using this method, modeling in great detail then removing nodes one at a time to see which nodes are significant and which can be removed for simplification.

System. Systems, sometimes referred to as, secondary systems are deal with components other than the main loads. Fans, dampers, and motors are all part of what the system entails. Strand describes HVAC simulation in as having three loops (Strand, Fisher et al. 2002). A visual representation of these three loops is displayed in Figure 6.2. Strand's designates the loops as the air loop, plant loop and condenser loop. Both the air loop and the condenser loop would fall in to the category of being part of the system. The plant loop is left to be in a category of its own which will be discussed later. It is interesting to note that generally programs will have a strong base in either load or system, but will leave the other one lacking (Sowell and Hittle 1995).

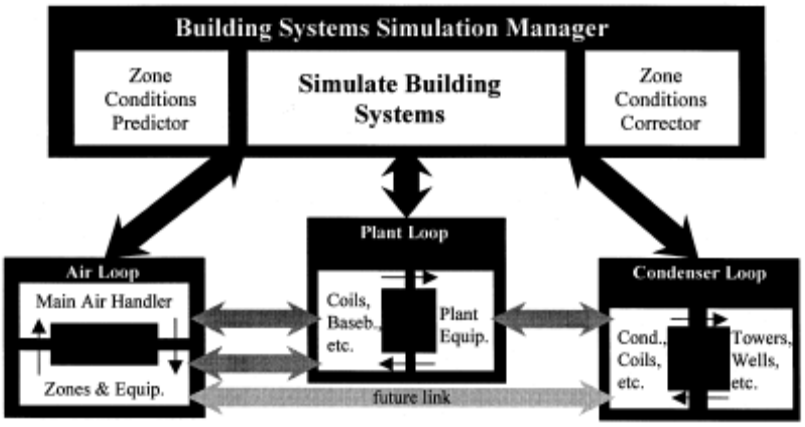

Figure 6.2: Loops of interest in a simulation model. Air and condenser loops fall into the system category (Strand, Fisher et al. 2002).

Plant. Most computer programs have greatly simplified the plant, or the operating HVAC component. Usually there is a catalogue of HVAC units comprised of air conditioners, heat pumps, furnaces, chillers, etc. and users are instructed to input an efficiency or curve fit coefficients obtained from manufacturers' data. It should be noted, however, that in Europe plants are modeled in great detail; a furnace model, for example, might include combustion calculations (Sowell and Hittle 1995).

Econonmics. In general, economics is the driving factor behind simulation. Whether the goal is to determine the amount of coal to deliver or the amount of electricity that is used, people are still concerned about the cost of creating the desired effects. Source energy is calculated in most programs, some programs will even calculate the cost of the source energy. In any case, comparisons between simulations with varying components, loads, or conditions provides insight that help engineers improve their designs.

Computational Methods

In general, two methods or models are widely used to mathematically describe building systems, or zone models. They are the heat balance method and the transfer function method.

Heat Balance Model. The heat balance model uses surface conduction, radiation, and convection at the surface of the building and convective heat transfer within the space. It is the most adaptive approach to building simulations. The AHSRAE handbook of fundamentals details the process (ASHRAE 1993). The solution uses basic energy balances, but several of them in order to balance all the sources of energy and physical components in the room. The governing calculations for the inside surface appear in Equation 6.1.

$$q_{i,\theta} = \left[h_{ci}\left(t_{a,\theta} - t_{i,\theta}\right) + \sum_{j=1\neq i}^{m} g_{ij}\left(t_{j,\theta} - t_{i,\theta}\right) \right] A_i + RS_{i,\theta} + RL_{i,\theta} + RE_{i,\theta} \qquad 6.1$$

For i=1, 2, 3, 4, 5, 6

where

m = number of surfaces in the room

$q_{i,\theta}$ = rate of heat conducted into surface i at inside surface at time θ

A_i = area of surface i

h_{ci} = convective heat transfer coefficient at interior surface i and interior surface j

g_{ij} = radiation heat transfer factor between interior surface i and interior surface j

$t_{a,\theta}$ = inside air temperature at time θ

$t_{i,\theta}$ = average temperature of interior surface i at time θ

$RS_{i,\theta}$ = rate of solar energy coming through windows and absorbed by surface i at time θ

$RL_{i,\theta}$ = rate of heat radiated from lights and absorbed by the surface i at time θ

$RE_{i,\theta}$ = rate of heat radiated form the equipment and occupants and absorbed by surface i at time θ

The set of equations formed by Equation 6.1 need to be solved simultaneously with the equations formed using Equation 6.2. This is necessary because the internal surface temperature is changing with time, which affects the conduction rate. The equations of Equation 6.2 are typically formed using the conduction transfer functions.

$$q_{in,\theta} = \sum_{m=1}^{M} Y_{k,m} t_{o,\theta-m+1} - \sum_{m=1}^{M} Z_{k,m} t_{in,\theta-m+1} + \sum_{m=1}^{M} F_m q_{in,\theta-m} \qquad 6.2$$

where

in = inside surface subscript

k = order of CTF

m = time index variable

M = number of nonzero CTF values

o = outside surface subscript

t = temperature

θ = time

x = exterior CTF values

Y = cross CTF values

Z = interior CTF values

F_m = flux history coefficients

Equation 6.3 is a space air energy balance and must be solved simultaneously with Equations 6.1 and 6.2.

$$Q_{L,\theta} = \left[\sum_{i=1}^{6} h_{ci}\left(t_{i,\theta} - t_{a,\theta}\right)\right] A_i + {}_{\sigma}CV_{L,t}\left(t_{o,\theta} - t_{a,\theta}\right) + {}_{\sigma}CV_{v,t}\left(t_{v,\theta} - t_{a,\theta}\right) + RS_{a,\theta} + RL_{a,\theta} + RE_{a,\theta} \qquad 6.3$$

where

σ = air density

C = air specific heat

$V_{i,\theta}$ = volume flow rate of outdoor air infiltrating into room at time θ

$t_{o,\theta}$ = outdoor air temperature at time θ

$V_{v,\theta}$ = volume rate of flow of ventilation air at time θ

$t_{v,\theta}$ = ventilation air temperature at time θ

$RS_{a,\theta}$ = rate of solar heat coming through windows and connected into room air at time θ

$RL_{a,\theta}$ = rate of heat from lights connected into room air at time θ

$RE_{a,\theta}$ = rate of heat from equipment and occupants and connected into room air at time θ

Transfer Function Method. The transfer function method is well suited for a computer. It approaches the problem with using a sol-air temperature to represent outdoor conditions, and it assumes a constant indoor temperature. It also assumes that both the indoor and outdoor heat transfer coefficients are constant. This method is outlined in chapter 26 of the ASHRAE Handbook of Fundamentals (ASHRAE 1993). The governing equation is shown as Equation 6.4. For addition help in using the equation, the reader is referred to the handbook.

$$q_{e,\theta} = A\left[\sum_{n=0} b_n\left(t_{e,\theta-n\delta}\right) - \sum_{n=1} d_n\left\{\left(q_{e,\theta-n\delta}\right)/A\right\} - t_{rc}\sum_{n-0} c_n\right] \qquad 6.4$$

where

$q_{e,\theta}$ = heat gain through wall or roof at calculation hour θ, Btu/h

A = indoor surface area of a wall or roof, ft^2

θ = time, h

δ = time interval, h

n = summation index (each summation has as many terms as there are non-negligible values of coefficients)

$t_{e,\theta-n\delta}$ = sol-air temperature at time θ-$n\delta$, °F

t_{rc} = constant indoor room temperature, °F

b_n, c_n, d_n = conduction transfer coefficients

Relevant Research

Several papers demonstrate building simulation with good supporting results. One of particular interest is by Sowell. Previously mentioned, he developed a program that uses the heat balance method predict the heat loads in a room. His program incorporates an arbitrary number of nodes (Sowell 1989). Using nodes in his program allowed him to step away from the lumped capacitance model that is largely used. Many simulations in the past had divided a room into only a small handful of zones, usually representing each zone as a portion of only the largest of the capacitances located in the zone. His program remedied this problem; much detail can be included in such a model.

A significant portion of his research dealt with lighting; particularly the non-linear aspect of fluorescent lighting and how the heat gain from it is incorporated into a building simulation (Sowell 1989). He used a program called LIGHTS to help supplement his program in HVACSIM+, Sowell Admits that the interface between the two programs needs some work (Sowell 1989); however, Sowell's research definitely presents a good starting path for the design of a psychrometric chamber simulation.

Kasahara's method of simulating a small building using a zone model has relevance to the proposed psychrometric chamber simulation. His method is more course than Sowell's in the calculation, but his model includes humidity calculations (Kasahara, Kuzuu et al. 2000). Kasahara's solution incorporated Kirchhoff's current law with the assumption that the air, while well mixed, was only flowing in one direction. It seems that the same idea could be used in the simulation of the psychrometric chamber because of the nature of the air flow. Using the zones described above, Kasahara created flow network and derived equations governing the room.

The most relevant research on this topic comes from Chatzidakis (Chatzidakis, Athienitis et al. 2002); which is based on an environmental test chamber located in Athens. The test chamber is built inside a building and is used to test semi trucks that require heating or cooling to maintain conditions in the cargo area. Chatzidakis used a transient finite difference model matrix to calculate the transient conditions leading up to the set point of the test facility.

The literature demonstrates that it is generally not possible to solve a problem as complex as building modeling by hand calculations. The solution in all reviewed literature was to use computers to model a building, or parts of a building and how they

interact with each other. A similar method will be used in modeling the psychrometric chamber.

Programs. The Package in which a simulation is executed is likely to play some role in the outcome of a simulation. Programs such as Energy Plus, AXCESS, TRACE, BLAST, TRNSYS and others have all been developed to simulate at least some part of a model. Unfortunately, time and resources are always limited and a comprehensive analysis of several programs is not feasible.

Due to the availability and openness of the source code, HVACSIM+ has been chosen as the engine of simulation. HVACSIM+ stands for the HVAC SIMulation PLUS other systems. It is a non-propriety building simulation program that was developed at the National Bureau of Standards (NBS). It is made up of a main simulation program, a library of HVAC system component models or Types, a building shell model, and interactive front and input data generation programs(Park, Clark et al.). The goal of the program is to help people better understand the interaction of buildings with the environment and with the loads. It too uses the basic LSPE approach to simulation. HVACSIM+ has many features that make it appealing for such a project. The program is used extensively at OSU and several Type models have been created. New Type models can easily be incorporated into HVACSIM+ through the use of a FORTRAN compiler. The option to customize the program is what is most appealing.

Three main papers serve as valuable resources in the operation and modification of the HVACSIM+ program. The first of these is a general user's guide which mostly describes the set up and general application of HVACSIM+. It includes some sample

simulations which could be used as a tutorial to the program (Clark and May 1985). The user's guide refers the reader to the reference manual for information about how to modify the program and create customized Type models. The reference manual also describes capabilities, operations, and limitations of the program. It is backed with models and validation in many areas (Clark 1985).

The third paper on HVACSIM+ is specific to building simulation. It details the shell models used in the original HVACSIM+ program. A zone envelope, building surface, and zone model are each included in the original program as Types 50, 51, and 52 respectively (Park, Clark et al. 1986).

Methodology

The heat balance method is the most adaptable, and simplest to use in the given situation because of the way that it breaks down the load into manageable parts. Chatzidakis used the heat balance method in his simulation (Chatzidakis, Athienitis et al. 2002). Using the same method will allow validation of the chamber model.

The chamber is broken into nodes for simulation purposes. Each wall, the ceiling, floor, and main chamber air mass is set as a control volume or node. Each node exchanges energy with those nodes surrounding it in the form of convection or radiation heat transfer; however, in the chamber model, radiation is neglected. Transient finite difference equations will be incorporated in the wall models.

Five main Type models; Types 803, 804, 805, 806, and 807; have been developed in order to sufficiently represent the interactions taking place in the simulation. Descriptions of each type and its governing equations are found below.

TYPE 803: Free Convection Heat Transfer

Type 803 calculates the free convection that takes place at a surface. This model was developed to model the heat transfer that takes place in the quiescent air that surrounds the psychrometric chamber. The subroutine uses physical properties of the air and adjacent surface to determine the amount of heat transfer that takes place across the interface. It outputs the heat transfer rate into the surface as well as the surrounding air.

Inputs for Type 803 are surface temperature and ambient temperature. Parameters include the height, width, and an integer input for surface position. The position input allows the user to specify the surface as the upper or lower face of a horizontal plane, or to specify that the surface is vertical.

A detailed explanation of free convection and several equations are given by Incropera and Dewitt. For simplicity, Equation 6.5, recommended by Churchill and Chu, is used to calculate the average Nusselt number for the vertical plane (Incropera and Dewitt 2002).

$$\overline{Nu}_L = \frac{\bar{h}L}{k_{fluid}} = \left\{ .825 + \frac{0.387 Ra_L^{1/6}}{\left[1 + (.492/\mathrm{Pr})^{9/16}\right]^{8/27}} \right\}^2 \qquad 6.5$$

The Nusselt number is used to find the average convection coefficient, *h*. The Raleigh number, Ra_L is calculated from the height and physical properties of the air at the film temperature. The Prandtl number, *Pr*, is also calculated using the film temperature.

Because gravity is a driving force in free convection, horizontal surfaces must be dealt with differently; the governing equations appear as Expression 6.6 below.

Upper heated plane or lower cooled plane:

$$\begin{aligned} \overline{Nu}_L &= .54 Ra_L^{1/4} \qquad \left(10^4 \le Ra_L \le 10^7\right) \\ \overline{Nu}_L &= .15 Ra_L^{1/3} \qquad \left(10^7 \le Ra_L \le 10^{11}\right) \end{aligned} \tag{6.6}$$

Lower heated plane or upper cooled plane:

$$\overline{Nu}_L = .27 Ra_L^{1/4} \qquad \left(10^5 \le Ra_L \le 10^{10}\right)$$

In horizontal configuration the Raleigh number is calculated using an adjusted length, *L* of the form *L = area/perimeter*. Upon calculation of the Nusselt number, the convection coefficient, *h*, is easily determined and used to get the overall heat transfer rate into the surface via Equation 6.7. Heat transfer into the surrounding air is opposite in sign.

$$q = hA\left(T_\infty - T_{surface}\right) \tag{6.7}$$

TYPE 804: Forced Convection Heat Transfer

Type 804 calculates the heat transfer rate due to forced convection at a surface using the physical properties of the moving air in conjunction with the surface temperatures of the adjacent plane. It has four inputs. Inputs include temperature of the surface and ambient air, mass flow rate through the space, and ambient pressure. Type

804 outputs the heat transfer rate into the wall and into the adjacent space. Parameters include flow surface length, heat transfer area, and flow area, which is used to determine the air velocity.

The heat transfer rates calculated by Type 804 are based on air moving across flat plates. This phenomenon can be seen in several places in the OSU chamber; one of the most obvious examples for uses of this type is for the walls in the main chamber. Air travels unidirectional through the room, entering through the floor and exiting through the ceiling. Air travels through the plenums and conditioning loop in approximately the same manner. For this reason, Type 804 will be used extensively.

The average Nusselt number for flat plates in parallel flow can be separated into two separate categories: turbulent and laminar flow. Both categories are described by Incropera and Dewitt (Incropera and Dewitt 2002) and are shown in Expression 6.8.

$$\overline{Nu}_L = \frac{\bar{h}L}{k_{fluid}} = \left(0.037\,\mathrm{Re}_L^{4/5} - 871\right)\mathrm{Pr}^{1/3} \qquad \left(500{,}000 \le \mathrm{Re}_L\right)$$
$$\overline{Nu}_L = \frac{\bar{h}L}{k_{fluid}} = 0.664\,\mathrm{Re}^{1/2}\,\mathrm{Pr}^{1/3} \qquad \left(\mathrm{Re}_L < 500{,}000\right) \qquad 6.8$$

The Reynolds number, Re_L, is calculated using the length, velocity, and kinematic viscosity. Length is given as a parameter; kinematic viscosity is determined at the film temperature using a preexisting subroutine and the density. Velocity is calculated from the mass flow rate input and the flow area specified as a parameter. Density is determined using the ideal gas law and the pressure input. Equation 6.7, above, is used to determine the heat transfer rate into and out of the surface.

TYPE 805: Room Model

Type 805 is a room model that has the assumption of being well mixed. It has thirteen inputs; nine of which represent heat gain from walls or objects in the room. The remaining four inputs include mass flow rate, supply air temperature, room temperature, and a signal to use initial conditions. It has one real output and a dummy output for ease of expansion. The valid output is the time derivative of the temperature change in the room; it must be connected to the room temperature input. It has three parameters; the initial room temperature, heat capacity of objects in the room, and room volume.

The governing equations for Type 805 are an adaptation to the Type 52 model developed by Clark (Clark and May 1985). The air in the room absorbs the heat transferred from the walls. Convection heat transfer from six surfaces is listed in the type model. Inputs are also specifically labeled for short wave radiation, long wave radiation and occupants in the room. It should be noted, however, that all of the heat transfer into the model is summed together, so the labels have little significance beyond identification. Heat from the supply, $\dot{Q}_{Supply}$, air is summed with the heat inputs. $\dot{Q}_{Supply}$ is determined from the following equation.

$$\dot{Q}_{Supply} = c_{p,air}\dot{m}_{Supply}\left(T_{Supply} - T_{Room}\right) \tag{6.9}$$

The differential equation is then determined with Equation 6.10. All physical properties of air are determined using the average of the two inlet temperatures.

$$\frac{dT}{dt} = \frac{\dot{Q}_{total,in} + \dot{Q}_{Supply}}{\left(C_{Objects} + c_{p,air}m_{roomair}\right)} \tag{6.10}$$

In the model, the total heat transfer into the room is used to heat both the air and the objects in the room. The new temperature in the room is computed using Equation 6.11.

$$T_{room} = \frac{Q_{total,in}}{m_{air} c_{P,air} + C_{P,Stuff}} + T_{air,in} \qquad 6.11$$

When the signal used to specify initial conditions is active, then $T_{air,in}$ is equal to the initial conditions specified as a parameter. This allows the user to easily specify the initial conditions of the room, which is necessary to determine the transient state.

TYPE 806: Air Cooler – User Specified Heat Removal

Type 806 represents the cooling (or heating) system. It has five inputs, one output and a single parameter. The inputs include mass flow rate, temperature in, heat transfer rate, temperature of the heat source, and a signal for initial conditions. Exiting temperature is the only output; initial temperature is declared as a parameter. The cooling system of any real application would be much more complex than the simple model demonstrated by Type 806, but development of the cooling system is beyond the scope of this project.

Type 806 is governed by Equation 6.12, below. The user can easily specify the rate of heat transfer from the air. The source temperature provides a limit so that the exiting air temperature, T_{out}, always falls in the range between T_{in} and T_{source}.

$$T_{out} = \frac{\dot{Q}}{\dot{m}_{air} c_{P,air}} + T_{in} \qquad 6.12$$

TYPE 807: Partition with Thermal Mass

Type 807 is used to approximate the temperature gradient in the walls surrounding the chamber. It uses convection and radiation from both sides of the wall to get heat flow into the wall. It uses heat flow and the surface temperatures from both sides to compute the new temperatures on each surface and at three intermediary points inside the wall. Table 6.1, below, shows the inputs and outputs for TYPE 807.

TYPE 803			
Inputs:	**units**	**Outputs:**	**units**
Radiation heat transfer, side A	kW	Energy storage in wall	kW
Radiation heat transfer, side B	kW	Heat transfer through wall	kW
Convection heat transfer, side A	kW	Temperature, Side A	C
Convection heat transfer, side B	kW	Temperature, Side B	C
Surface temperature, side A	C	Temperature, Midpoint	C
Surface temperature, side B	C		

Table 6.1: Inputs and outputs associated with TYPE 807

The equations governing the transient behavior of the wall are slightly modified from their source (Incropera and Dewitt 2002), and appear below as Equation 6.13 and 6.14.

$$T_{surface}^{p+1} = \frac{2}{\rho C_p A}\left(q_{radiation} + q_{convection} + \frac{kA}{\Delta x}\left(T_{mid}^{p} - T_{surface}^{p}\right)\right) + T_{surface}^{p} \qquad 6.13$$

$$T_{m}^{p+1} = \frac{\alpha}{(\Delta x)^2}\left(T_{m+1}^{p} + T_{m-1}^{p}\right) + \left(1 - 2\frac{\alpha}{(\Delta x)^2}\right)T_{m}^{p} \qquad 6.14$$

where

$T_{surface}^{p}$ is the temperature of the surface at the current time step

$T_{surface}^{p+1}$ is the temperature of the surface at the future time step

T_{mid}^{p} is the current temperature of the inner wall node

ρ is density

C_p is specific heat capacity of the wall A is the heat transfer area

k is the coefficient of conduction

α is the thermal diffusivity of the wall

Δx is the distance between nodes

$q_{radiation}$ and $q_{convection}$ are the heat transfer rates of the radiation and convection to the surface respectively

T_m^p is the current temperature of a specified node, m

T_m^{p+1} is the future temperature of a specified node, m

These finite difference formulae must meet stability requirements based on the the material properties, Δx, and the time step. If the wall is broken into 4 different nodes, then the chamber wall data meets stability criteria for these functions at time steps below about 1 minute.

The model assumes that the wall is homogenous. Chamber walls at Oklahoma State and at the test facility in Athens are made up primarily of urethane foam with a thin steel skin. Excellent conduction properties and material thinness create a stability criterion for the skin that is on the order of microseconds. Future development of a wall model with more than one section could serve future users of HVACSIM+. The homogenous assumption is necessary to keep the program time step in a semi-reasonable regime.

Connecting the Components

To simulate the system, the components are connected together. Type 807 wall units interface with the room, Type 805, via the forced convection calculator, Type 804, and with the external environment through the free convection calculator, Type 803. Room models can also be used for ducts and plenums. Each Type 805 room model passes outlet temperature to the next room model, or to Type 806 for conditioning purposes.

Simulation of the chamber can be broken down into as many pieces as one would like; however, it is suggested to keep it as simple as possible because the complex algorithm used by HVACSIM+ to solve the system of equations can be difficult to work with. One who wishes to make the model more complex is invited to read about the hierarchal system solver that is incorporated in HVACSIM+ (Clark 1985). The interested engineer will have to analyze how to break the simulation into blocks and superblocks. Adding components to the workspace makes this task ever more important and difficult to accomplish correctly.

Component Validation

After a stand alone test for each component was performed, sets of three or four components were then combined in mock simulations to ensure that component outputs were reasonable. Results were very encouraging, but further validation seemed necessary.

The literature review did not yield much information about typical transition times, nor did it reveal any experimental test results for transient conditions. The best verification that could be found is from the simulation results obtained from Chatzidakis (Chatzidakis, Athienitis et al. 2002).

To begin his simulation, Chatzidakis had the car, or test specimen, inside the test chamber with both the car and chamber at equilibrium with the surrounding, 25 °C, see Figure 6.3. When the simulation is started, the test chamber and the car simultaneously begin their conditioning loops. From the equilibrium point, the car heats its entire volume and contents to its set point of 32.5 °C using a 3 kW capacity heater. Similarly, the chamber cools its contents to a 7.5 °C set point using 20 kW of cooling capacity.

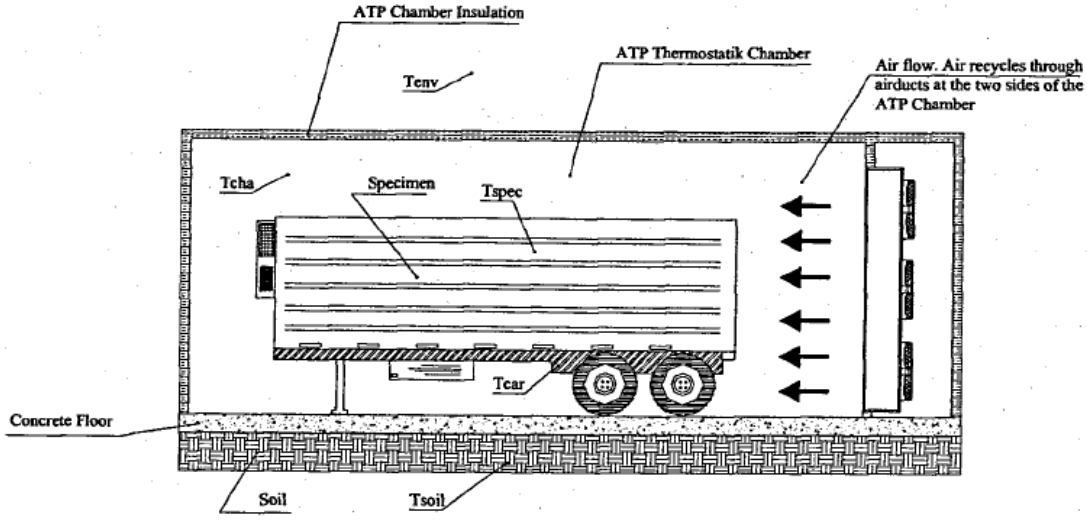

Figure 6.3: Schematic of test chamber in Athens with specimen inside (Chatzidakis, Athienitis et al. 2002).

Although no data points were given, Chatzidakis adequately described the simulation parameters and presented the following graph, Figure 6.4, which shows his simulation results. It took about 1.5 hours for the chamber to reach the set point temperature. The test specimen reached its set point temperature in about half an hour.

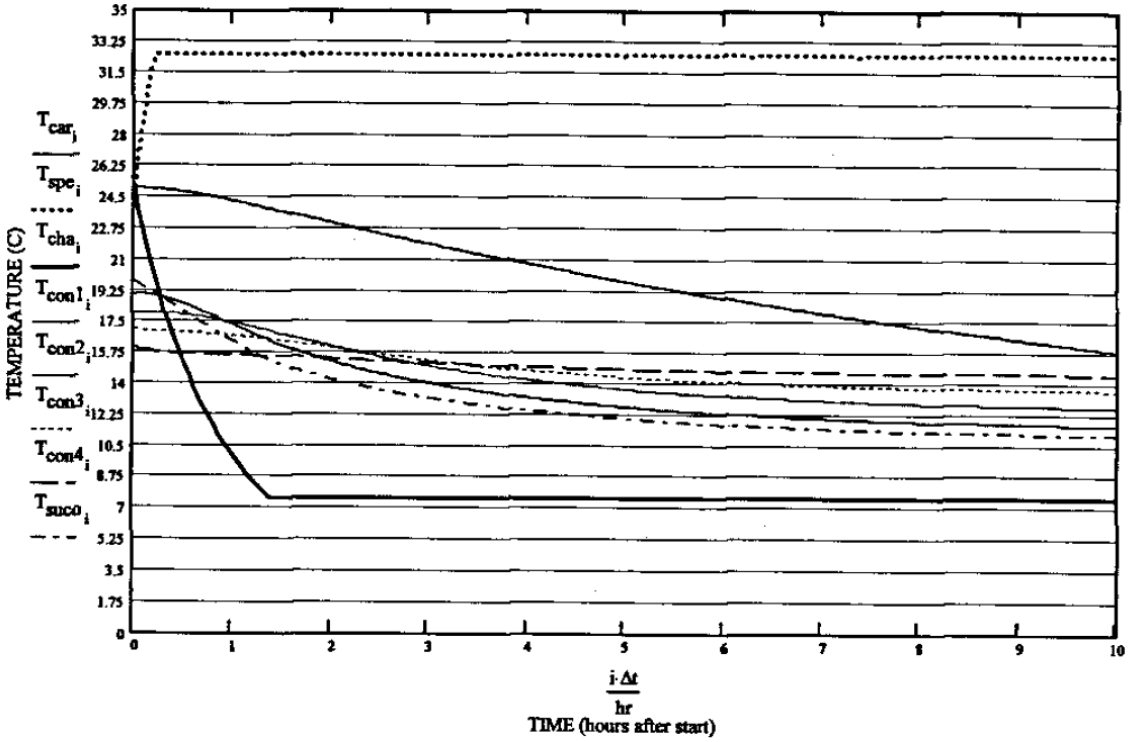

Figure 6.4: Simulation results from Chatzidakis. Note particularly T_{spe}, T_{cha}, T_{con1}, and T_{con3}, representing the car cavity, test chamber, surface concrete and middle concrete temperatures respectively (Chatzidakis, Athienitis et al. 2002)

For validation, Chatzidakis' simulation was mimicked using the developed Type models. The results of the simulation appear in Figure 6.5, the connections can be seen in Appendix D. It can be seen that both the chamber and the test specimen reflect Chatzidakis's results. The variations are likely associated with the minor assumptions of a few parameters not included in Chatzidakis' report; further variation may be due to the difference in approach to solving the problem. This difference is particularly evident when comparing the results of the concrete temperature curves.

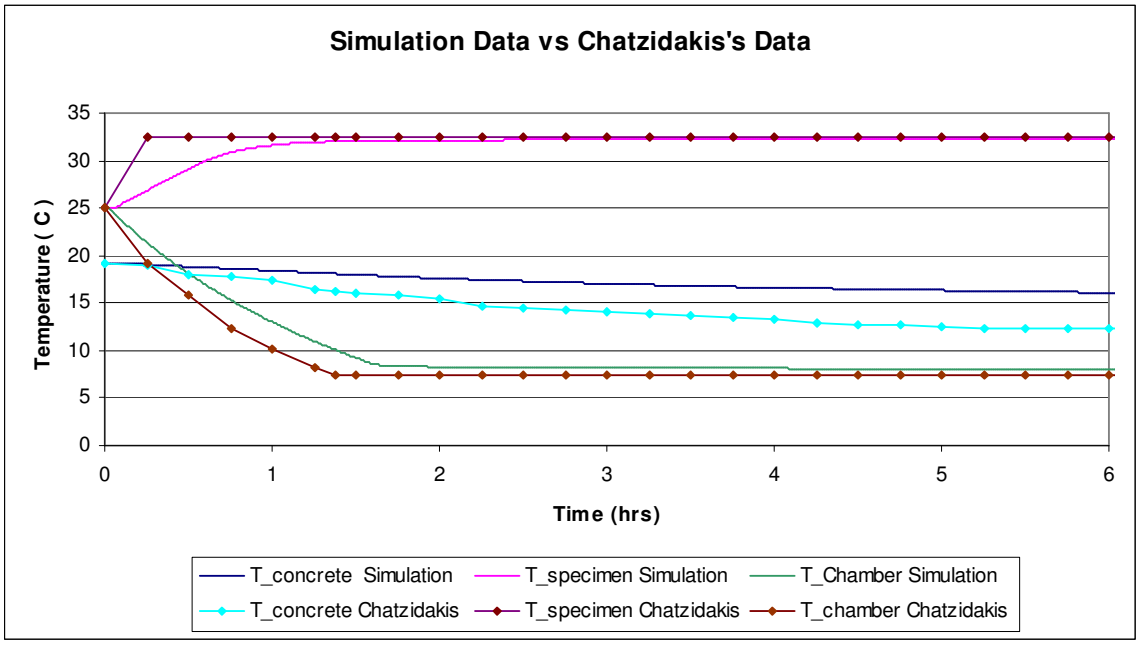

Figure 6.5: Validation results. Simulation modeling results for the chamber in Athens using results from the custom HVACSIM+ program compared to results from Chatzidakis's paper.

Results

Design data from the OSU psychometric room was used to develop a model of the chamber and its ducts. In the OSU chamber, only the outdoor chamber was modeled, no test specimen was inside. The following graph, Figure 6.6, shows the chamber, conditioning loop, and underfoot plenum approach the set point of 7.5 °C from an initial starting condition of 25 °C. The chamber takes the longest to get to the set point, reaching it in about 3 hours.

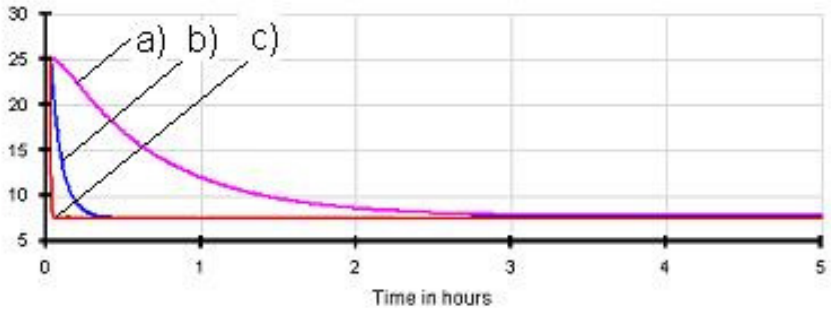

Figure 6.6: Soaking for set point of 7.5°C. a) chamber b) plenum c) conditioning loop

Several other set points were simulated; they appear in Figure 6.7. The model is such that the chamber never really reaches the set point temperature, but hovers very near to it. Figure 6.7 demonstrates that the time it takes for the chamber to reach temperatures that differ from the set point by 1, 2, and 5°C. The results are reasonable; the soaking time from 25°C to within 1° of -40°C is 4.4 hours. Simulations with a set point between -20 and -30°C do not get within 1 degree of the set point. This is likely attributed to the transition of laminar to turbulent convection coefficients.

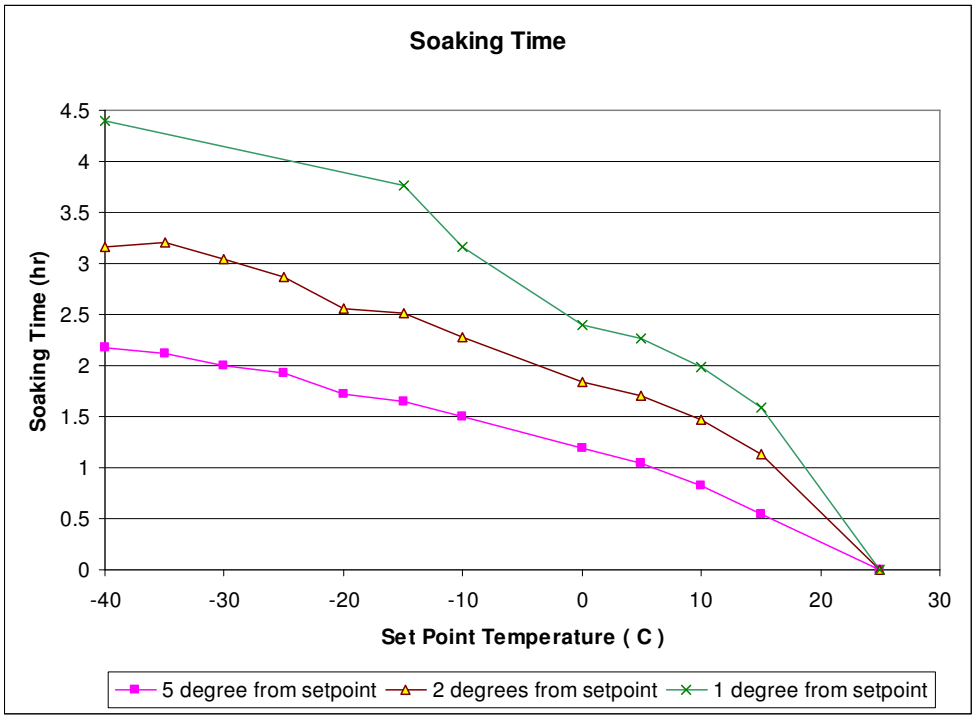

Figure 6.7: Transient time to reach set point based on a 25 °C starting point, note that some setpoints do not get to within 1°C

Simulation was carried out to 10 hours for several set points. The limit of each set point was determined and plotted in Figure 6.8. The figure demonstrates the time it takes for the temperature curve of the chamber to become asymptotic, or for it to reach its temperature limit within two decimal places. It also shows that, with the exception of the -30° set point, the final difference between the set point temperature and the chamber temperature increases with decreasing temperature, which is what would be expected.

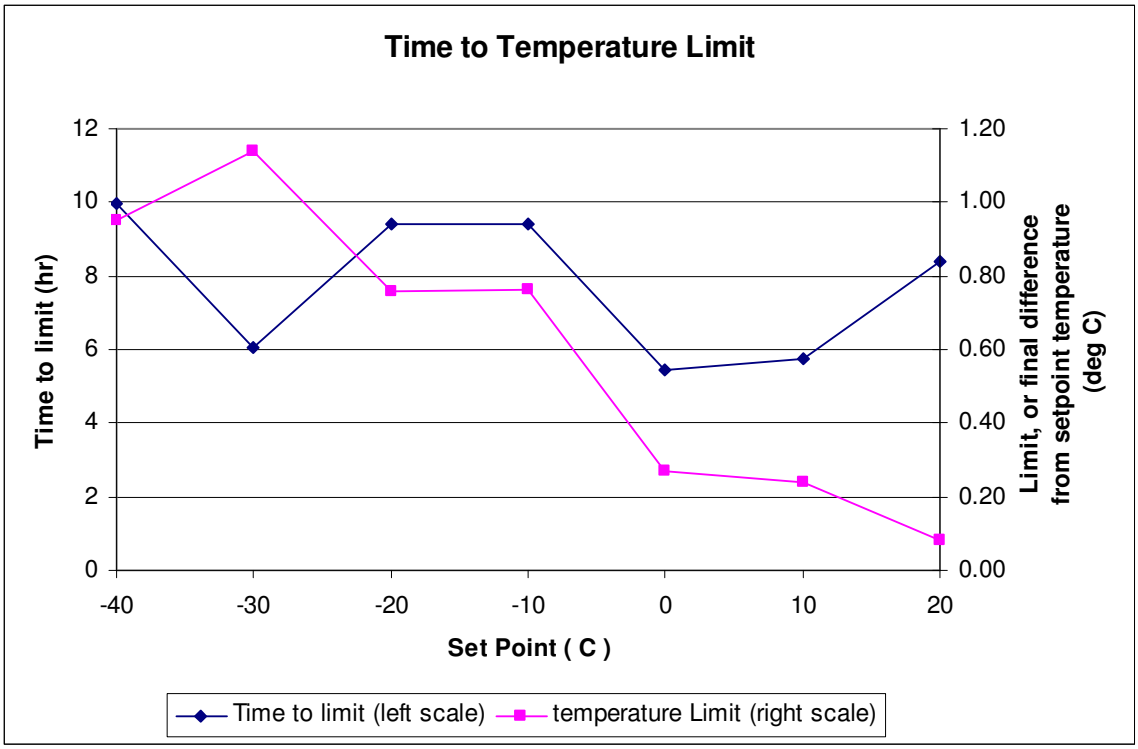

Figure 6.8: Time for chamber temperature curve to become asymptotic and variation from set point temperature at that time.

Sensitivity Analysis

Because the thermo physical properties of the panels are based on some general assumptions, it seems wise to perform a sensitivity analysis on the model to see how sensitive the soaking time is to variations in thermo physical properties of the panels. Three properties were selected for variation: Specific heat capacity, density, and thermal conductivity. These properties were systematically varied according to Table 6.2. The original estimated value for the previous simulations remains as the middle value. The high and low values are +15% and -15% of the middle value respectively, the set point of the chamber is set to 0°C.

Input Parameters				Resuts				
Specific Heat, Cp (kJ/kg-K)	Density (kg/m3)	Thermal Conductivity, k (W/m-K)	run	limit (°C)	Time (minutes) w/in 5°C	w/in 2°C	w/in 1°C	To limit
1.045	70	0.026	OOO	0.58	81.6	143.2	231.6	541.6
1.045	70	0.0299	OO+	0.60	81.6	143.2	233.2	528.2
1.045	70	0.0221	OO -	0.55	81.6	143.2	230.7	552.4
1.045	80.5	0.026	O+O	0.59	82.4	145.7	247.4	560.7
1.045	80.5	0.0299	O++	0.61	82.4	145.7	249.1	554.1
1.045	80.5	0.0221	O+ -	0.57	82.4	145.7	246.6	565.7
1.045	59.5	0.026	O - O	0.57	81.6	139.9	217.4	500.8
1.045	59.5	0.0299	O - +	0.60	81.6	139.9	218.3	475.8
1.045	59.5	0.0221	O - -	0.54	81.6	139.9	216.6	524.1
1.20175	70	0.026	+OO	0.59	82.4	145.7	247.4	560.7
1.20175	70	0.0299	+O+	0.61	82.4	145.7	249.1	554.1
1.20175	70	0.0221	+O -	0.57	82.4	145.7	246.6	565.7
1.20175	80.5	0.026	++O	0.61	**82.5**	**149.1**	266.6	571.6
1.20175	80.5	0.0299	+++	**0.63**	**82.5**	**149.1**	**268.3**	568.3
1.20175	80.5	0.0221	++ -	0.59	**82.5**	**149.1**	265.0	**575.0**
1.20175	59.5	0.026	+ - O	0.58	81.6	142.4	229.9	537.4
1.20175	59.5	0.0299	+ - +	0.60	81.6	142.4	230.7	522.4
1.20175	59.5	0.0221	+ - -	0.55	81.6	142.4	228.2	549.1
0.88825	70	0.026	- OO	0.57	81.6	139.9	217.4	500.8
0.88825	70	0.0299	-O+	0.60	81.6	139.9	218.3	475.8
0.88825	70	0.0221	- O -	0.54	81.6	139.9	216.6	524.1
0.88825	80.5	0.026	- +O	0.58	81.6	142.4	229.9	537.4
0.88825	80.5	0.0299	- ++	0.60	81.6	142.4	230.7	522.4
0.88825	80.5	0.0221	- + -	0.55	81.6	142.4	228.2	549.1
0.88825	59.5	0.026	- - O	0.58	**81.1**	136.9	206.1	437.8
0.88825	59.5	0.0299	- - +	0.61	**81.1**	136.9	206.9	**406.1**
0.88825	59.5	0.0221	- - -	**0.54**	**81.1**	**136.1**	**205.3**	473.6
High and Low (+, -) inputs vary by +/- 15% from middle value (O)			max	0.63	82.5	149.1	268.3	575.0
			min	0.54	81.1	136.1	205.3	406.1
		Maximum difference		0.09	1.4	13.0	63.0	168.9

Table 6.2: Input parameters and results for analysis of model sensitivity to variation in thermo physical properties

Results of these variations also appear in Table 6.2. Maximum and minimum overall changes in soaking time and temperature limits correspond closely to the runs where all variables were set at their corresponding high and low values, respectively.

In order to see if one property had a larger influence than another, each property was plotted for its low, middle, and high value while holding constant the other two properties. Figure 6.9, 6.10, 6.11 displays the results corresponding to the time it takes for the chamber to transition to 1°C, or within one degree of the set point temperature.

Figure 6.9 demonstrates that, while holding density and specific heat constant, the thermal conductivity a weak effect on the soaking time. Increasing the thermal conductivity from the lowest to highest value, or 30% of the nominal value, only increases the soaking time approximately 5 minutes, or about 2% of the nominal 232 minutes. Contrastingly, increasing the specific heat or density, while keeping other properties constant, results in a 35 minute increase in soaking time between the low and high values, as seen in Figure 6.10 and 6.11. The data reveals that on average, a 15% change in density or specific heat is proportional to a 43% change in soaking time.

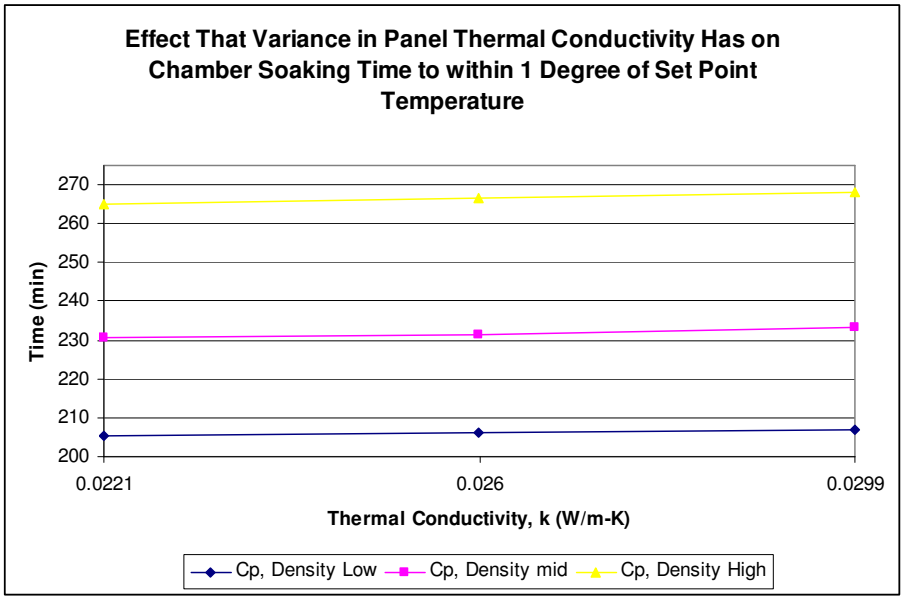

Figure 6.9: Effect that variance in panel thermal conductivity has in the chamber soaking time to within one degree of the set point temperature

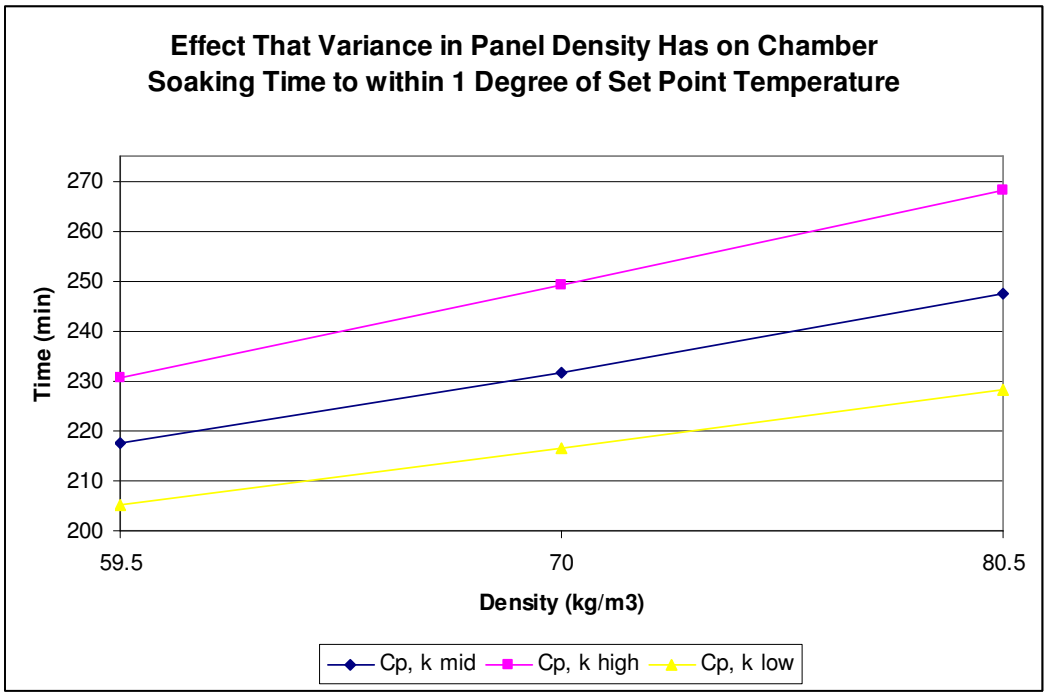

Figure 6.10: Effect that variance in panel density has in the chamber soaking time to within one degree of the set point temperature

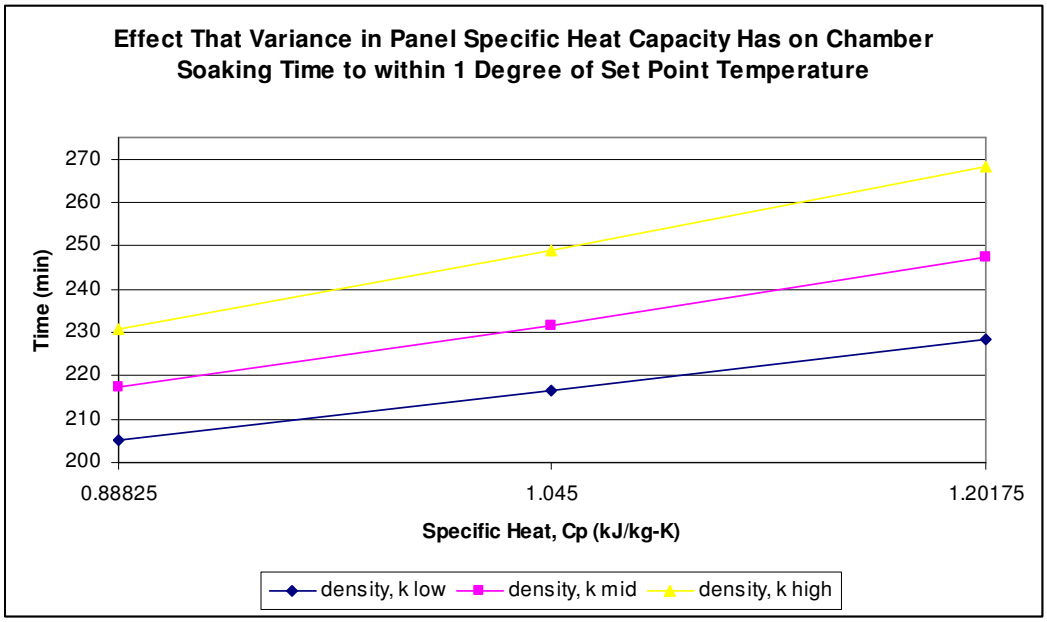

Figure 6.11: Effect that variance in panel specific heat capacity has in the chamber soaking time to within one degree of the set point temperature

The reason behind the similarity in simulation results when changing density or specific heat can be seen in Equations 6.13, and 6.14, both of these variables appear as a

product of each other, therefore a 15% change in either makes an identical change in either equation. Contemplating how the equations are working sheds light on the results that appear in the above figures. The reason that these variables increase the soaking time is that, with every time step, the updated temperature is undershooting the overall change. Therefore, the overall time to reach the set point temperature is increased.

Although the thermal conductivity does not seem to play a significant role in the simulated soaking time, it is more significant than the density and specific heat in determining the temperature limit; this significance can be seen in Figures 6.12 and 6.13. The temperature limit was determined by running the simulation to 10 hours. After simulating 10 hours of operation, the temperature has clearly reached an asymptotic value, which differs from the set point temperature. In other words, the temperature limit is the steady state value of the simulation.

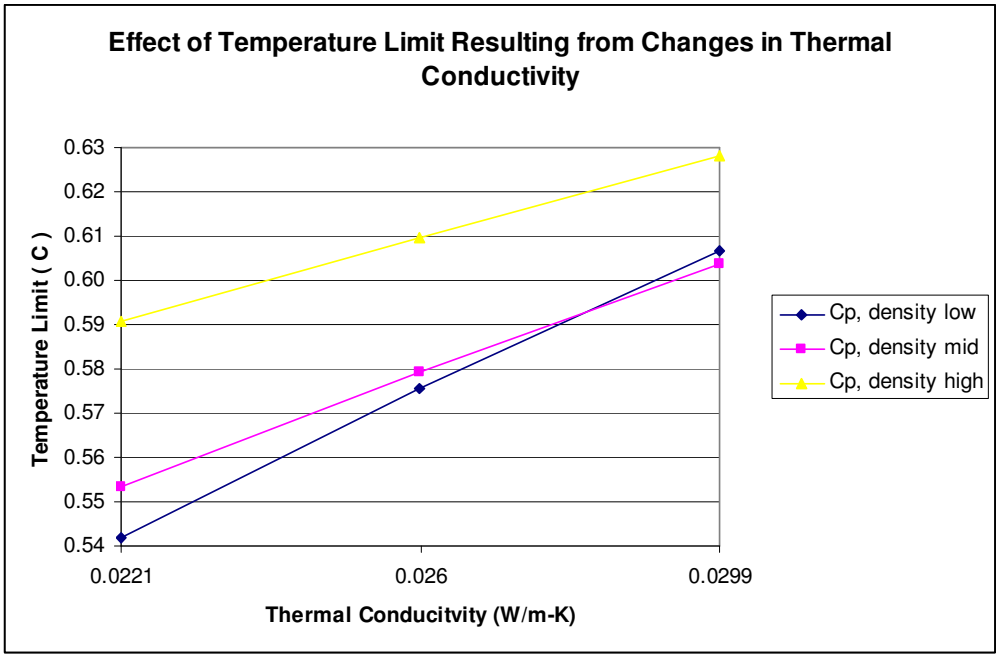

Figure 6.12: Effect of temperature limit resulting from changes in thermal conductivity

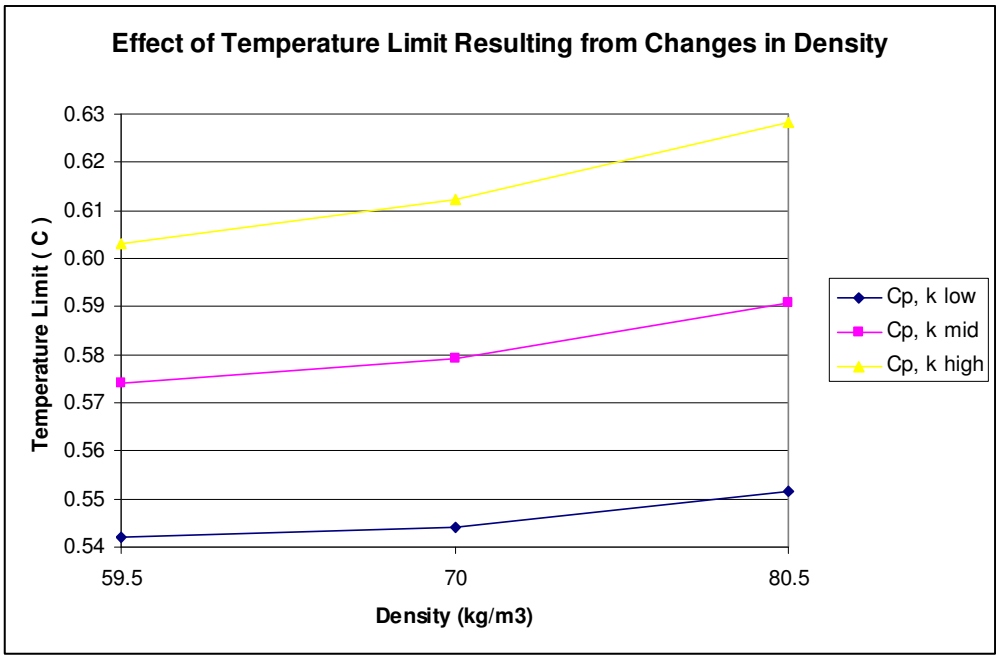

Figure 6.13: Effect of temperature limit resulting from changes in Density

Figures 6.12 and 6.13 demonstrate that on average, a 15% increase in the thermal conductivity results in a 4% increase in the temperature limit; whereas a 15% increase in either the density or the specific heat capacity only increases the temperature limit by 1%. Furthermore, this increase in temperature limit corresponds to a decrease in the time it takes to reach the temperature limit in the case of the thermal conductivity, as seen in Figure 6.14. Intuitively, this makes sense because the temperature limit is closer to the initial conditions. The figure also demonstrates that, in the case of increasing density or specific heat, the time it takes to get to the temperature limit increases, correlates to the increasing need in energy to change the temperature of the unit.

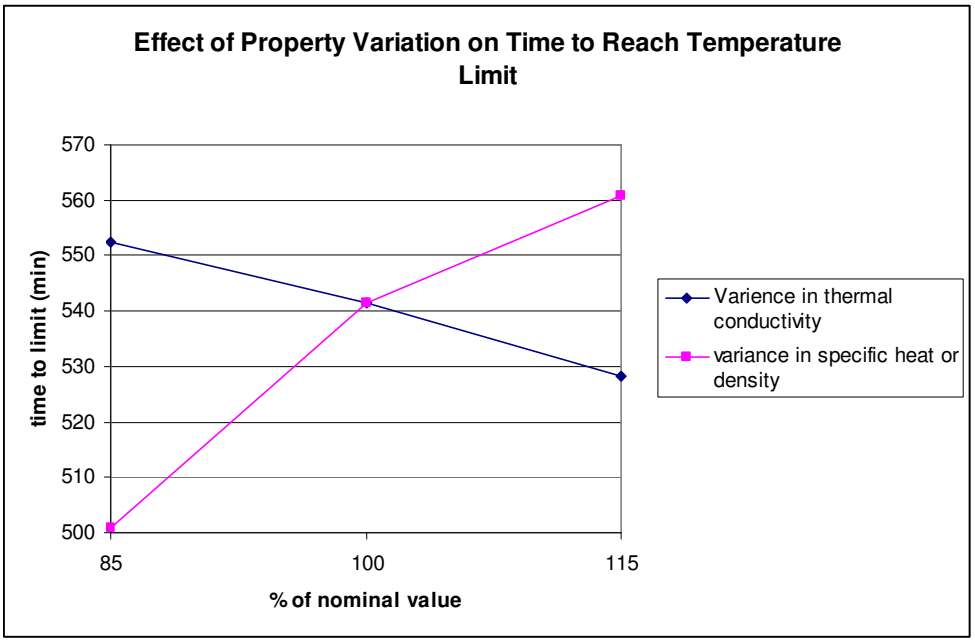

Figure 6.14: Effect of property variation on time it takes for simulation to reach the temperature limit. Values correspond to the middle range setting settings of the variables that are held constant.

Modeling Conclusions

In this section, several method of building simulation have been researched and discussed. Type subroutines have successfully been developed and implemented for use in the transient model of the OSU psychrometric chamber. Data has been used to validate the model. The projected soaking time for various temperatures is estimated. In practice, the actual soaking time of the chamber will depend on the control methods implemented; however, it this model should provide a good estimate. A sensitivity model gives some insight into the importance of selecting appropriate thermo physical properties of the panels when modeling the chamber.

CHAPTER VII

CONCLUSION AND FUTURE RESEARCH

A comprehensive design of the psychrometric chamber structure has been developed; including the design of a mezzanine, trolley crane, and staging area. The chamber has been constructed in the basement and of the ATRC on the OSU campus. As part of the construction, the mechanical components of the chamber have been installed. These components include the cooling coils and associated hydronic system, heating coils, and supporting electrical items. A model of the chamber soaking time has also been developed and validated using a model found in the literature.

Specifically conclusions of this thesis are as follows:

- A new psychrometric chamber at OSU was designed and constructed. The structure consists of two adjacent rooms, one to simulate outdoor climate conditions and the other to replicate the indoor environments of residential and commercial buildings.
    - The constructed chamber, with dimensions of 25’ x 40’ x 20’, sits in the basement of the Advanced Technology Research Center on the Oklahoma State University, Stillwater campus.

- The designed chamber temperature rage is -40 to130°F (-40 to 54 °C) and 10 to 90% relative humidity. Maximum capacity is approximately 15 tons (52.7 kW). Maximum airflow rate is approximately 8000cfm.
- The chamber consists of sheet metal panels filled with a polyurethane foam core. The average thermal conductivity of the panels is estimated to be 0.026 - 0.033 W/m-K (0.015 - 0.019 Btu/hr-ft-F). Simulation analysis suggests chamber operation down to about -25°F (-32°C) before formation of condensate on the exterior walls.

- A mezzanine and crane lift were also designed and constructed. The mezzanine houses much of the conditioning equipment; the crane has a capacity of 4,000 lbs. A staging area has also been designed.
- A literature review of the existing knowledge in the field revealed that air enthalpy methods, described in the ARI standard 210 and ASHRAE standard 116, is the most suitable method for testing units. The chamber was specifically designed with these methods in mind for testing split system and unitary equipment.
- Hydronic cooling loops for indoor and outdoor chambers were designed and installed. Dynalene HC-50, with a freezing temperature of -58°F (-50°C), is used in the outdoor loop to allow good heat transfer at low temperature; water is the heat transfer fluid of the indoor loop

- Based on preliminary simulations using customized subroutines in HVACSIM+, the soaking time of the chamber from 25 to 0°C (77 to 32°F) is expected to be about 2.5 hours. The soaking time down to -40°F is approximately 4 hours.
- A sensitivity analysis demonstrated a correlation between increasing soaking time and increasing density and specific heat values. Increasing thermal conductivity corresponded to an increase in the steady state temperature.
- The chamber structure and supporting systems have been constructed and await operation.

Much work has been completed on the OSU psychrometric chamber, this thesis outlines the design and construction, up to chamber start up. However, this is not the end of the work and research that could be done concerning the chamber; much more research could be done to better understand and improve the operating psychrometric chamber.

Future Work and Research

Calibration

I suspect that the next student to take on this project will have his hands full as he or she tries to get the chamber to respond correctly to changes in load and set point. Just maintaining conditions with no live thermal load will present a significant challenge; which, I believe, will increase as the set point temperature diverges from ambient conditions. A significant control issue will be when the set point of the chamber is right around freezing and frost begins to form on the cooling coils. Switching outdoor

conditioning loops to defrost mode while maintaining conditions will require some innovation.

As currently operating, the psychrometric chamber will only be able to reach about 55°F. The airflow laboratory has a chiller that may be connected to the chamber to bring it down to about -10°F. This chiller has a small capacity, but could definitely be used in heat pump testing. It is suggested that, as funds permit, a chiller dedicated to the chamber be purchased. This chiller should approach -50°F if the -40°F set point is to be reached inside the chamber. This chiller could be connected to the chamber cooling loop through the heat exchanger; however the losses associated with the heat exchanger may warrant the direct connection of the chiller into the cooling line.

Modeling

Future research work in modeling the complete chamber system could yield interesting results and will likely allow one to make suggestions to options for changes in the operations and control of the chamber.

Control. The most obvious modeling that would have significant benefit is the modeling of the control of the chamber; this may be done in parallel with the calibration of the chamber. Modeling the control and operation of the chamber will give better understanding to the options for control and may allow the optimization for control. The optimization could be focused on energy saving measure or on the best way to maintain the set point.

Coil Frosting. Much is still not understood about frost accumulation on coils. Modeling this aspect of the chamber could help in other areas of the HVAC&R field. In any case, modeling this phenomenon would give way to better prediction for defrosting method of the chamber conditioning coils.

Airflow. As currently built, the airflow patterns inside the chamber are a speculation of how it should behave. Modeling the airflow in a CFD program should give ways to improve the uniformity of the airflow throughout the chamber.

This list is not exhaustive, several other points of interest could be touched on concerning the chamber. But, again the key research is not with the chamber itself, but with the research that will go on inside its walls.

REFERENCES

AHRI (2008). ARI Standard 210/240: Performance Rating of Unitary Air-Conditioning & Air-Source Heat Pump Equipment. Arlington, VA, Air-Conditioning, Heating, and Refrigeration Institute.

Armstrong, P. R., S. B. Leeb, et al. (2006). Control with building mass - Part II: Simulation, Chicago, IL, United States, Amer. Soc. Heating, Ref. Air-Conditoning Eng. Inc., Atlanta, GA 30329, United States.

ASHRAE (1993). 1993 ASHRAE Handbook Fundamentals I-P Edition. Atlanta, GA, American Society of Heating, Refrigeration and Air-Conditioning Engineers, Inc.

ASHRAE (1995). Standard 116 -1995: Methods of Testing for Rating of Seasonal Efficiency of Unitary Air Conditioners and Heat Pumps, American Society of Heating, Refrigerating, and Air-conditioning Engineers, Inc.

Brandemuehl, M. J., M. J. Lepore, et al. (1990). Modeling and testing the interaction of conditioned air with building thermal mass, St. Louis, MO, USA, Publ by ASHRAE, Atlanta, GA, USA.

Chatzidakis, S. K., A. K. Athienitis, et al. (2002). "A Numerical Simulation Study of a New Environmental Chamber." ASHRAE Transaction 108: 113-118.

Clark, D. R. (1985). HVACSIM+ Building Systems and Equipment Simulation Program Reference Manual. Gaithersburg, MD, United States Department of Commerce.

Clark, D. R., C. W. Hurley, et al. (1985). DYNAMIC MODELS FOR HVAC SYSTEM COMPONENTS, Chicago, IL, USA, ASHRAE, Atlanta, GA, USA.

Clark, D. R. and W. B. May (1985). HVACSIM+ Building Systems and Equipment Simulation Program - User's Guide. Gaithersburg, United States Department of Commerce.

Cremaschi, L. and E. Lee (2008). "Design and Heat Transfer Analysis of a New Psychrometric Environmental Chamber for Heat Pump and Refrigeration Systems Testing." ASHRAE Transaction 114(2): 619-631.

Incropera, F. P. and D. P. Dewitt (2002). Fundamentals of Heat and Mass Transfer. Hoboken, New Jersey, John Wiley & Sons, Inc.

Kasahara, M., Y. Kuzuu, et al. (2000). "Physical model of an air-conditioned space for control analysis." ASHRAE Transactions 106 (PA: 304-317.

NCDC, N. C. D. C. and U. S. D. o. Commerce. (2009, November 8, 2007). "NOAA Satellite and Information Service." Retrieved January 6, 2009, from http://www.ncdc.noaa.gov/oa/climate/globalextremes.html#lowpre.

Park, C., D. R. Clark, et al. An Overview of HVACSIM+, A Dynamic Building/HVAC/Control Systems Simulation Program. Gaithersburg, MD.

Park, C., D. R. Clark, et al. (1986). HVACSIM+ Building Systems and Equipment Simulation Program: Building Loads Calculation. Gaithersburg, MD, United States Department of Commerce.

Shigley, J. E. and C. R. Mischke (2002). Mechanical Engineering Design. Boston, McGraw-Hill.

Sowell, E. E. and P. Haves (2001). "Efficient solution strategies for building energy system simulation." Energy and Buildings **33**(4): 309-317.

Sowell, E. F. (1989). General zone model for HVACSIM/sup +/. User's manual. UK, Univ. Oxford.

Sowell, E. F. and D. C. Hittle (1995). Evolution of building energy simulation methodology, Chicago, IL, USA, ASHRAE, Atlanta, GA, USA.

Strand, R. K., D. E. Fisher, et al. (2002). Modular HVAC simulation and the future integration of alternative cooling systems in a new building energy simulation program, Honolulu, HI, United States, Amer. Soc. Heating, Ref. Air-Conditoning Eng. Inc.

Tom, S., Ph.D., P.E. (2008). "Managing Energy And Comfort." ASHRAE Journal(June): 18-26.

APPENDICES

Appendix A: Chamber Parts

The complete chamber design is too complex to include here. The complete chamber structure assembly contains about 4,900 parts. This number is comprised of 400 unique part numbers. This appendix contains a sampling of these parts. The parts were designed at AAON, but were drafted later using a demo version of Solid Edge; please excuse the water mark.

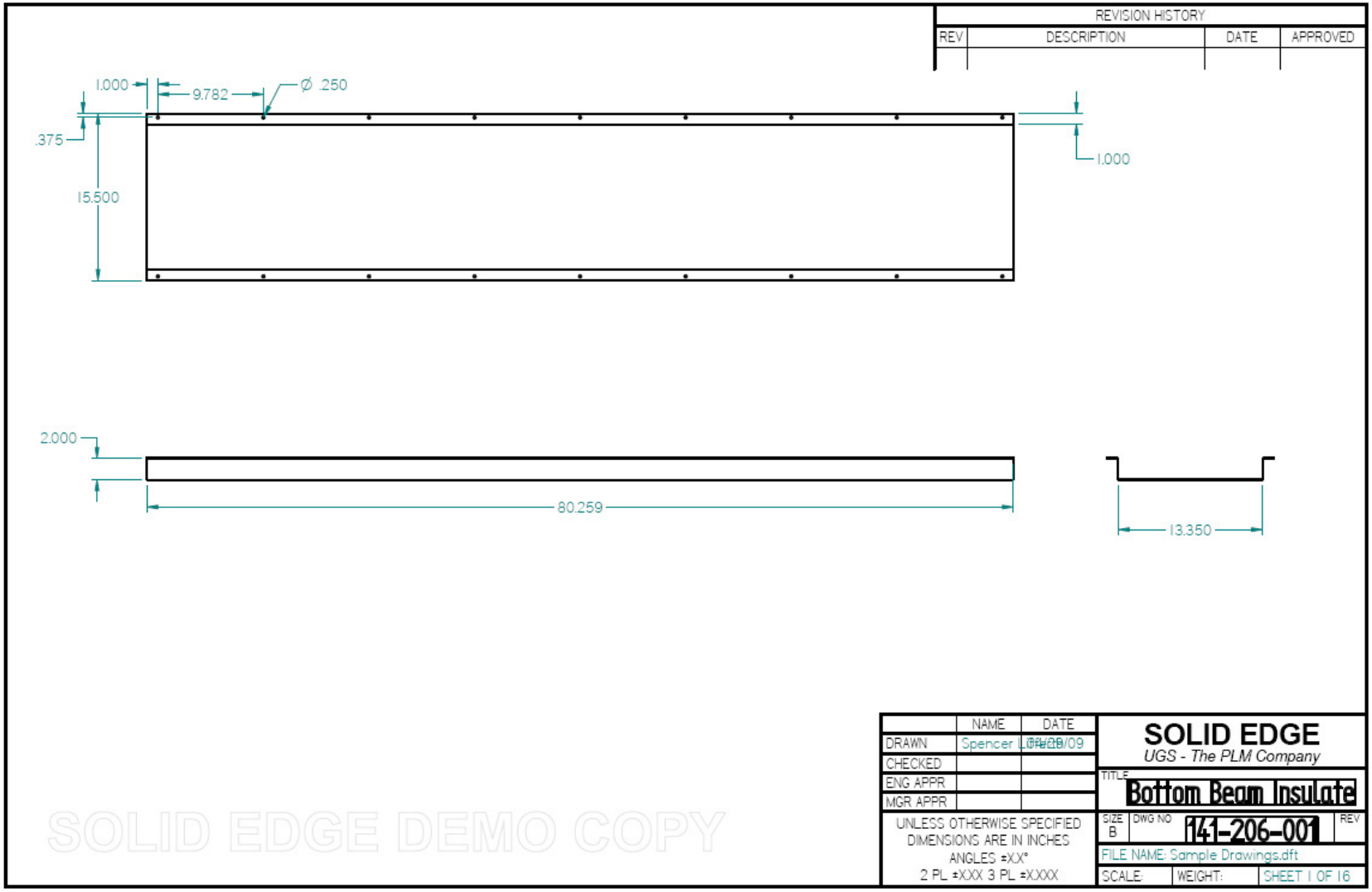
REVISION HISTORY
REV
DESCRIPTION
DATE
APPROVED
1.000
9.782
Ø .250
.375
15.500
1.000
2.000
80.259
13.350
NAME
DATE
DRAWN
Spencer Lott
4/28/09
CHECKED
ENG APPR
MGR APPR
UNLESS OTHERWISE SPECIFIED
DIMENSIONS ARE IN INCHES
ANGLES ±X.X°
2 PL ±X.XX 3 PL ±X.XXX
SOLID EDGE
UGS - The PLM Company
TITLE
Bottom Beam Insulate
SIZE
B
DWG NO
141-206-001
REV
FILE NAME: Sample Drawings.dft
SCALE:
WEIGHT:
SHEET 1 OF 16
SOLID EDGE DEMO COPY

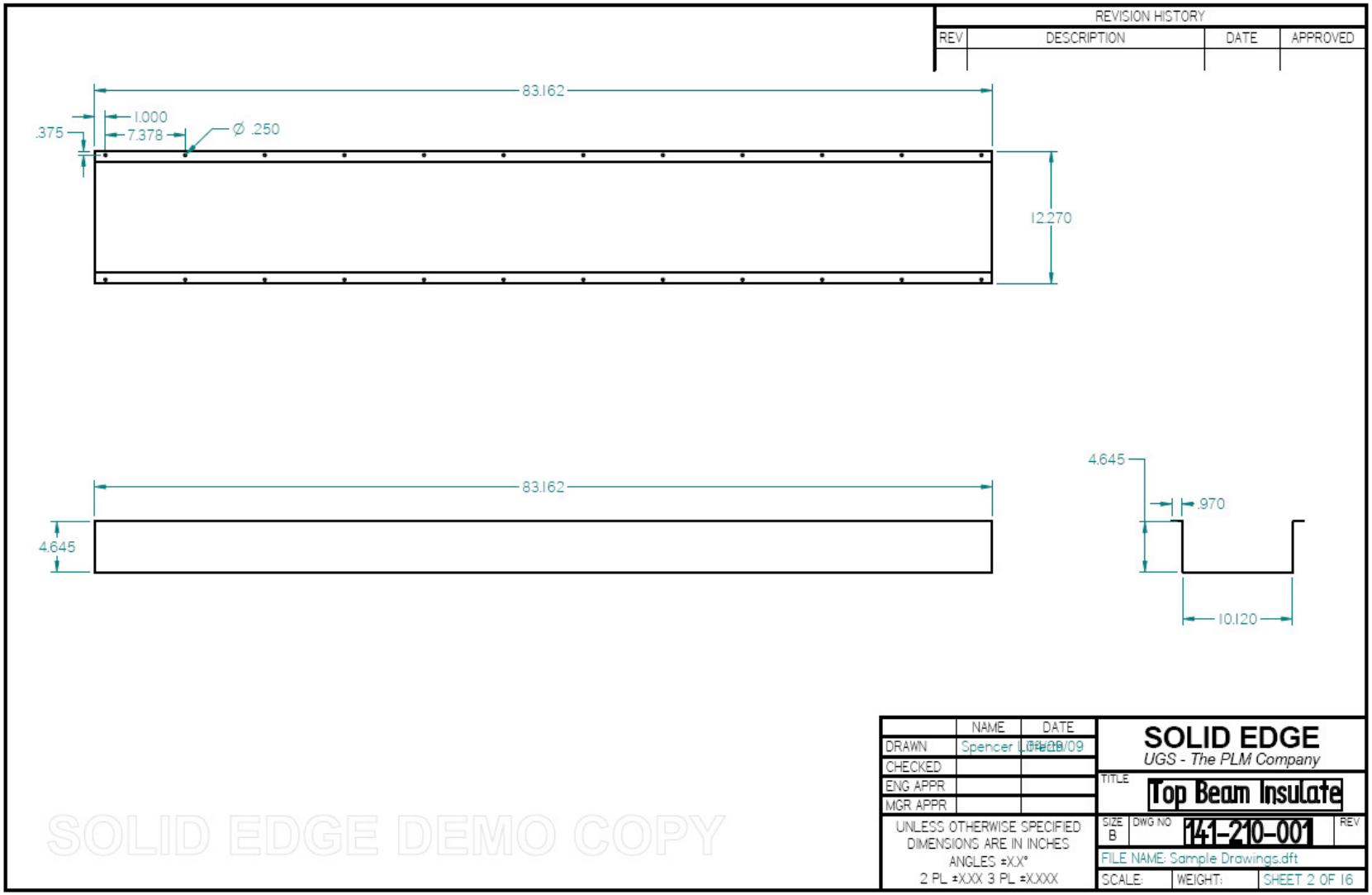
REVISION HISTORY
REV
DESCRIPTION
DATE
APPROVED
83.162
1.000
7.378
Ø .250
.375
12.270
83.162
4.645
4.645
.970
10.120
NAME
DATE
DRAWN
Spencer L. Pace
CHECKED
ENG APPR
MGR APPR
UNLESS OTHERWISE SPECIFIED
DIMENSIONS ARE IN INCHES
ANGLES ±X.X°
2 PL ±X.XX 3 PL ±X.XXX
SOLID EDGE
UGS - The PLM Company
TITLE
Top Beam Insulate
SIZE
B
DWG NO
141-210-001
REV
FILE NAME: Sample Drawings.dft
SCALE:
WEIGHT:
SHEET 2 OF 16
SOLID EDGE DEMO COPY

REVISION HISTORY			
REV	DESCRIPTION	DATE	APPROVED

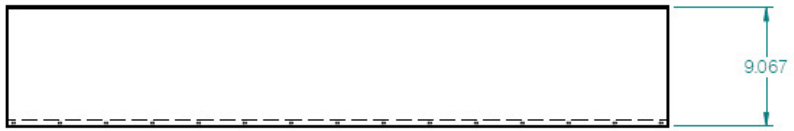

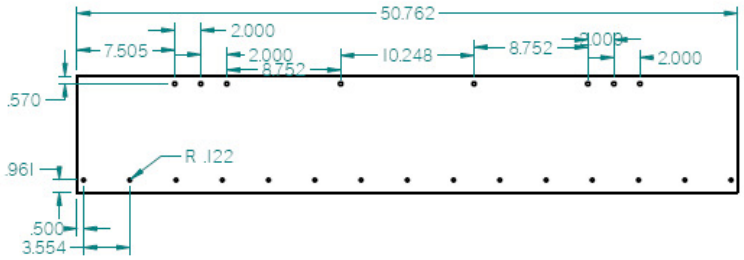

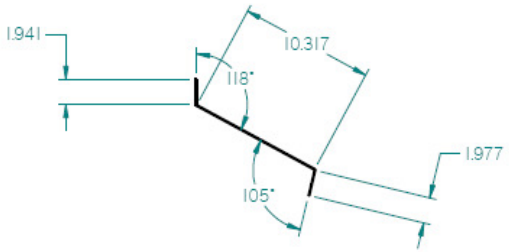

	NAME	DATE
DRAWN	Spencer L	3/4/09
CHECKED		
ENG APPR.		
MGR APPR.		

UNLESS OTHERWISE SPECIFIED
DIMENSIONS ARE IN INCHES
ANGLES ±X.X°
2 PL ±.XXX 3 PL ±.XXXX

SOLID EDGE
UGS - The PLM Company

TITLE: Coil Support Rail

SIZE: B | DWG NO: 142-190-001 | REV:

FILE NAME: Sample Drawings.dft

SCALE: | WEIGHT: | SHEET 3 OF 16

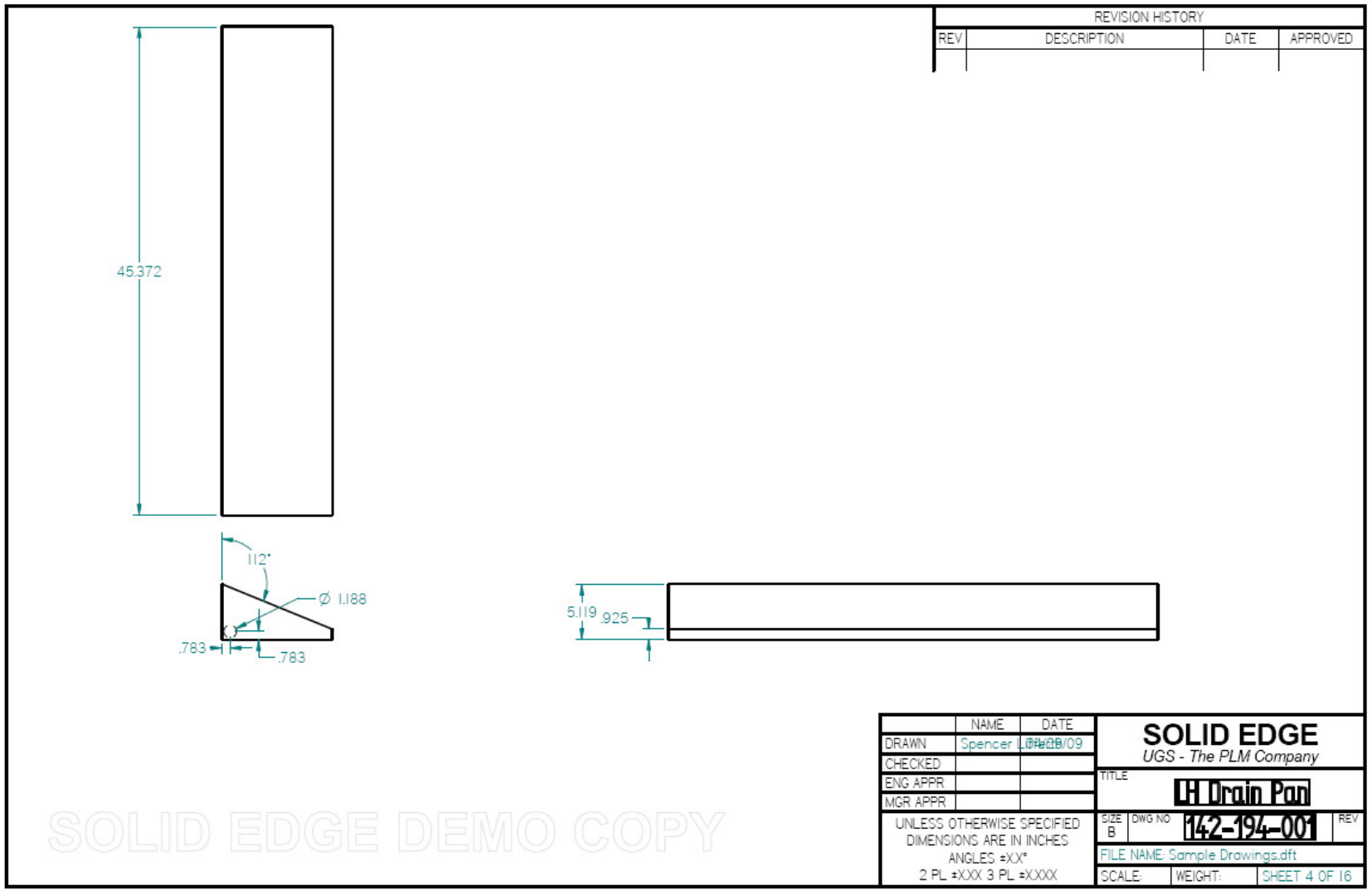
REVISION HISTORY
REV
DESCRIPTION
DATE
APPROVED
45.372
112°
Ø 1.188
.783
.783
5.119
.925
NAME
DATE
DRAWN
Spencer Lofthus
CHECKED
ENG APPR
MGR APPR
UNLESS OTHERWISE SPECIFIED
DIMENSIONS ARE IN INCHES
ANGLES ±X.X°
2 PL ±.XXX 3 PL ±.XXXX
SOLID EDGE
UGS - The PLM Company
TITLE
LH Drain Pan
SIZE
B
DWG NO
142-194-001
REV
FILE NAME: Sample Drawings.dft
SCALE:
WEIGHT:
SHEET 4 OF 16
SOLID EDGE DEMO COPY

REVISION HISTORY			
REV	DESCRIPTION	DATE	APPROVED

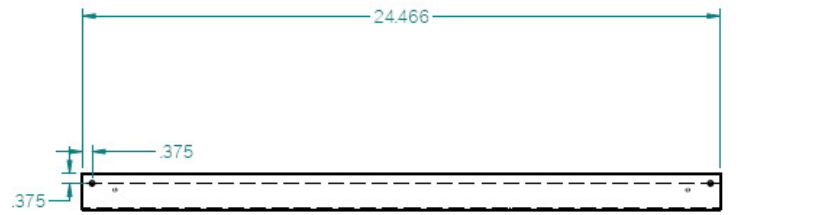

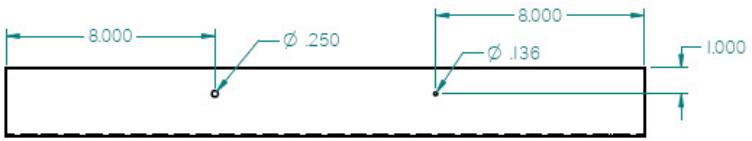

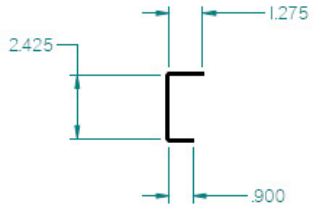

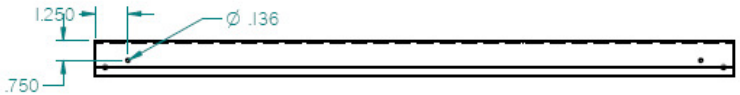

	NAME	DATE
DRAWN	Spencer Lopez	10/29/09
CHECKED		
ENG APPR.		
MGR APPR.		

UNLESS OTHERWISE SPECIFIED
DIMENSIONS ARE IN INCHES
ANGLES ±X.X°
2 PL ±.XXX 3 PL ±.XXX

SOLID EDGE
UGS - The PLM Company

TITLE: Grate Channel

SIZE: B | DWG NO: 141-258-001 | REV:

FILE NAME: Sample Drawings.dft

SCALE: | WEIGHT: | SHEET 5 OF 16

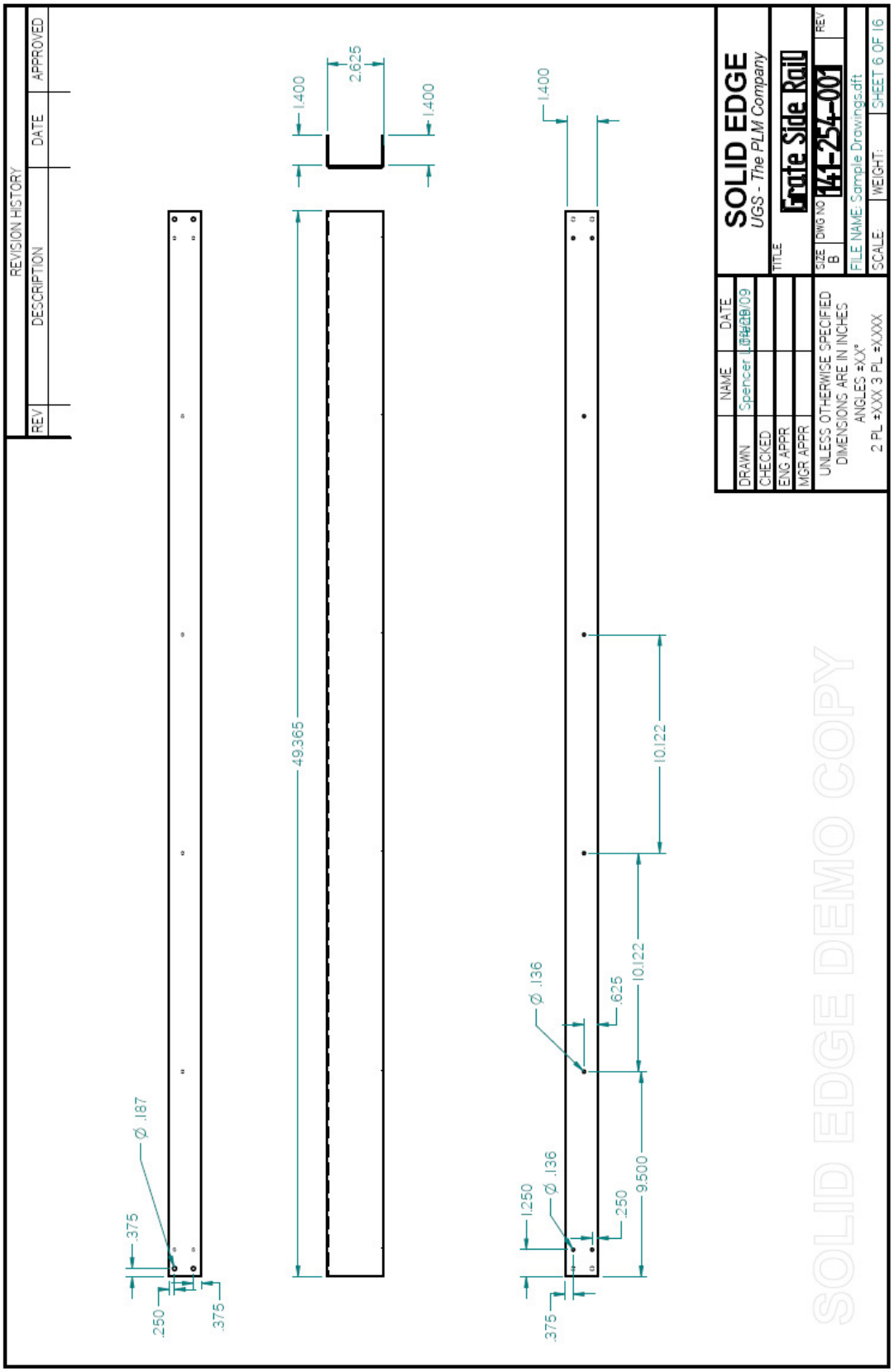
REVISION HISTORY
REV
DESCRIPTION
DATE
APPROVED
SOLID EDGE
UGS - The PLM Company
NAME
DATE
DRAWN
Spencer L
CHECKED
ENG APPR
MGR APPR
TITLE
Grate Side Rail
SIZE
B
DWG NO
141-254-001
REV
UNLESS OTHERWISE SPECIFIED
DIMENSIONS ARE IN INCHES
ANGLES ±X.X°
2 PL ±.XXX 3 PL ±.XXXX
FILE NAME Sample Drawings.dft
SCALE
WEIGHT:
SHEET 6 OF 16
1.400
2.625
1.400
49.365
1.400
10.122
10.122
Ø .136
.625
Ø .187
.375
1.250
Ø .136
.250
9.500
.250
.375
.375
SOLID EDGE DEMO COPY

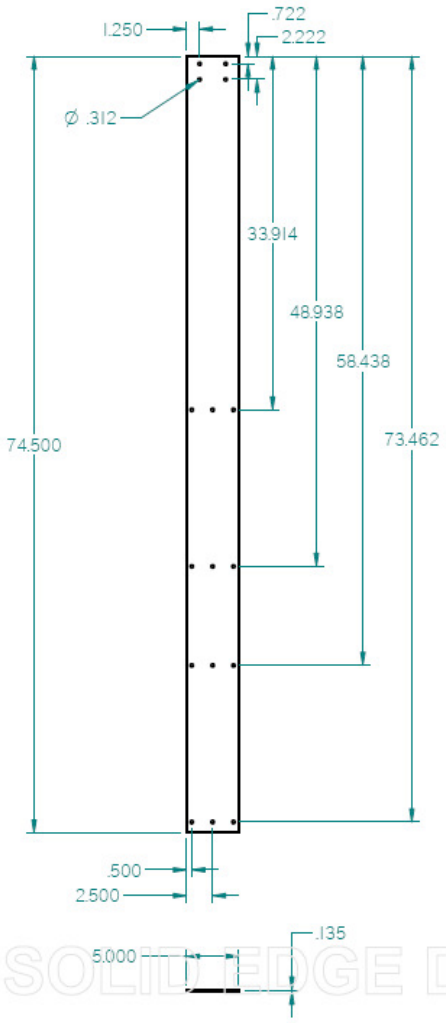

REVISION HISTORY			
REV	DESCRIPTION	DATE	APPROVED

	NAME	DATE
DRAWN	Spencer L. Hall	3/4/09
CHECKED		
ENG APPR		
MGR APPR		

UNLESS OTHERWISE SPECIFIED
DIMENSIONS ARE IN INCHES
ANGLES ±X.X°
2 PL ±.XXX 3 PL ±.XXX

SOLID EDGE
UGS - The PLM Company

TITLE: Coil Hanger Bar

SIZE: B | DWG NO: 142-216-001 | REV:

FILE NAME: Sample Drawings.dft

SCALE: | WEIGHT: | SHEET 7 OF 16

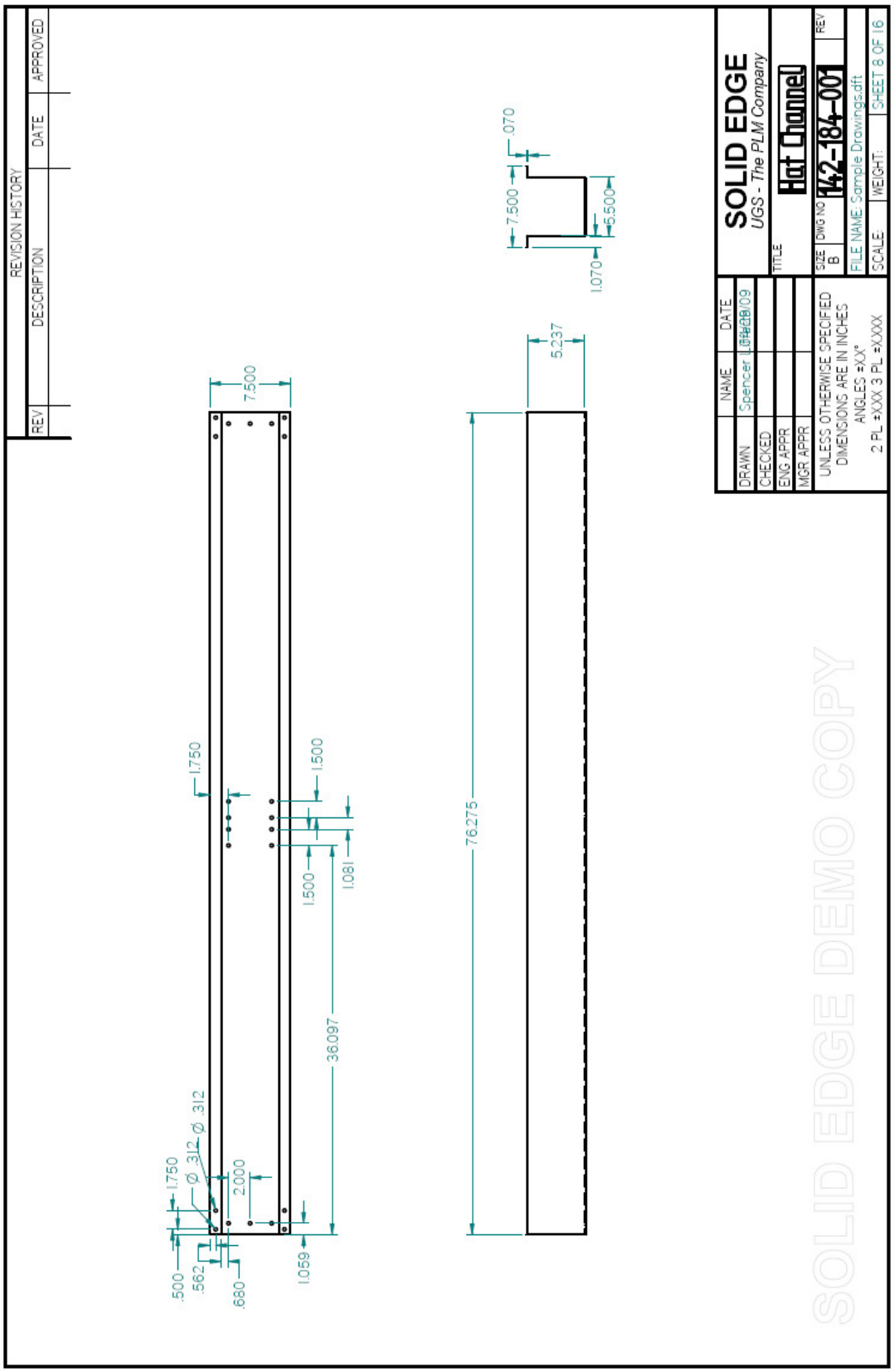
REVISION HISTORY
REV
DESCRIPTION
DATE
APPROVED
7.500
1.750
1.500
1.500
1.081
36.097
1.750
Ø .312
Ø .312
2.000
.500
.562
.680
1.059
76.275
5.237
.070
7.500
5.500
1.070
SOLID EDGE
UGS - The PLM Company
DRAWN
CHECKED
ENG APPR
MGR APPR
NAME
DATE
Spencer L
28/09
TITLE
Hat Channel
UNLESS OTHERWISE SPECIFIED
DIMENSIONS ARE IN INCHES
ANGLES ±X.X°
2 PL ±.XXX 3 PL ±.XXXX
SIZE
B
DWG NO
142-184-001
REV
FILE NAME Sample Drawings.dft
SCALE
WEIGHT:
SHEET 8 OF 16
SOLID EDGE DEMO COPY

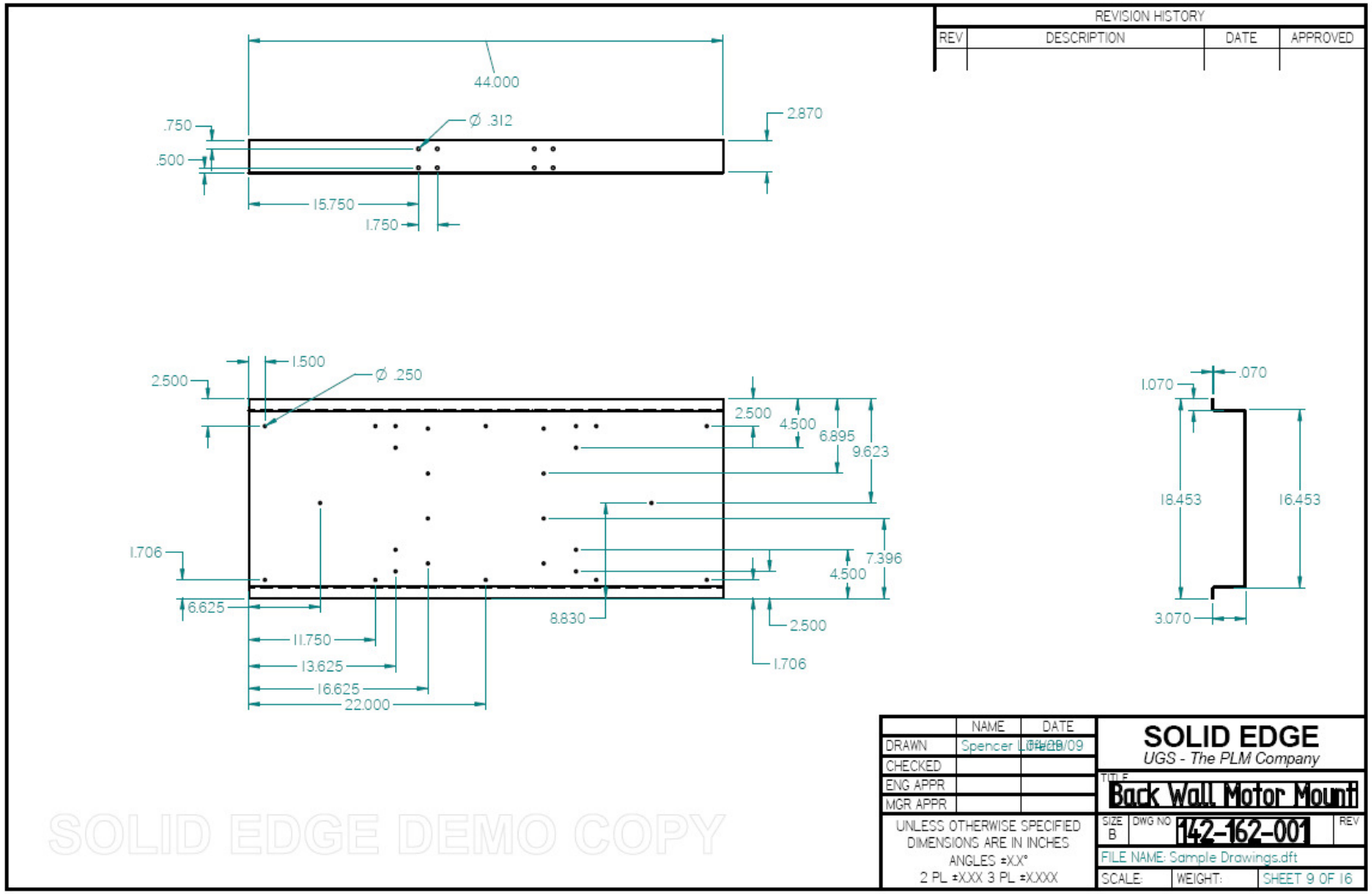
REVISION HISTORY
REV
DESCRIPTION
DATE
APPROVED
44.000
.750
.500
Ø .312
2.870
15.750
1.750
2.500
1.500
Ø .250
4.500
6.895
9.623
1.706
7.396
6.625
8.830
11.750
13.625
16.625
22.000
1.070
.070
18.453
16.453
3.070
NAME
DATE
DRAWN
Spencer L
CHECKED
ENG APPR
MGR APPR
UNLESS OTHERWISE SPECIFIED
DIMENSIONS ARE IN INCHES
ANGLES ±X.X°
2 PL ±.XXX 3 PL ±.XXXX
SOLID EDGE
UGS - The PLM Company
TITLE
Back Wall Motor Mount
SIZE
B
DWG NO
142-162-001
REV
FILE NAME: Sample Drawings.dft
SCALE:
WEIGHT:
SHEET 9 OF 16
SOLID EDGE DEMO COPY

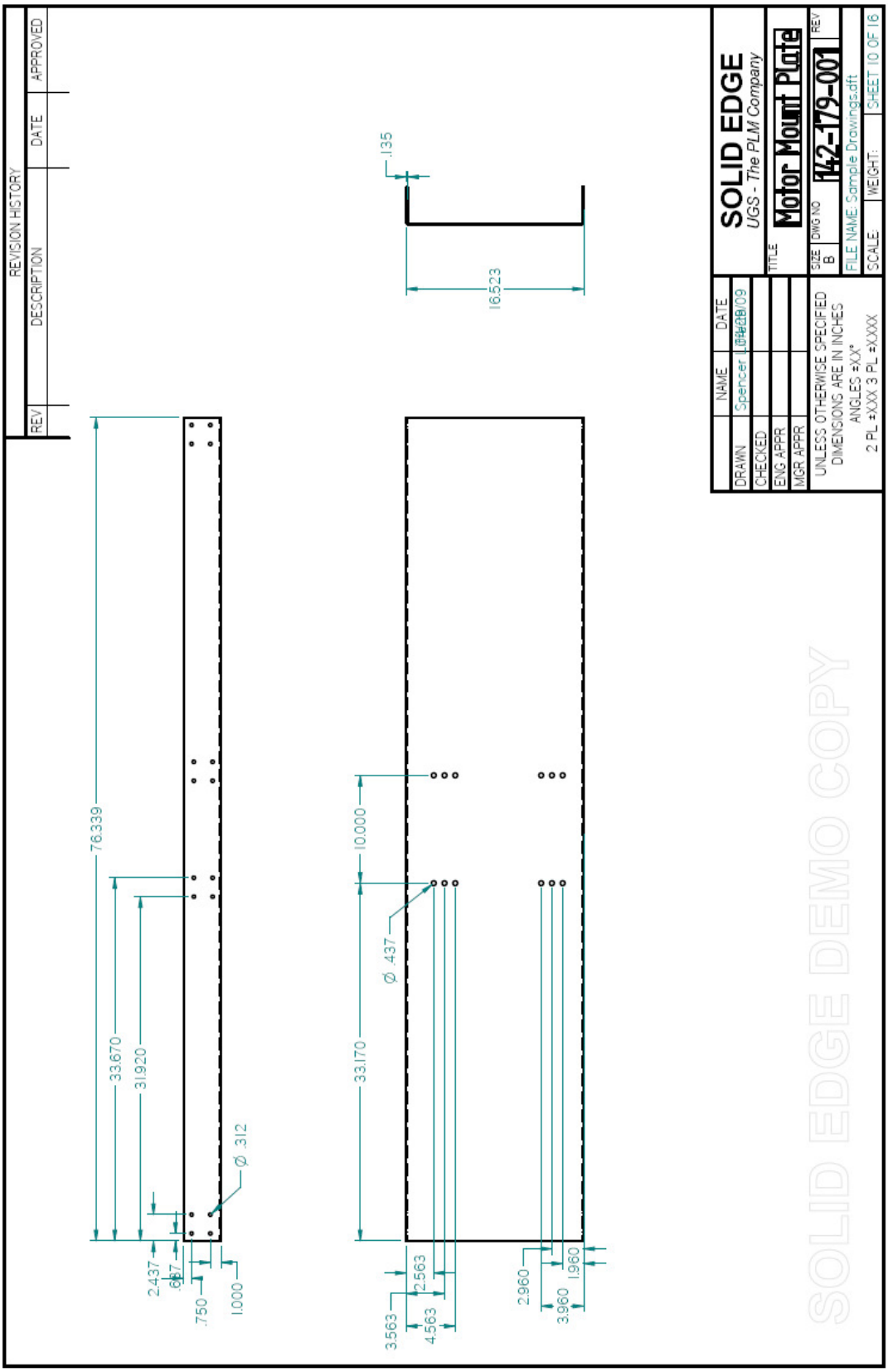
REVISION HISTORY
REV
DESCRIPTION
DATE
APPROVED
SOLID EDGE
UGS - The PLM Company
NAME
DATE
DRAWN
Spencer
CHECKED
ENG APPR
MGR APPR
TITLE
Motor Mount Plate
SIZE
B
DWG NO
142-179-001
REV
FILE NAME: Sample Drawings.dft
SCALE:
WEIGHT:
SHEET 10 OF 16
UNLESS OTHERWISE SPECIFIED
DIMENSIONS ARE IN INCHES
ANGLES ±XX°
2 PL ±XXX 3 PL ±XXXX
76.339
33.670
31.920
2.437
.667
.750
1.000
Ø .312
33.170
10.000
Ø .437
3.563
2.563
4.563
2.960
3.960
1.960
.135
16.523
SOLID EDGE DEMO COPY

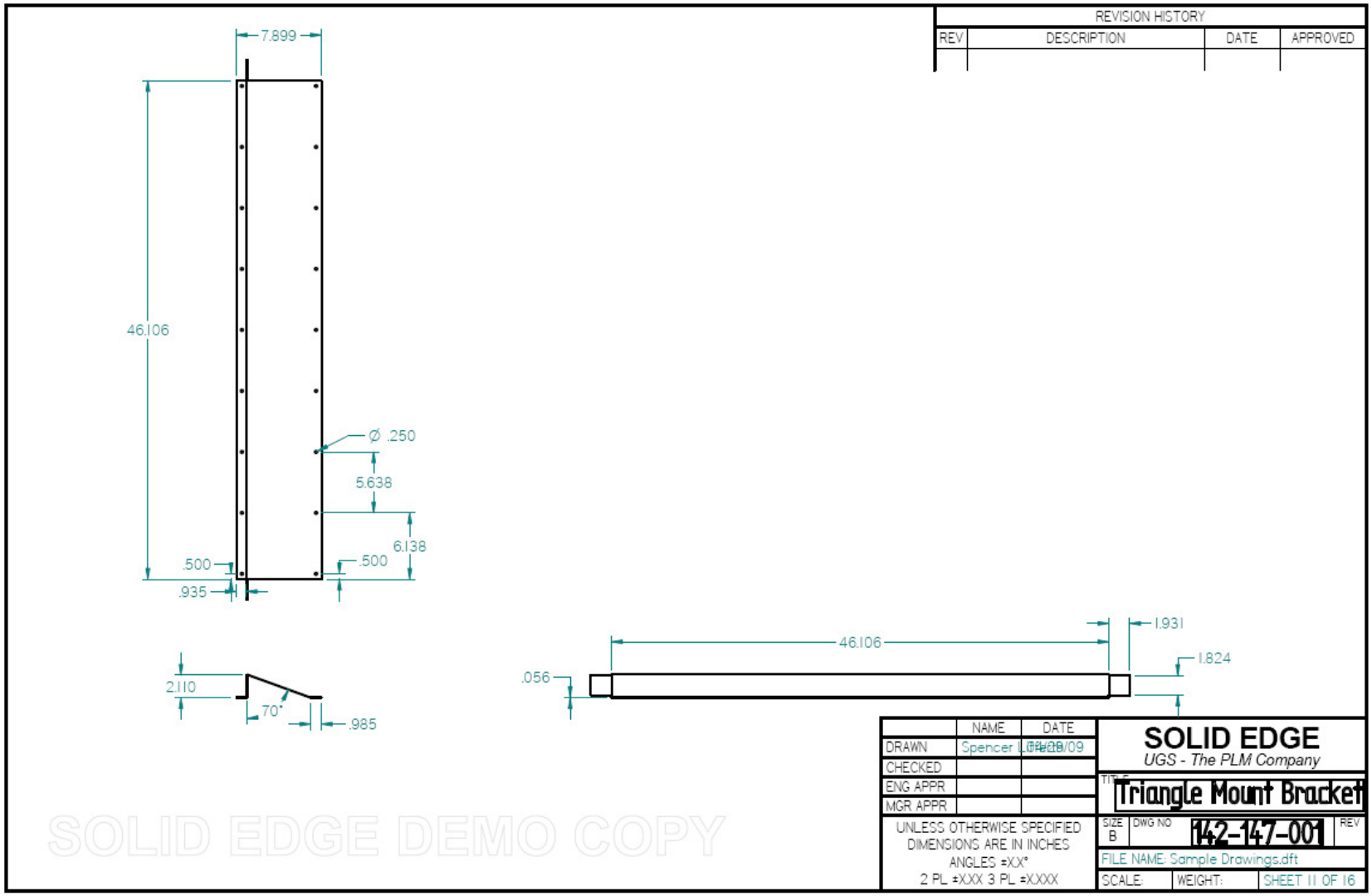
REVISION HISTORY
REV
DESCRIPTION
DATE
APPROVED
7.899
46.106
Ø .250
5.638
6.138
.500
.500
.935
2.110
70°
.985
46.106
1.931
1.824
.056
NAME
DATE
DRAWN
Spencer
CHECKED
ENG APPR
MGR APPR
UNLESS OTHERWISE SPECIFIED
DIMENSIONS ARE IN INCHES
ANGLES ±X.X°
2 PL ±.XXX 3 PL ±.XXXX
SOLID EDGE
UGS - The PLM Company
TITLE
Triangle Mount Bracket
SIZE
B
DWG NO
142-147-001
REV
FILE NAME: Sample Drawings.dft
SCALE:
WEIGHT:
SHEET 11 OF 16
SOLID EDGE DEMO COPY

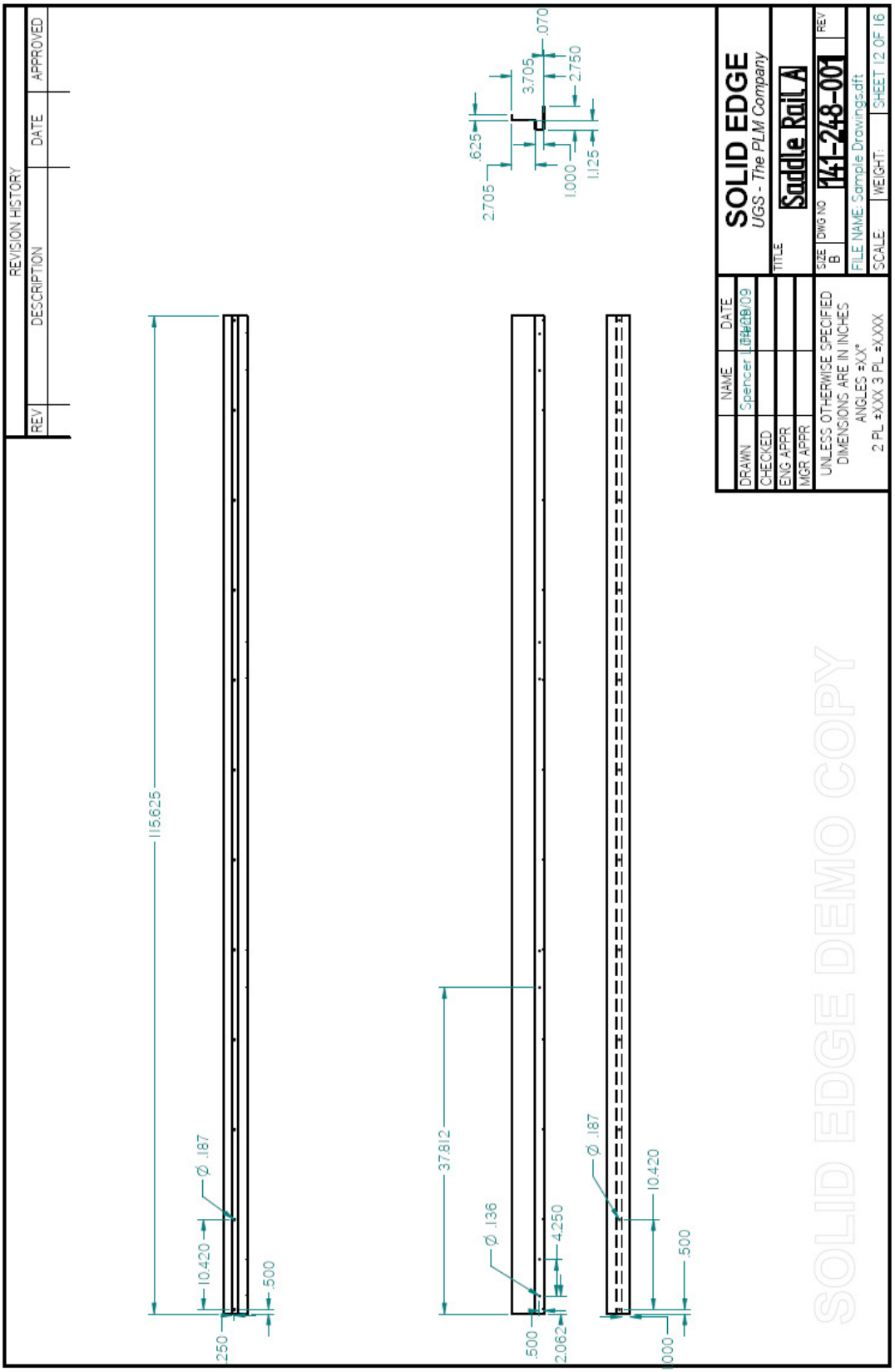
REVISION HISTORY
REV
DESCRIPTION
DATE
APPROVED
115.625
Ø .187
10.420
.500
.250
37.812
Ø .136
4.250
.500
2.062
Ø .187
10.420
.500
1.000
.625
2.705
3.705
.070
2.750
1.000
1.125
SOLID EDGE
UGS - The PLM Company
DRAWN
CHECKED
ENG APPR
MGR APPR
NAME
DATE
Spencer
TITLE
Saddle Rail A
SIZE
B
DWG NO
141-248-001
REV
UNLESS OTHERWISE SPECIFIED
DIMENSIONS ARE IN INCHES
ANGLES ±XX°
2 PL ±XXX 3 PL ±XXXX
FILE NAME: Sample Drawings.dft
SCALE:
WEIGHT:
SHEET 12 OF 16
SOLID EDGE DEMO COPY

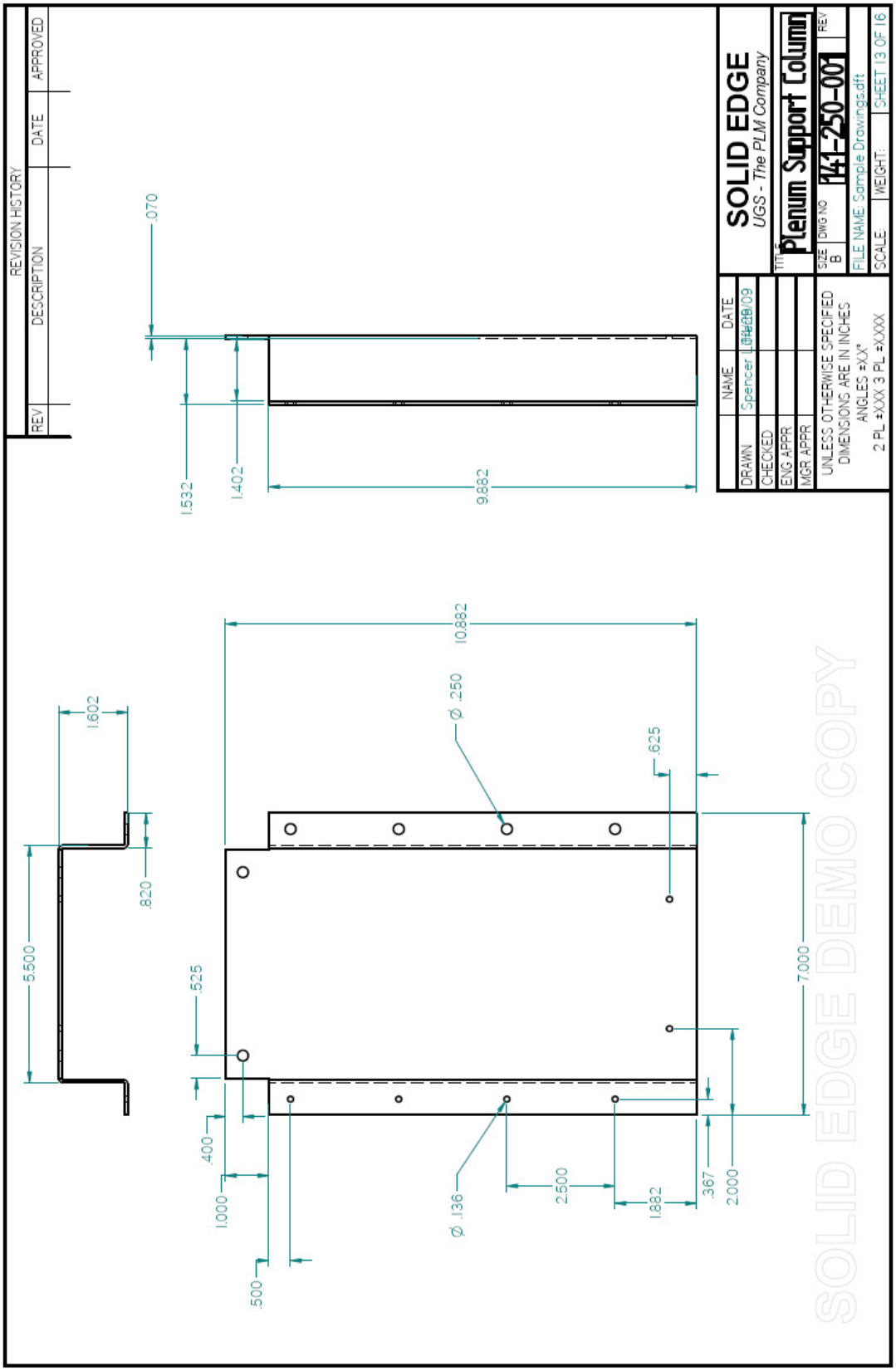
REVISION HISTORY
REV
DESCRIPTION
DATE
APPROVED
.070
1.532
1.402
9.882
10.882
Ø .250
.625
1.602
.820
5.500
.525
7.000
.400
1.000
.500
Ø .136
2.500
1.882
.367
2.000
SOLID EDGE
UGS - The PLM Company
NAME
DATE
DRAWN
Spencer
CHECKED
ENG APPR
MGR APPR
UNLESS OTHERWISE SPECIFIED
DIMENSIONS ARE IN INCHES
ANGLES ±X.X°
2 PL ±.XXX 3 PL ±.XXXX
TITLE
Plenum Support Column
SIZE
B
DWG NO
141-250-001
REV
FILE NAME Sample Drawings.dft
SCALE
WEIGHT:
SHEET 13 OF 16
SOLID EDGE DEMO COPY

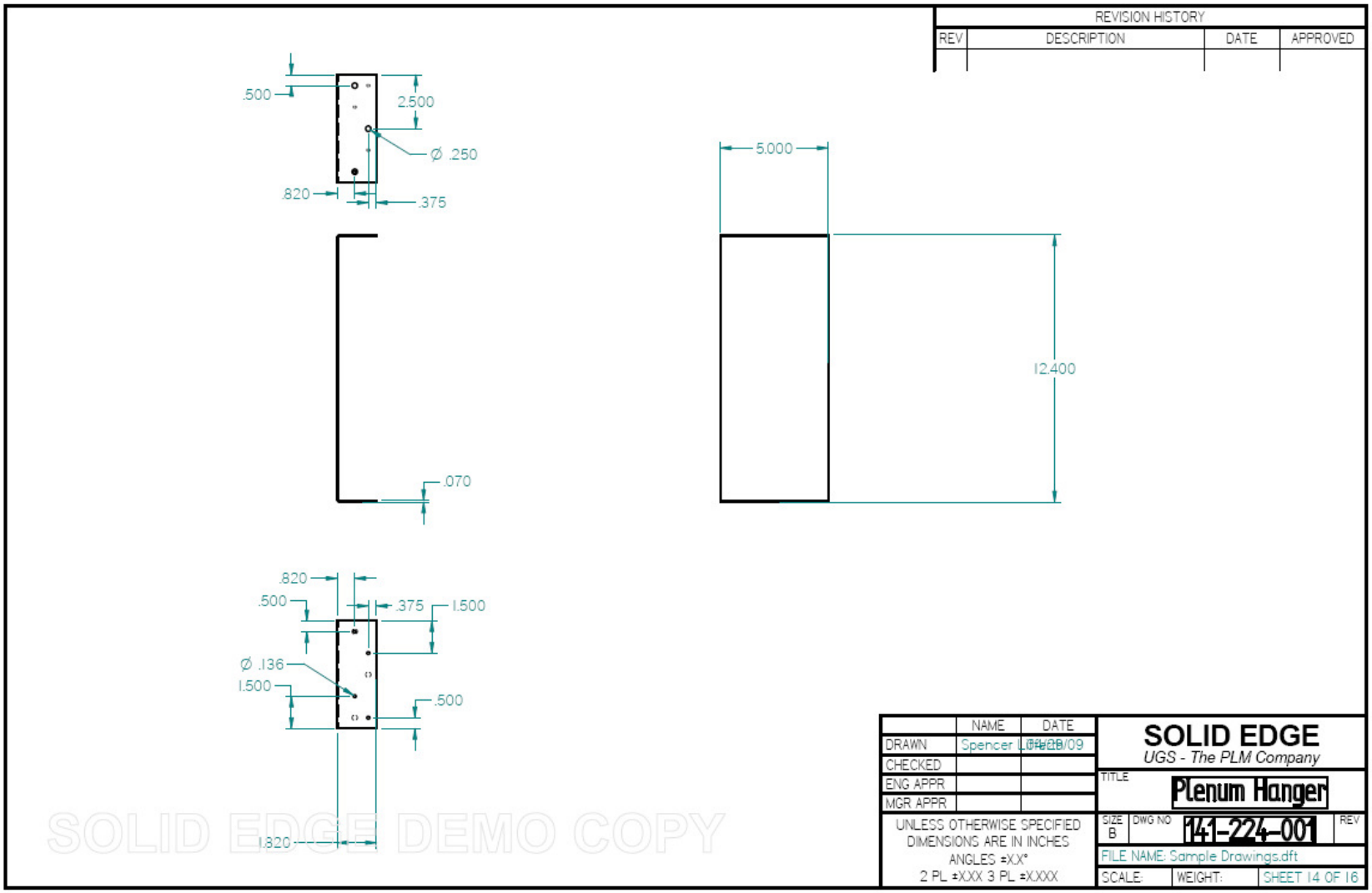
REVISION HISTORY
REV
DESCRIPTION
DATE
APPROVED
.500
2.500
Ø .250
.820
.375
.070
5.000
12.400
.820
.500
.375
1.500
Ø .136
1.500
.500
1.820
NAME
DATE
DRAWN
Spencer Lee
CHECKED
ENG APPR.
MGR APPR.
UNLESS OTHERWISE SPECIFIED
DIMENSIONS ARE IN INCHES
ANGLES ±X.X°
2 PL ±X.XX 3 PL ±X.XXX
SOLID EDGE
UGS - The PLM Company
TITLE
Plenum Hanger
SIZE
B
DWG NO
141-224-001
REV
FILE NAME: Sample Drawings.dft
SCALE:
WEIGHT:
SHEET 14 OF 16
SOLID EDGE DEMO COPY

REVISION HISTORY			
REV	DESCRIPTION	DATE	APPROVED

NOTE: This is a typical panel half, with the part number showing in the bottom. See next Sheet for a parametric list of other panels

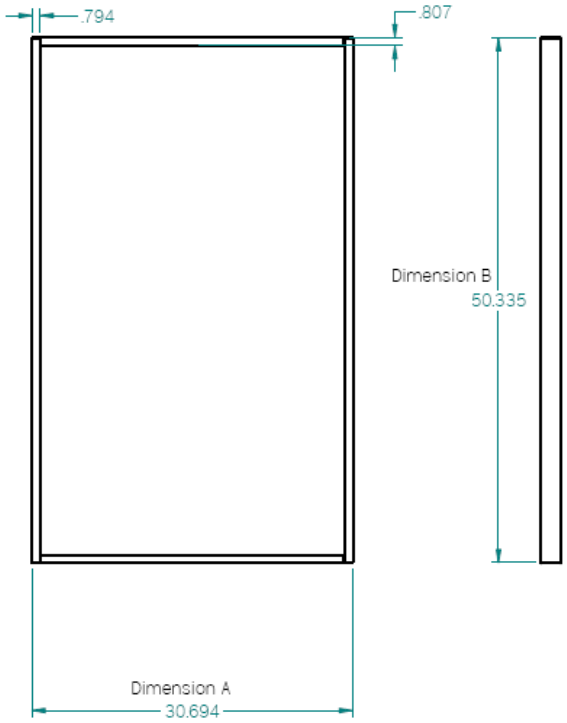

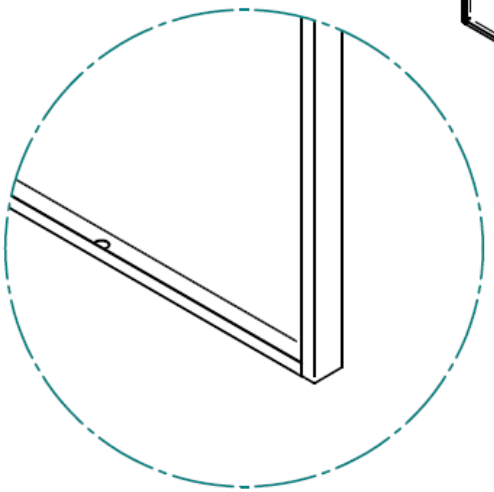

DETAIL A

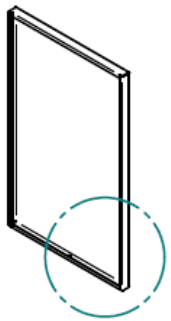

A

	NAME	DATE
DRAWN	Spencer	6/29/09
CHECKED		
ENG APPR.		
MGR APPR.		

UNLESS OTHERWISE SPECIFIED
DIMENSIONS ARE IN INCHES
ANGLES ±X.X°
2 PL ±.XXX 3 PL ±.XXXX

SOLID EDGE
UGS - The PLM Company

TITLE: Typical Panel Half

SIZE	DWG NO	REV
B		

FILE NAME: Sample Drawings.dft

SCALE:	WEIGHT:	SHEET 15 OF 16

REVISION HISTORY			
REV	DESCRIPTION	DATE	APPROVED

		Dimension					Dimension		
Quantity	Panel Part Number	A	B	C	Quantity	Panel Part Number	A	B	C
86	140-626-M00	24.5	10.3.9	1.938	32	140-654-M00	46.2	50.5	1.938
2	140-640-M00	27.4	108.8	1.938	4	140-642-M00	30.8	50.5	1.938
2	140-636-M00	27.4	107.6	1.938	5	140-652-M00	46.2	25.6	1.938
3	140-629-M00	25.9	110.8	1.938	8	140-614-M00	14.6	103.9	1.938
20	140-625-M00	23.9	131.3	1.938	2	140-619-M00	18.0	103.9	1.938
20	140-624-M00	23.9	118.9	1.938	2	140-611-M00	11.1	103.9	1.938
3	140-628-M00	25.9	105.6	1.938	7	140-637-M00	78.4	27.4	1.938
2	140-658-M00	124.7	12.0	1.938	2	140-601-M00	46.0	50.2	0.938
2	140-643-M00	103.8	6.7	0.938	4	140-633-M00	54.4	27.4	1.938
2	140-645-M00	103.8	18.0	1.938	12	140-632-M00	26.2	103.9	1.938
4	140-651-M00	115.8	18.0	1.938	1	140-662-M00	50.2	54.9	1.938
4	140-649-M00	115.8	18.0	0.938	8	140-650-M00	34.1	103.9	1.938
4	140-653-M00	115.8	18.0	0.438	8	140-634-M00	27.4	90.0	1.938
14	140-648-M00	33.0	77.9	1.938	1	140-663-M00	50.2	78.0	1.938
4	140-647-M00	115.8	6.8	0.938	2	140-635-M00	78.4	22.9	1.938
10	140-616-M00	17.7	130.0	1.938	12	140-627-M00	25.9	90.0	1.938
4	140-610-M00	10.4	117.9	1.938	1	140-630-M00	54.4	22.9	1.938
10	140-615-M00	17.7	106.6	0.938	2	140-622-M00	19.8	103.9	1.938
4	140-576-M00	10.4	106.6	0.938					

	NAME	DATE
DRAWN	Spencer L	04/29/09
CHECKED		
ENG APPR		
MGR APPR		

UNLESS OTHERWISE SPECIFIED
DIMENSIONS ARE IN INCHES
ANGLES ±X.X°
2 PL ±.XXX 3 PL ±.XXXX

SOLID EDGE
UGS - The PLM Company

TITLE: **Panel Sizes**

SIZE B | DWG NO | REV

FILE NAME: Sample Drawings.dft

SCALE: | WEIGHT: | SHEET 16 OF 16

Appendix B: Staging Area Design

At the time that the thesis was completed, the staging area had not yet been constructed. The design is included here for construction purposes.

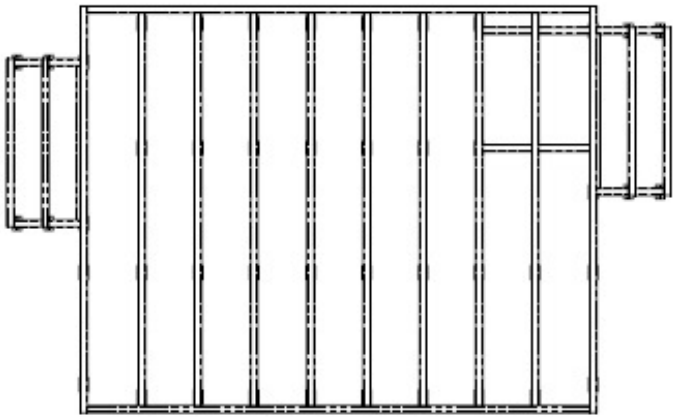

Plan View

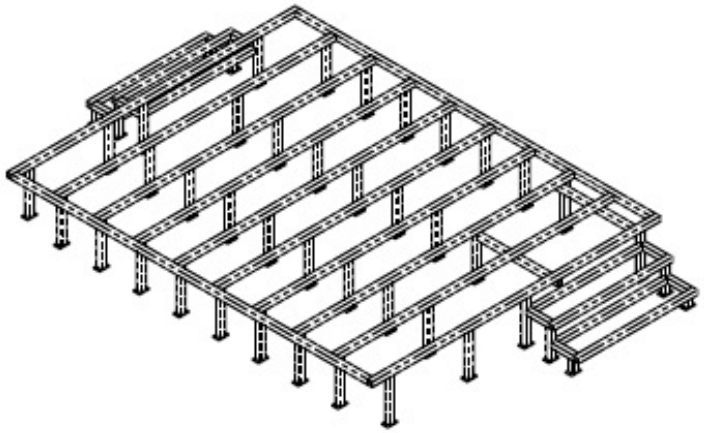

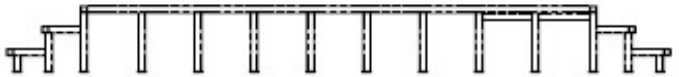

North Elevation

West Elevation

		UNLESS OTHERWISE SPECIFIED:		NAME	DATE
		DIMENSIONS ARE IN INCHES TOLERANCES: FRACTIONAL ± ANGULAR: MACH ± BEND ± TWO PLACE DECIMAL ± THREE PLACE DECIMAL ±	DRAWN		
			CHECKED		
			ENG APPR.		
			MFG APPR.		
		BREAK SHARP GEOMETRIC TOLERANCING PER:	Q.A.		
		MATERIAL	COMMENTS:		
		FINISH			
NEXT ASSY	USED ON				
APPLICATION		DO NOT SCALE DRAWING			

PROPRIETARY AND CONFIDENTIAL

THE INFORMATION CONTAINED IN THIS DRAWING IS THE SOLE PROPERTY OF <INSERT COMPANY NAME HERE>. ANY REPRODUCTION IN PART OR AS A WHOLE WITHOUT THE WRITTEN PERMISSION OF <INSERT COMPANY NAME HERE> IS PROHIBITED.

TITLE:

All Views

SIZE	DWG. NO.	REV
B	5 - 1	
SCALE: 1:50	WEIGHT:	SHEET 1 OF 10

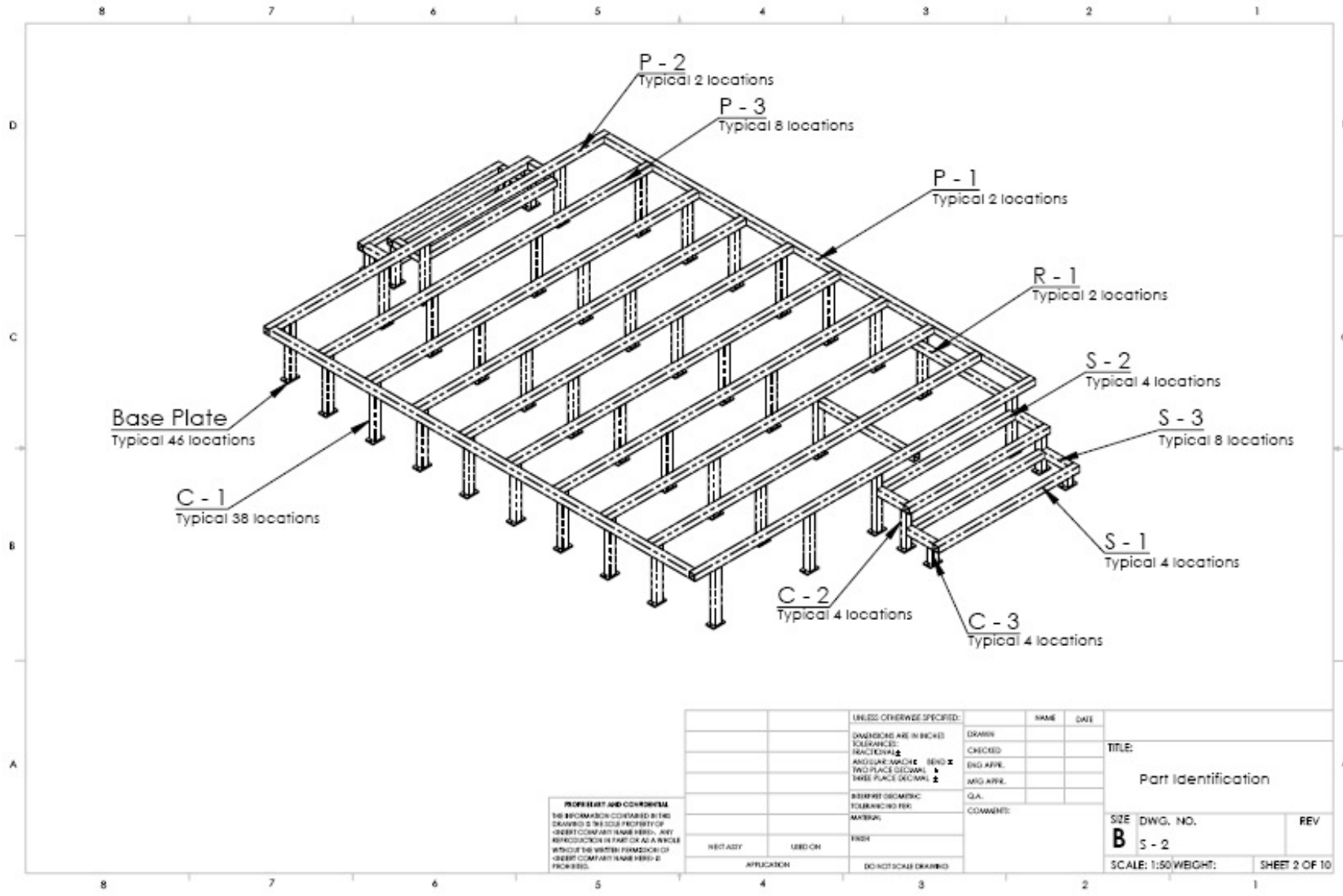
P - 2
Typical 2 locations
P - 3
Typical 8 locations
P - 1
Typical 2 locations
R - 1
Typical 2 locations
S - 2
Typical 4 locations
S - 3
Typical 8 locations
S - 1
Typical 4 locations
C - 3
Typical 4 locations
C - 2
Typical 4 locations
Base Plate
Typical 46 locations
C - 1
Typical 38 locations
UNLESS OTHERWISE SPECIFIED:
DRAWN
CHECKED
ENG APPR.
MFG APPR.
Q.A.
COMMENTS:
NAME
DATE
TITLE:
Part Identification
SIZE
B
DWG. NO.
S - 2
REV
SCALE: 1:50 WEIGHT:
SHEET 2 OF 10

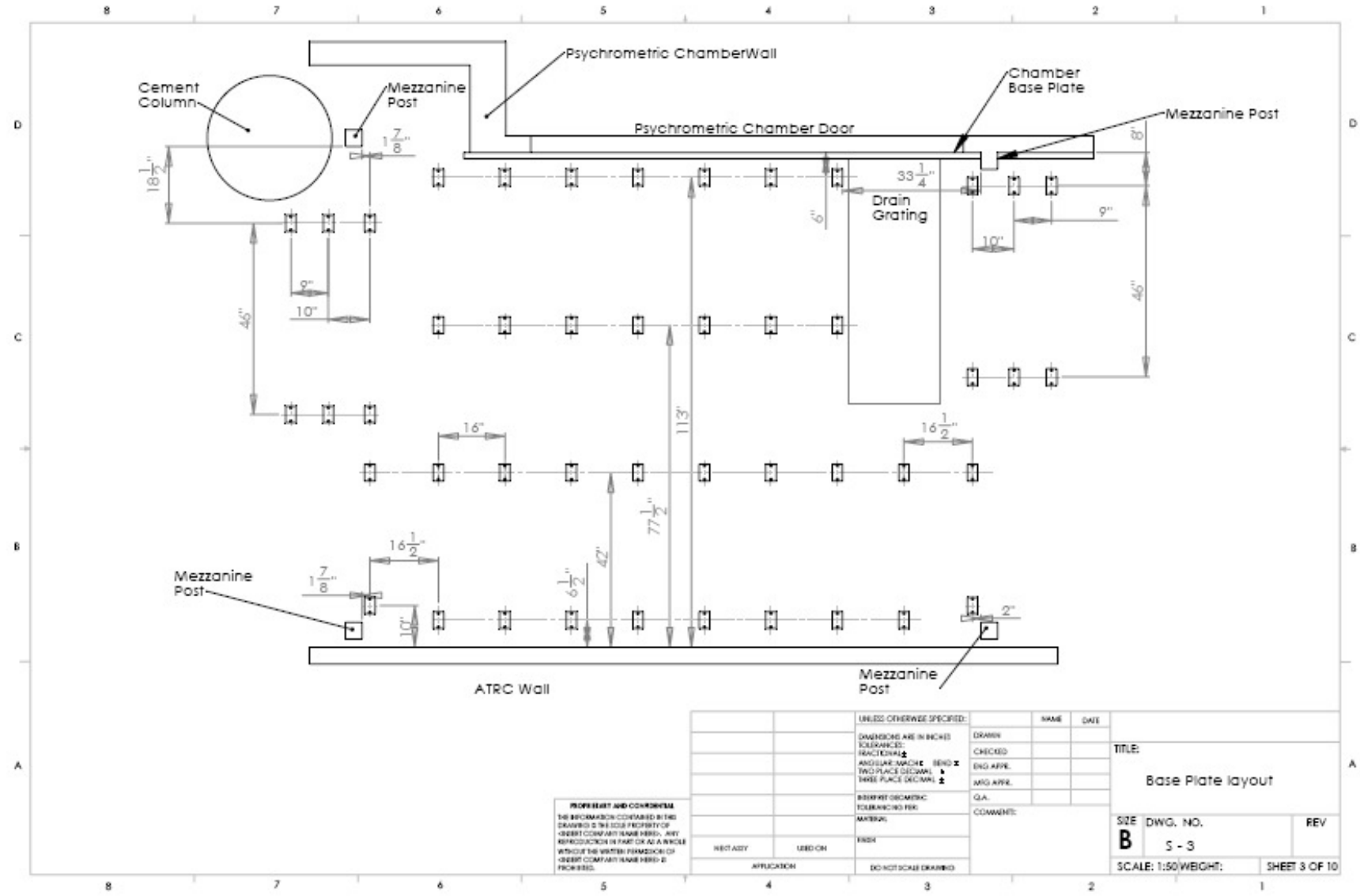
Psychrometric ChamberWall
Cement Column
Mezzanine Post
Chamber Base Plate
Psychrometric Chamber Door
Mezzanine Post
Drain Grating
Mezzanine Post
ATRC Wall
Mezzanine Post
TITLE:
Base Plate layout
SIZE B
DWG. NO. S - 3
REV
SCALE: 1:50 WEIGHT:
SHEET 3 OF 10

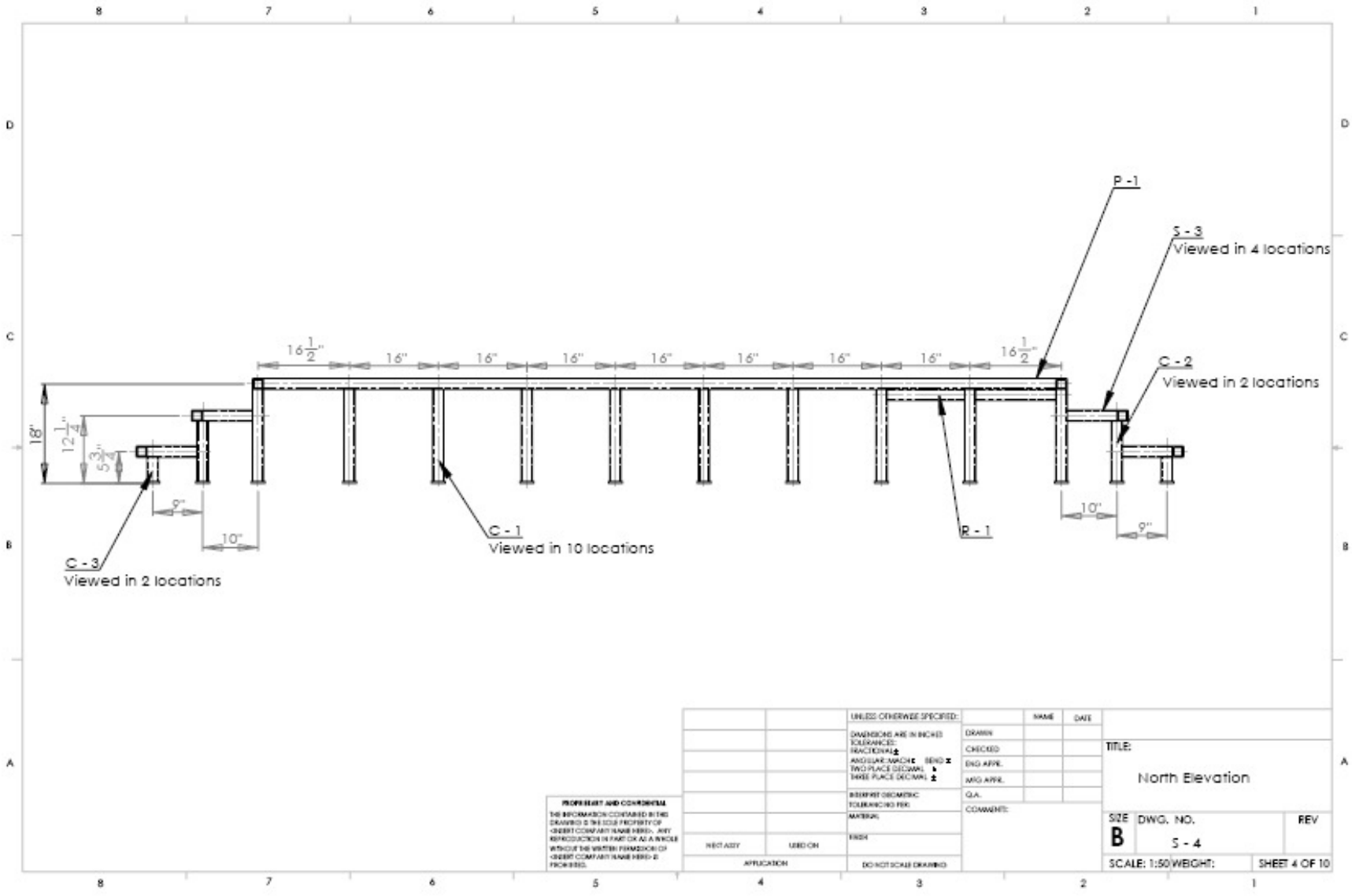
P - 1
S - 3
Viewed in 4 locations
C - 2
Viewed in 2 locations
C - 1
Viewed in 10 locations
C - 3
Viewed in 2 locations
R - 1
16 1/2"
16"
18"
12 1/4"
5 3/4"
9"
10"
North Elevation
S - 4
B
SCALE: 1:50 WEIGHT:
SHEET 4 OF 10

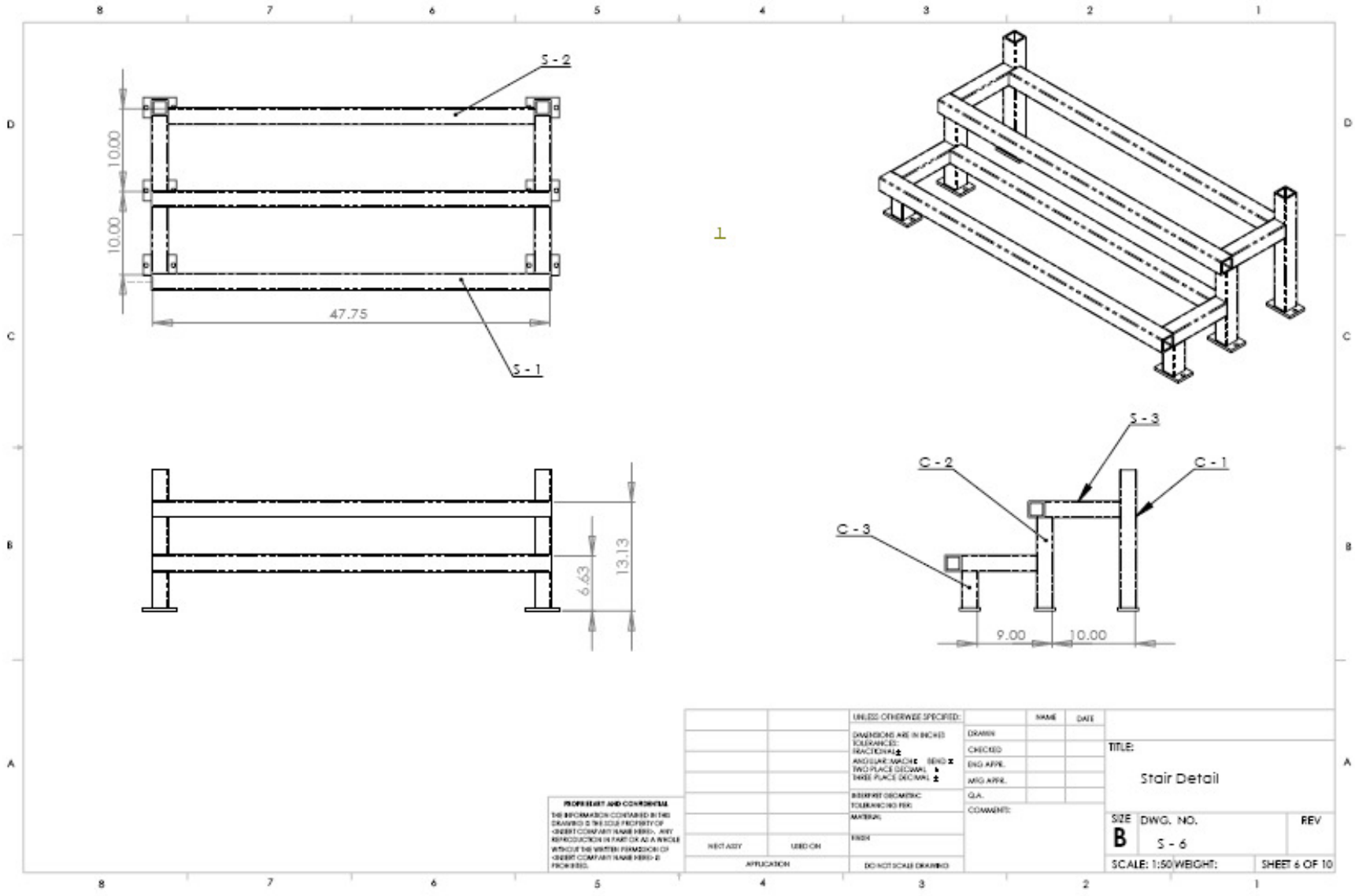
S - 2
10.00
10.00
47.75
S - 1
S - 3
C - 2
C - 1
C - 3
9.00
10.00
6.63
13.13
UNLESS OTHERWISE SPECIFIED:
DRAWN
CHECKED
ENG APPR.
MFG APPR.
Q.A.
COMMENTS:
NAME
DATE
TITLE:
Stair Detail
SIZE
B
DWG. NO.
S - 6
REV
SCALE: 1:50
WEIGHT:
SHEET 6 OF 10
NEXT ASSY
USED ON
APPLICATION
DO NOT SCALE DRAWING

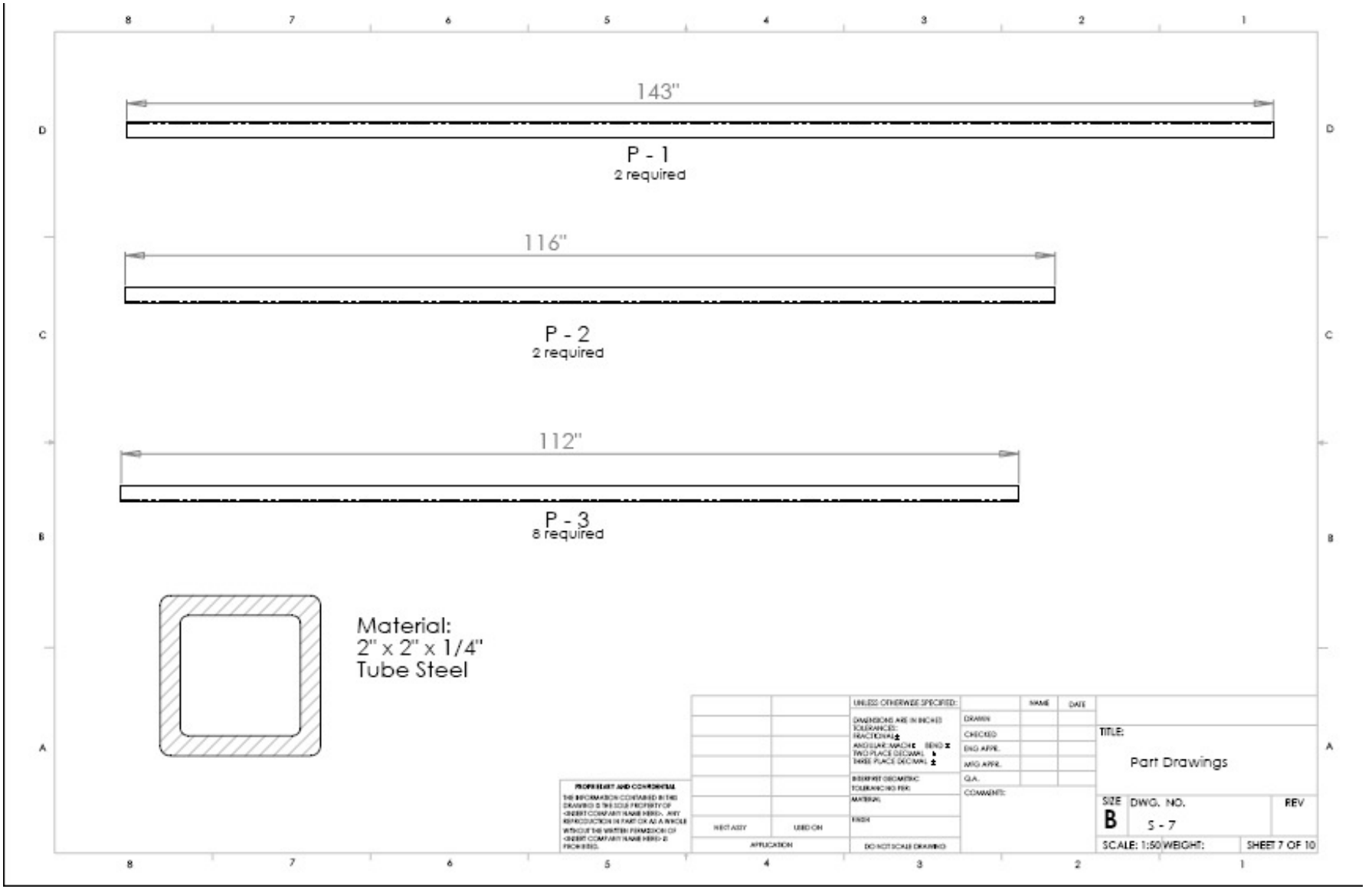
143"
P - 1
2 required
116"
P - 2
2 required
112"
P - 3
8 required
Material:
2" x 2" x 1/4"
Tube Steel
Part Drawings
S - 7
SCALE: 1:50 WEIGHT:
SHEET 7 OF 10

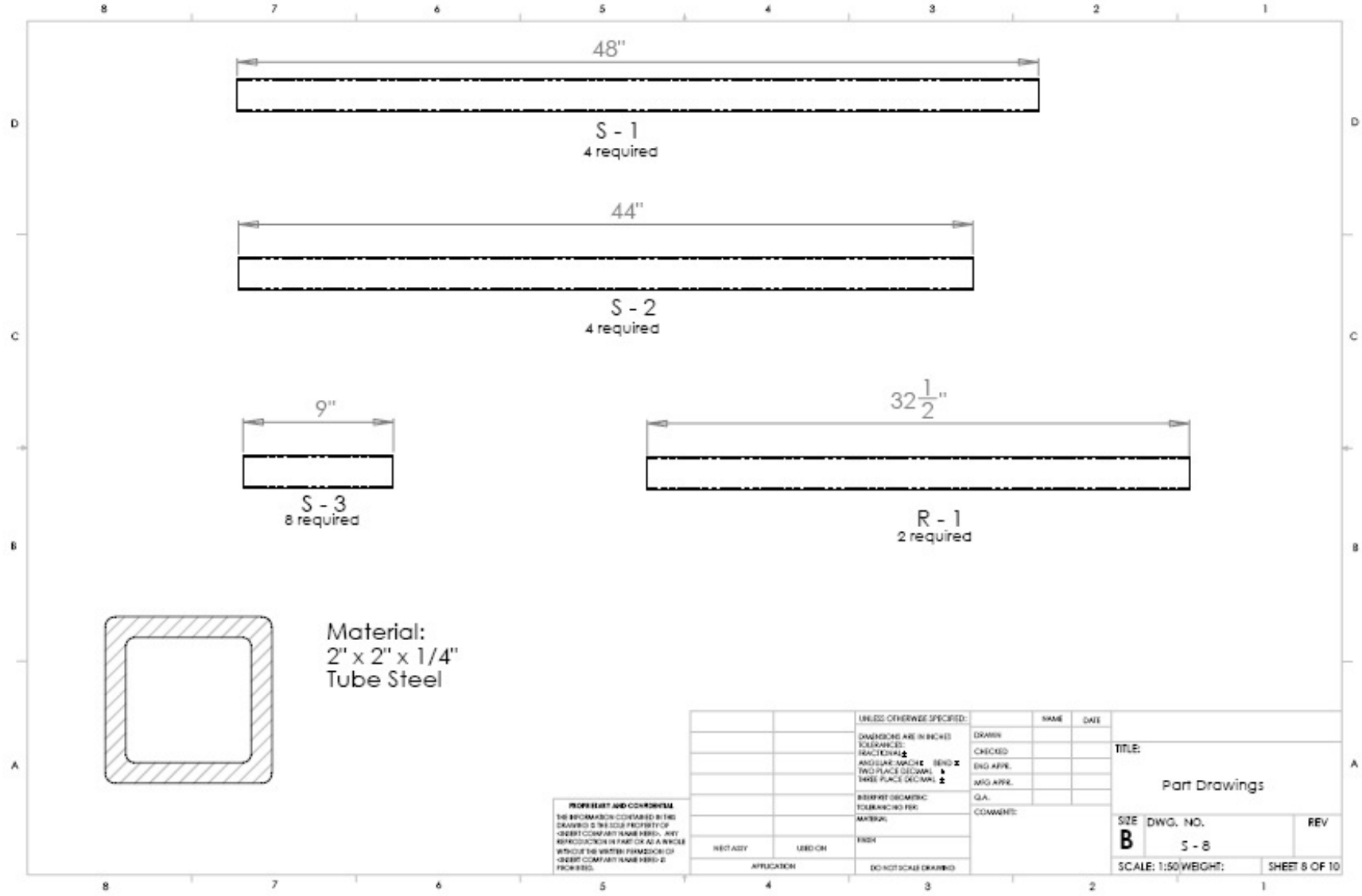
48"
S - 1
4 required
44"
S - 2
4 required
9"
S - 3
8 required
32 1/2"
R - 1
2 required
Material:
2" x 2" x 1/4"
Tube Steel
Part Drawings
SIZE B
DWG. NO. S - 8
REV
SCALE: 1:50 WEIGHT:
SHEET 8 OF 10

C - 1
38 required

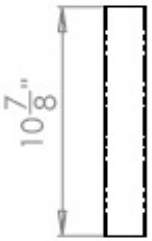

C - 2
4 required

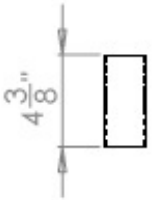

C - 3
4 required

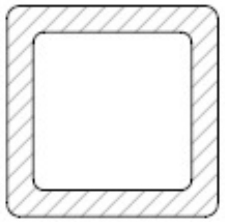

Material:
2" x 2" x 1/4"
Tube Steel

		UNLESS OTHERWISE SPECIFIED:		NAME	DATE
		DIMENSIONS ARE IN INCHES TOLERANCES: FRACTIONAL ± ANGULAR: MACH ± BEND ± TWO PLACE DECIMAL ± THREE PLACE DECIMAL ±	DRAWN		
			CHECKED		
			ENG APPR.		
			MFG APPR.		
			Q.A.		
			COMMENTS:		
		BREAK SHARP EDGES TOLERANCING PER:			
		MATERIAL			
NEXT ASSY	USED ON	FINISH			
APPLICATION		DO NOT SCALE DRAWING			

PROPRIETARY AND CONFIDENTIAL
THE INFORMATION CONTAINED IN THIS DRAWING IS THE SOLE PROPERTY OF <INSERT COMPANY NAME HERE>. ANY REPRODUCTION IN PART OR AS A WHOLE WITHOUT THE WRITTEN PERMISSION OF <INSERT COMPANY NAME HERE> IS PROHIBITED.

TITLE:
Part Drawings

SIZE	DWG. NO.	REV
B	S - 9	
SCALE: 1:50	WEIGHT:	SHEET 9 OF 10

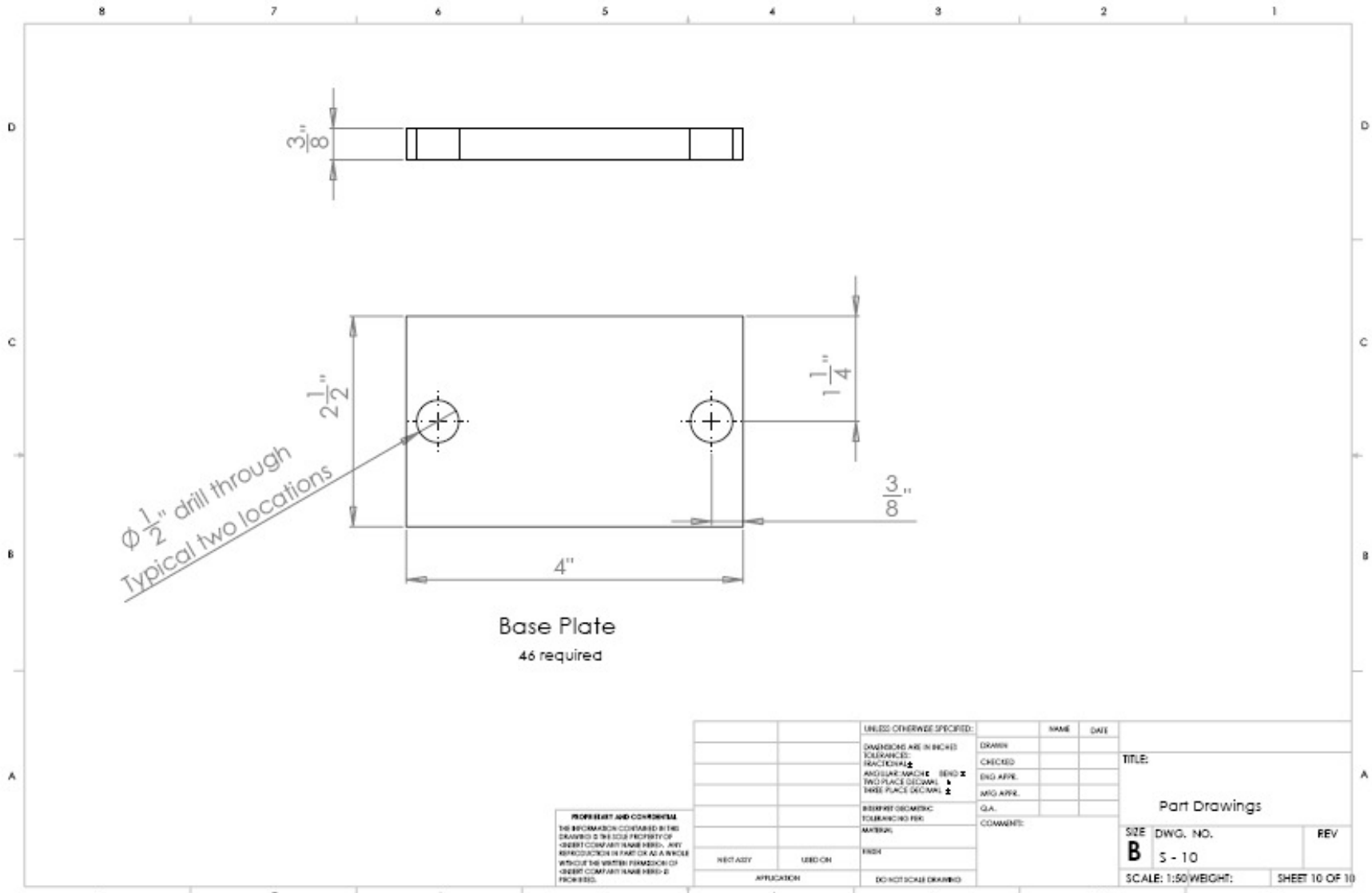
3/8"
2 1/2"
1 1/4"
3/8"
4"
ϕ 1/2" drill through
Typical two locations
Base Plate
46 required
UNLESS OTHERWISE SPECIFIED:
DRAWN
CHECKED
ENG APPR.
MFG APPR.
Q.A.
COMMENTS:
NAME
DATE
TITLE:
Part Drawings
SIZE
B
DWG. NO.
S - 10
REV
SCALE: 1:50
WEIGHT:
SHEET 10 OF 10
PROPRIETARY AND CONFIDENTIAL
NEXT ASSY
USED ON
APPLICATION
DO NOT SCALE DRAWING

Appendix C: Detailed Schematics of Conditioning Loop

This appendix contains detailed schematics of the conditioning loop, including estimated pipe lengths. Locations of fittings and valves are also specified.

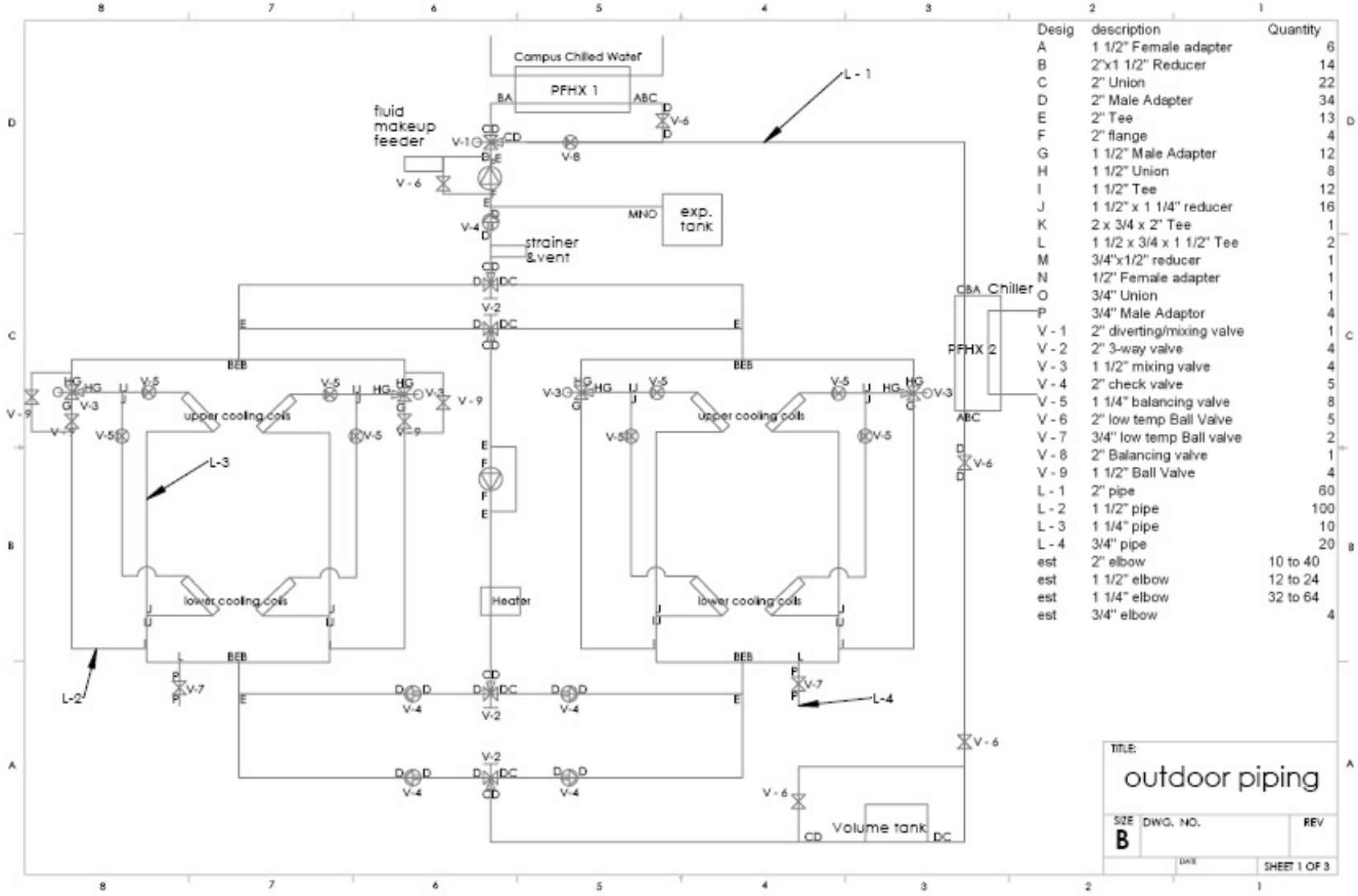

Desig	description	Quantity
A	1 1/2" Female adapter	6
B	2"x1 1/2" Reducer	14
C	2" Union	22
D	2" Male Adapter	34
E	2" Tee	13
F	2" flange	4
G	1 1/2" Male Adapter	12
H	1 1/2" Union	8
I	1 1/2" Tee	12
J	1 1/2" x 1 1/4" reducer	16
K	2 x 3/4 x 2" Tee	1
L	1 1/2 x 3/4 x 1 1/2" Tee	2
M	3/4"x1/2" reducer	1
N	1/2" Female adapter	1
O	3/4" Union	1
P	3/4" Male Adaptor	4
V - 1	2" diverting/mixing valve	1
V - 2	2" 3-way valve	4
V - 3	1 1/2" mixing valve	4
V - 4	2" check valve	5
V - 5	1 1/4" balancing valve	8
V - 6	2" low temp Ball Valve	5
V - 7	3/4" low temp Ball valve	2
V - 8	2" Balancing valve	1
V - 9	1 1/2" Ball Valve	4
L - 1	2" pipe	60
L - 2	1 1/2" pipe	100
L - 3	1 1/4" pipe	10
L - 4	3/4" pipe	20
est	2" elbow	10 to 40
est	1 1/2" elbow	12 to 24
est	1 1/4" elbow	32 to 64
est	3/4" elbow	4

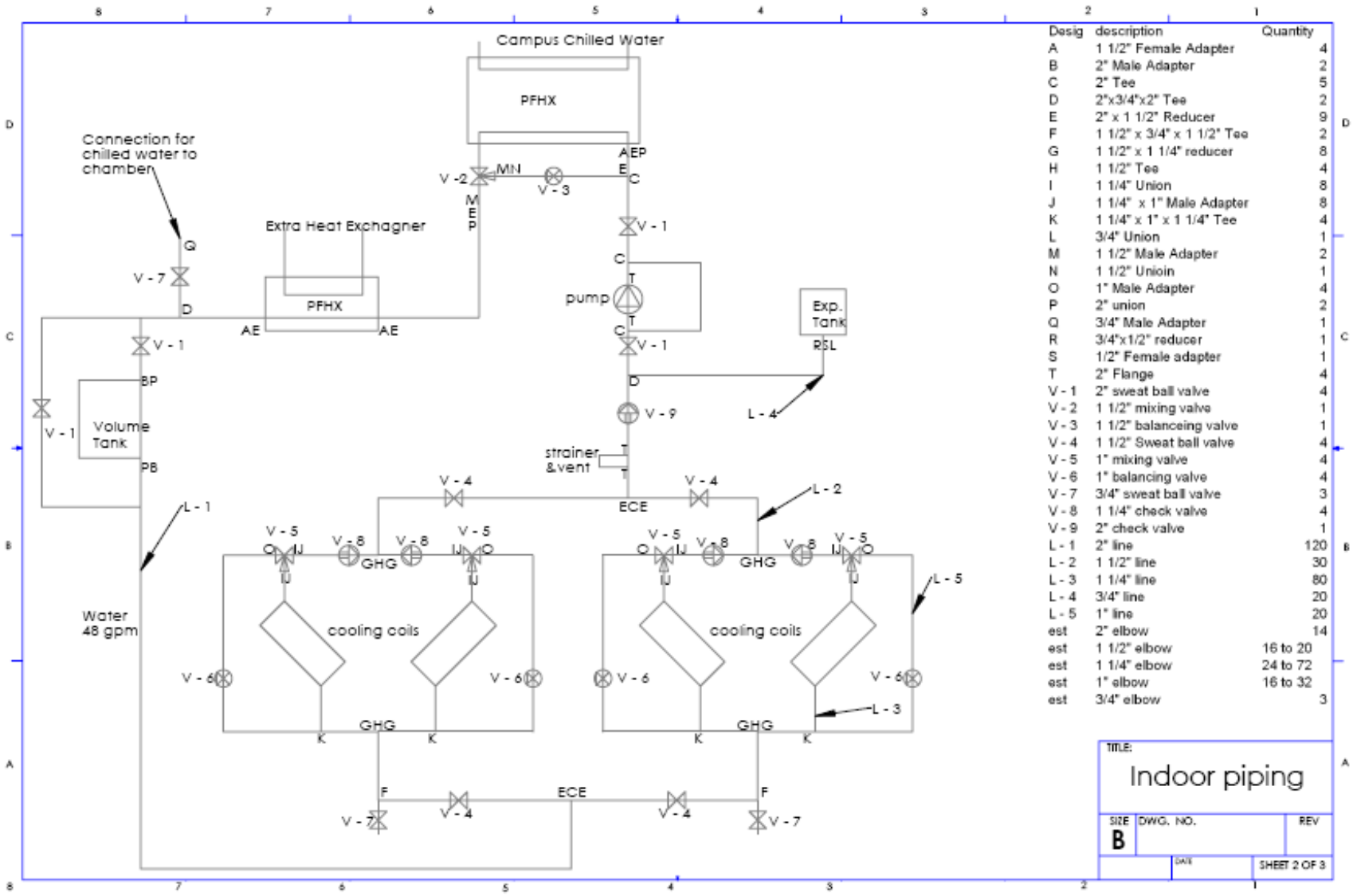

Desig	description	Quantity
A	1 1/2" Female Adapter	4
B	2" Male Adapter	2
C	2" Tee	5
D	2"x3/4"x2" Tee	2
E	2" x 1 1/2" Reducer	9
F	1 1/2" x 3/4" x 1 1/2" Tee	2
G	1 1/2" x 1 1/4" reducer	8
H	1 1/2" Tee	4
I	1 1/4" Union	8
J	1 1/4" x 1" Male Adapter	8
K	1 1/4" x 1" x 1 1/4" Tee	4
L	3/4" Union	1
M	1 1/2" Male Adapter	2
N	1 1/2" Unioin	1
O	1" Male Adapter	4
P	2" union	2
Q	3/4" Male Adapter	1
R	3/4"x1/2" reducer	1
S	1/2" Female adapter	1
T	2" Flange	4
V - 1	2" sweat ball valve	4
V - 2	1 1/2" mixing valve	1
V - 3	1 1/2" balanceing valve	1
V - 4	1 1/2" Sweat ball valve	4
V - 5	1" mixing valve	4
V - 6	1" balancing valve	4
V - 7	3/4" sweat ball valve	3
V - 8	1 1/4" check valve	4
V - 9	2" check valve	1
L - 1	2" line	120
L - 2	1 1/2" line	30
L - 3	1 1/4" line	80
L - 4	3/4" line	20
L - 5	1" line	20
est	2" elbow	14
est	1 1/2" elbow	16 to 20
est	1 1/4" elbow	24 to 72
est	1" elbow	16 to 32
est	3/4" elbow	3

TITLE: Indoor piping

SIZE B | DWG. NO. | REV

DATE | SHEET 2 OF 3

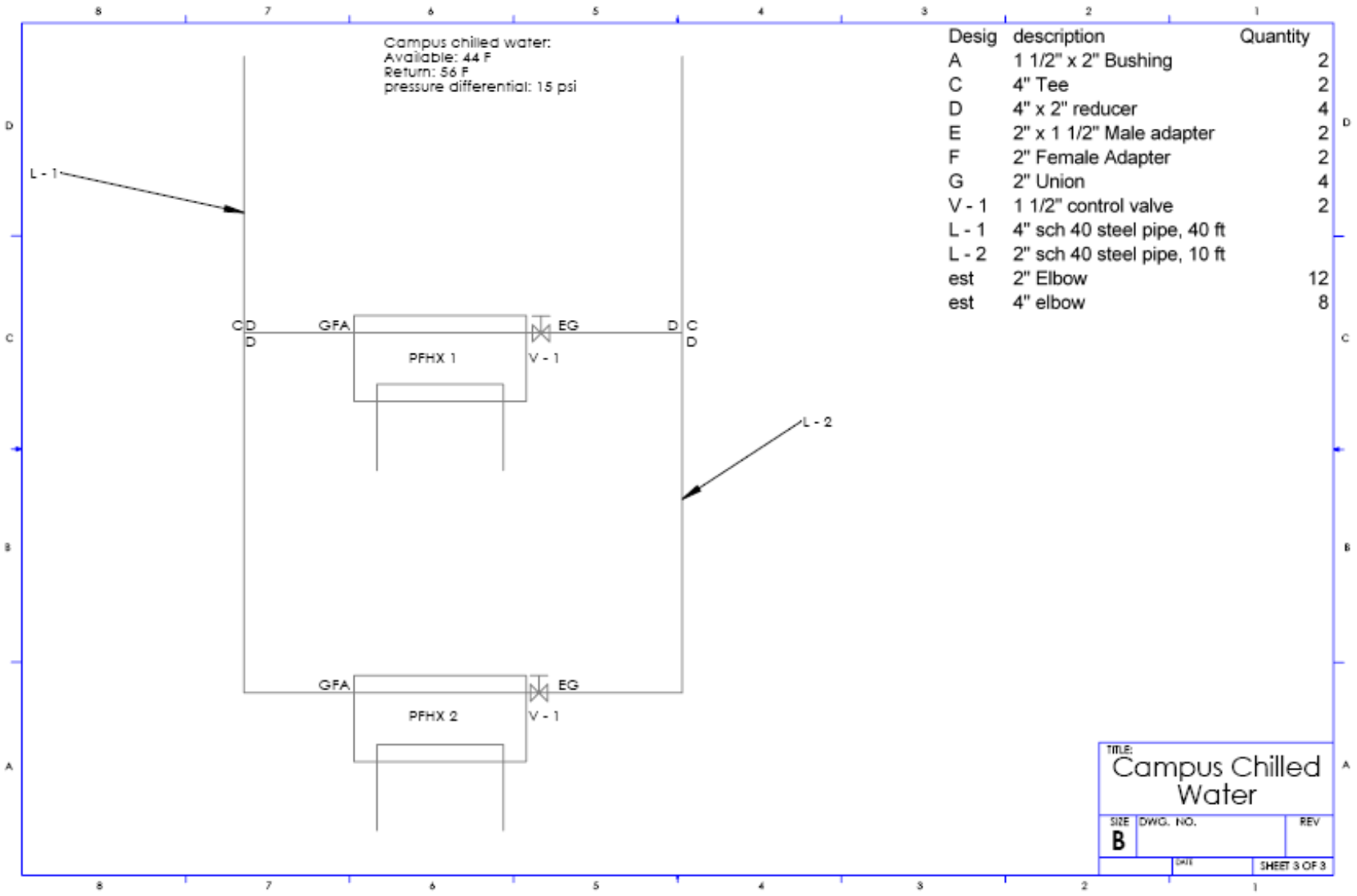
Campus chilled water:
Available: 44 F
Return: 56 F
pressure differential: 15 psi
L - 1
L - 2
C D D
GFA
EG
D C D
PFHX 1
V - 1
GFA
EG
PFHX 2
V - 1
Desig description Quantity
A 1 1/2" x 2" Bushing 2
C 4" Tee 2
D 4" x 2" reducer 4
E 2" x 1 1/2" Male adapter 2
F 2" Female Adapter 2
G 2" Union 4
V - 1 1 1/2" control valve 2
L - 1 4" sch 40 steel pipe, 40 ft
L - 2 2" sch 40 steel pipe, 10 ft
est 2" Elbow 12
est 4" elbow 8
TITLE:
Campus Chilled Water
SIZE B
DWG. NO.
REV
DATE
SHEET 3 OF 3

Appendix D: HVACSIM+ Workspace

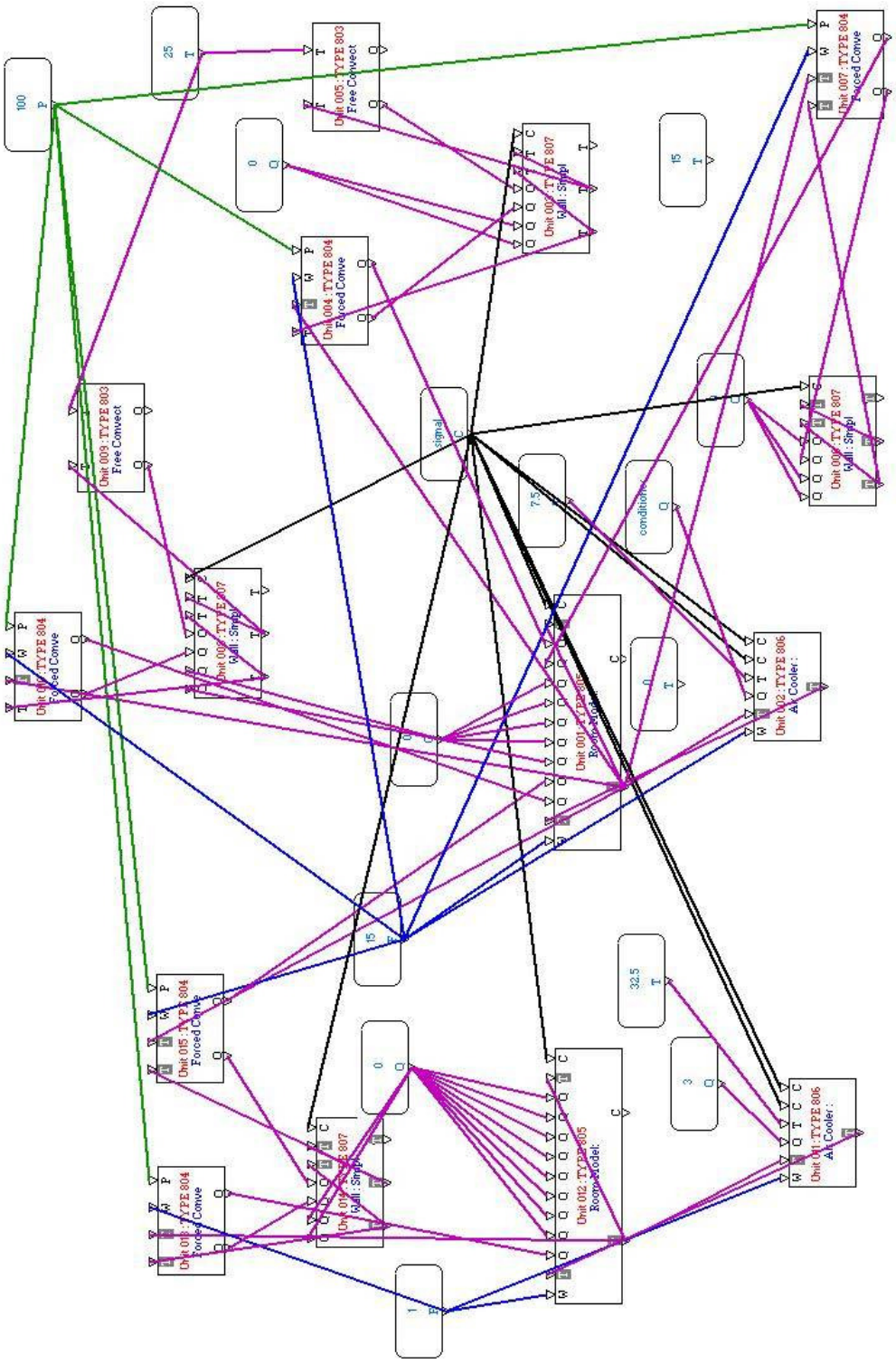

HVACSIM+ workspace for validation using Chatzidakis's data

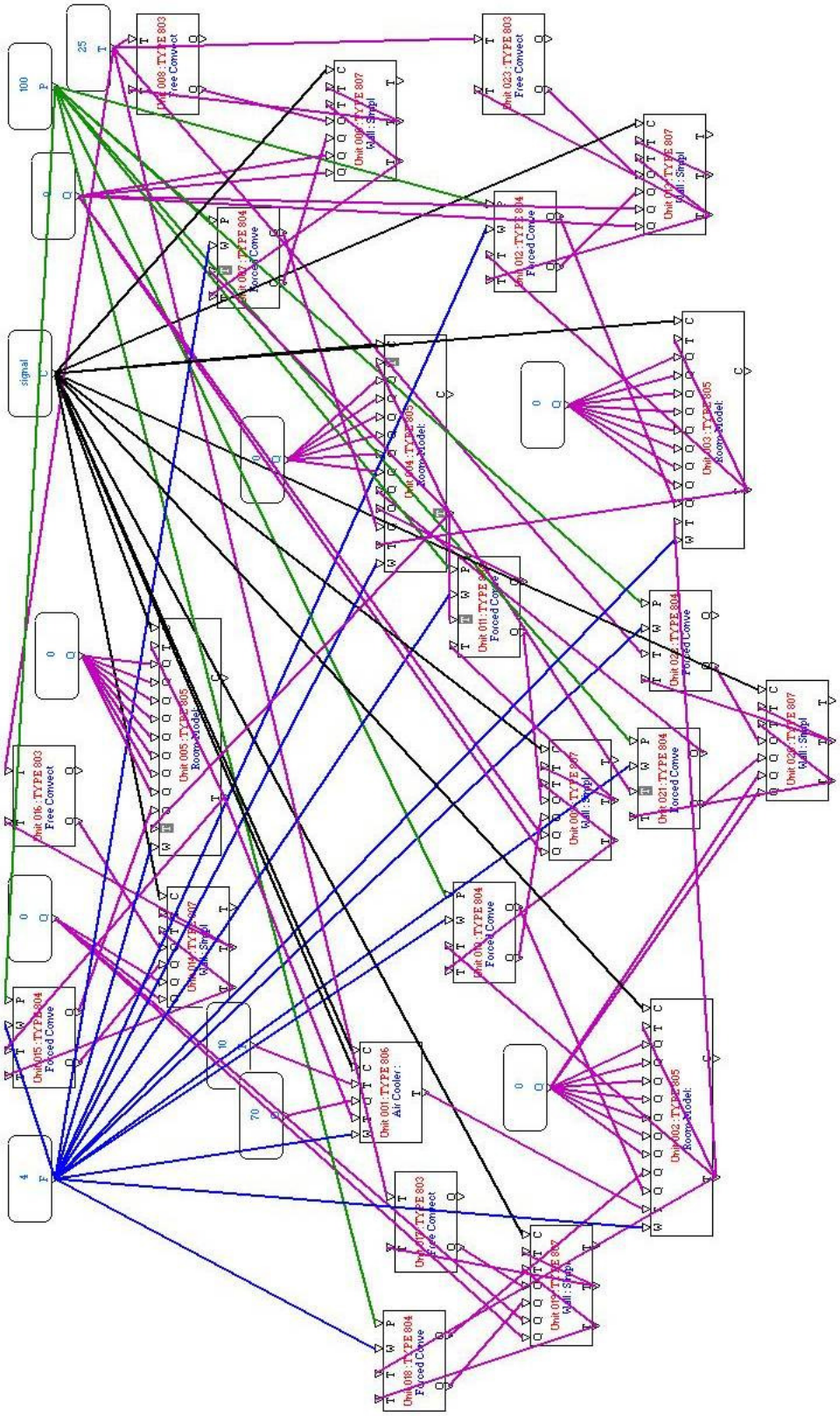

HVACSIM+ workspace for modeling the OSU psychrometric chamber

VITA

Spencer Owen Lifferth

Candidate for the Degree of

Master of Science

Thesis: DESIGN AND CONSTRUCTION OF A NEW PSYCHROMETRIC CHAMBER

Major Field: Mechanical and Aerospace Engineering

Biographical:

Education:
Completed the requirements for the Master of Science in Mechanical Engineering at Oklahoma State University, Stillwater, Oklahoma in May 2009.

Completed the requirements for the Bachelor of Science in Mechanical Engineering at Brigham Young University, Provo, Utah in April 2007.

Professional Memberships:
ASHRARE

Name: Spencer Owen Lifferth Date of Degree: May, 2009

Institution: Oklahoma State University Location: Stillwater, Oklahoma

Title of Study: DESIGN AND CONSTRUCTION OF A NEW PSYCHROMETRIC CHAMBER

Pages in Study: 155 Candidate for the Degree of Master of Science

Major Field: Mechanical and Aerospace Engineering

Scope and Method of Study:

Design and construct a new psychrometric on campus at Oklahoma State University using fundamental structural and thermal analysis

Findings and Conclusions:

The complete design and construction of a psychrometric chamber resulted in the following conclusions:

- Chamber dimensions of 25' x 40' x 20
- Temperature rage of -40 to130°F (-40 to 54 °C) and 10 to 90% relative humidity
- Cooling capacity of 15 tons (52.7 kW) and airflow rate of approximately 8000cfm.
- The chamber consists of sheet metal panels filled with a polyurethane foam core; the estimated thermal conductivity of a panel is 0.026 - 0.033 W/m-K (0.015 - 0.019 Btu/hr-ft-F).
- Simulation suggests chamber operation down to about -25°F (-32°C) before formation of condensate on the exterior walls
- The chamber was specifically designed to incorporate industry standards for testing using the indoor and outdoor air enthalpy methods
- Low and high temperature hydronic cooling systems were designed and installed for chamber operation
- Based on preliminary simulations using customized subroutines in HVACSIM+, the soaking time of the chamber for 25 to 0°C (77 to 32°F) is expected to be about 2.5 hours. The soaking time down to -40°F is approximately 4 hours.
- The chamber structure and supporting systems have been constructed and await operation.

ADVISER'S APPROVAL: Lorenzo Cremaschi